HIGGS MEDIATED SUPERSYMMETRY BREAKING

By

SIMON KNAPEN

A dissertation submitted to the

Graduate School—New Brunswick

Rutgers, The State University of New Jersey

in partial fulfillment of the requirements

for the degree of

Doctor of Philosphy

Graduate Program in Physics and Astronomy

written under the direction of

Professor David Shih

and approved by

_____

_____

_____

_____

_____

New Brunswick, New Jersey

October, 2014

ABSTRACT OF THE DISSERTATION

Higgs Mediated Supersymmetry Breaking

By SIMON KNAPEN

Dissertation Director:

Professor David Shih

We study the role the Higgs sector can play in mediating supersymmetry breaking in the context of the MSSM and its most minimal extension. Higgs-messenger interactions can supplement gauge mediated supersymmetry breaking in important ways: they may provide a solution to the μ/B_μ problem and at the same time generate generate large trilinear Higgs-squark couplings, which are well motivated in the light of the observation of a Higgs boson with mass near 126 GeV. We identify the A/m_H problem, which is analogous of the μ/B_μ problem, as well as several solutions. Moreover we present a general framework for studying Higgs mediated supersymmetry breaking, which enables us to study the possible implications of strongly coupled hidden sectors.

Preface

This thesis is the result of a my graduate training at New High Energy Theory Center at Rutgers University, under the direction of professor David Shih and professor Matthew Strassler. During my graduate education I was fortunate to be given to opportunity to work on a variety of topics with many different collaborators. For this thesis however I have attempted to craft a single, coherent story, and for this reason only a selection of my papers is included. The other papers were all published in peer-reviewed journals, and can be conveniently accessed at http://arxiv.org/.

This thesis is organized as follows: Chapter one contains a brief review of weak scale supersymmetry, intended to sketch the context in which my work may be relevant. Chapters two, three and four consist out of papers on the subject that I wrote with my collaborators and chapter five contains a brief conclusion and outlook.

Acknowledgments

This thesis is merely the endpoint of a truly amazing adventure. I have had the privilege to undertake my journey in truly exceptional circumstances, and I could not have imagined a more exciting time nor place to do so. In terms of the timing, I am grateful to the Higgs boson, for postponing its dramatic appearance on the stage of science until my arrival at the scene, rather than being discovered at LEP many years ago. This has added excitement to my studies in ways that I could not have imagined.

However more important have been the extraordinary people that I have the pleasure of meeting along the road, sometimes in unexpected places. In the first place I am grateful to David Shih, whose advising has been of critical importance for this undertaking to reach a successful conclusion. Aside from bestowing me with indispensable technical skills, David made me appreciate the importance of truly detailed reasoning when building up an argument. His passion for physics has only augmented my own, for which I am very grateful. I am very proud to be the first of large contingent of scientists to be formed under David's guidance.

At various stages throughout my studies I have been exceptionally fortunate to have had the opportunity to learn from several other mentors in addition to David. Of particular significance in this category have been Matt Strassler and Nathaniel Craig. Matt first introduced me in this field and provided me with valuable advice ever after. I am grateful to have had the opportunity to learn from his sharp intuition and exceptional clarity. I am also indebted to Nathaniel for the large amount of physics I learned from him during our frequent collaborations in the later phase of my studies. Moreover I greatly benefited from his career advice and from his ability to find the shortest path towards the solution of any given problem.

Many teachers have contributed in various ways to my education at Rutgers. I am grateful to Tom Banks, Allison Brooks, Daniel Friedan, Chuck Keeton, Wim Kloet, Greg

Moore, Joel Shapiro, Matt Strassler, Scott Thomas and Sacha Zamolodchikov. Of these, Scott and Matt deserve special recognition for teaching me many things that are critical to my functioning as a scientist in my field.

In addition to David, Matt and Nathaniel, I would further like to thank Aria Basirnia, Daniel Egana, Eva Halkiadakis, Diego Redigolo, Pietro Longhi, Claudia Seitz and Yue Zhao for the fruitful collaborations and friendship over the years. I also greatly enjoyed many lengthy discussions with Michael Park, which have contributed significantly to my growth as a physicist.

I have found the department of physics and astronomy at Rutgers to be a very welcoming place were the right conditions have been created for innovation to thrive, in research as well as in education. Besides my thesis research, I have attempted to also make a few modest contributions to the latter. For these projects Michael Manhart has been my fixed compagnon-de-route; somehow working with Michael made every problem always easy. Aside from my interactions with Michael, I was able to grow as an educator by working with Aatish Bathia, Baki Brahmia, Deepak Iyer and Saurabh Jha.

However my greatest thanks goes to those who stayed behind. To my parents and Jonas, who had to deal with the consequences of the decision of a son/brother to move across the world to pursue a distant dream. My gratitude for their sacrifice is unlimited.

Finally I thank Tong for the continuous support and for patiently putting up with all the lost evenings and weekends. Without her I would be nowhere.

Dedication

To my parents,

who taught me the value of education

Table of Contents

Chapter 1

Introduction

On the 4th of July 2012, the ATLAS and CMS collaborations announced the observation of a new particle decaying to a photons and Z-bosons (figure 1.1) [1, 2]. Subsequent measurements have demonstrated that the new particle furthermore decays to W-bosons, tau-leptons and b-quarks. At the time of this writing, all decay rates are consistent with the decay modes associated with a standard model Higgs boson (See figure 1.2). The decay width with respect to the W and Z bosons is of particular importance: if the new particle is indeed a Higgs boson, the strength of this decay is fully determined by the masses of the electroweak gauge bosons. As such, this measurement is a very strong test of the Higgs mechanism and gives us very high confidence that the new particle is indeed a Higgs boson. A detailed and technical description of the Higgs mechanism would easily fill a full chapter of this thesis, and many of the details are not immediately relevant to understand the broader context in which this thesis was written. Moreover such detailed, pedagogical descriptions are available in any standard text on quantum field theory. Nevertheless, given the importance of the subject, a brief, qualitative description is appropriate here.

1.1 Breaking electroweak symmetry

Quantum field theory is the framework in which we understand relativistic quantum mechanics, and when it comes to precise quantitive predictions it is unmatched in all of science. (The anomalous magnetic moment of the electron was predicted and confirmed to 1 part in a billion.) The fact that we deal with relativistic systems implies we would like to preserve a Lorentz covariance formulation as much as possible. In many cases this if a fairly trivial requirement, but in some (important) exceptional cases this approach comes at a price. An extremely important example in this category is the case of spin 1 particles. A massless

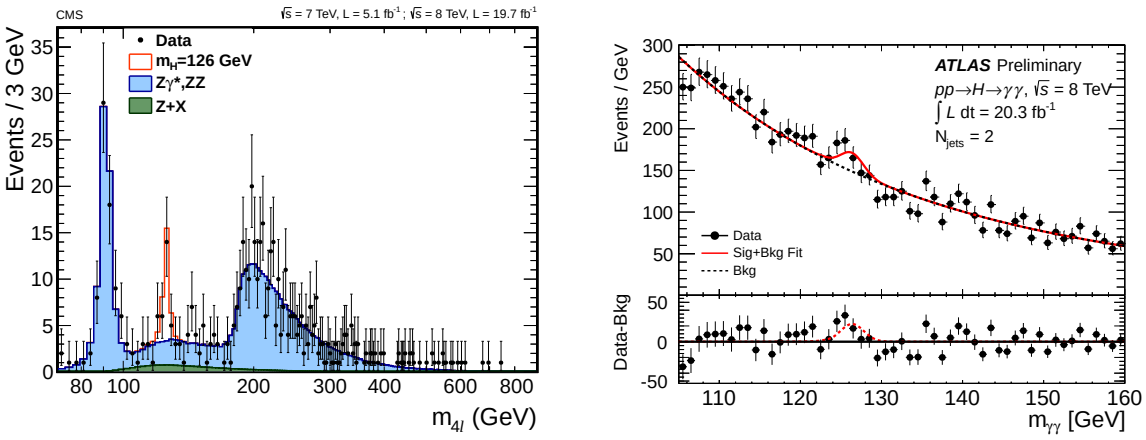

Figure 1.1: The Higgs boson as observed in the ZZ channel (left, CMS collaboration [3]) and in the $\gamma\gamma$ channel (right, ATLAS [4]) collaboration.

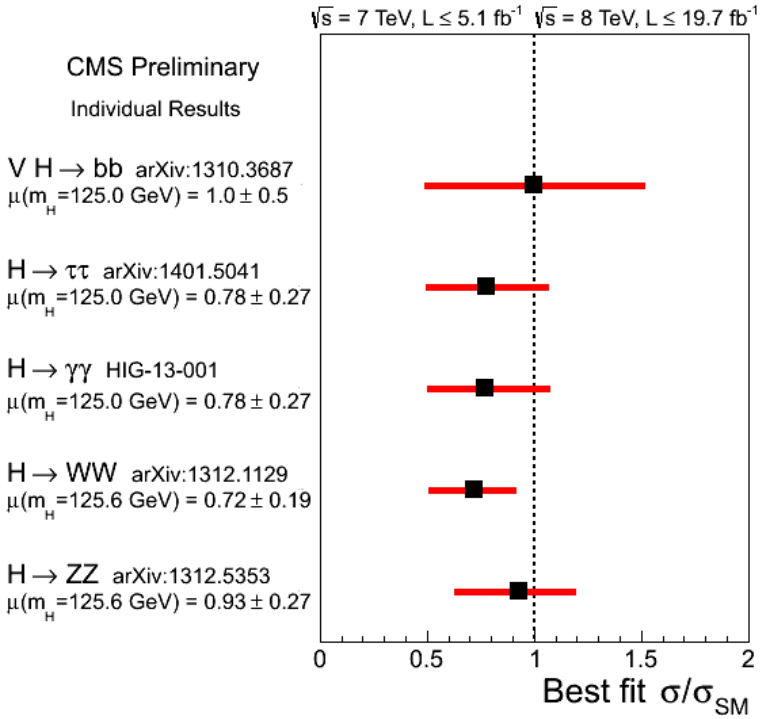

Figure 1.2: The Higgs boson as observed in the ZZ channel (left, CMS collaboration [5]) and in the $\gamma\gamma$ channel (right, ATLAS [4]) collaboration.

spin one particle has 2 degrees of freedom or polarization states (-1 and +1), a massive spin 1 particle has 3 degrees of freedom, associated with the -1, 0, and 1 polarization states. Both cases clash with the requirement of Lorentz covariance: A spin 1 field transforms as a vector under the Lorentz group and must therefore be written as

$$A^\mu \quad \text{with} \quad \mu \in \{0, 1, 2, 4\}. \tag{1.1}$$

The A^μ field has therefore *four* degrees of freedom, 2 more than a massless spin 1 particle and 1 more than a massive spin one particle. We are therefore confronted with the choice of either giving up Lorentz covariance all together or to allow for extra, unphysical degrees of freedom into the theory. As it turns out, the latter is the lesser of the two evils. Now that we accepted these extra, unphysical bookkeeping devices into our calculations, we must make sure that their effect drops out in the final answer for every physical observable. This is ensured by a special symmetry, called **gauge symmetry**. For instance, for a massless spin 1 particle, there is no longitudinal polarization and the component of A^μ aligned with the propagation direction of the particle should not have any physical meaning. This means that we must demand that all physical observables must always be invariant under

$$A^\mu \to A^\mu + \partial^\mu f \tag{1.2}$$

where f is an arbitrary differentiable function. This gauge symmetry therefore simply acts as a firewall between the physical and unphysical degrees of freedom, and failure to enforce it will result in unphysical contributions to physical observables. Typically this sort of mistake would manifest itself as a violation of unitarity in some scattering amplitude. To obtain a massive spin 1 particle, one can simply promote this spurious degree of freedom to a physical degree of freedom[1].

If our spin one particle has no interactions with other spin one particles, this could be the end of the story. However if there are such interactions, the situation is more complicated, at least for massive particles. The reason is that now two transversely polarized particles can scatter into a longitudinal one, as shown in the vertices of the diagram in figure 1.3(a). However if we simply added back the longitudinal mode like we did in the none-interacting

[1]This is know as the Stueckelberg mechanism.

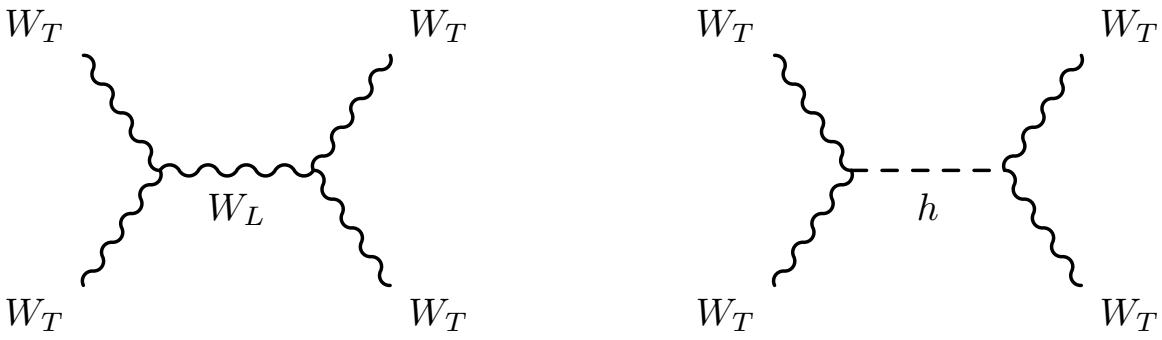

(a) Exchange of longitudinal mode (b) Exchange of Higgs particle

Figure 1.3: Scattering of massive spin 1 bosons, suggestively labeled with W. The diagram on the left grows with energy and would induce unitarity violation at high center of mass energies. Adding in a contribution from exchanging a Higgs boson fixes this problem.

case, the scattering cross section for the longitudinal modes (figure 1.3(a)) keeps rising with energy until unitarity is violated. As we discussed earlier, this is a hallmark of gauge invariance being violated somewhere in our initial setup. But even if one didn't know about gauge invariance, one could simply postulated a new, ad hoc particle with exactly the right couplings to the spin 1 bosons to correct for this nonsensical behavior (figure 1.3(b)). This particle is the Higgs boson. The existence of the Higgs boson is therefore a direct consequence of having a self-consistent quantum field theory of massive, interacting spin one particles[2].

The Higgs mechanism furthermore has an elegant interpretation in terms of the spontaneous symmetry breaking. This goes as follows: The interactions of spin one particles always exhibit a global symmetry, which we must then extend to a more general gauge symmetry to ensure that the unphysical degrees of freedom decouple. For the standard model W bosons, this global symmetry is the $SU(2)$ weak isospin. For massive spin 1 bosons, this global symmetry is broken by the mass term in the Lagrangian. While this is harmless on the level of the global symmetry, we must ensure that the associated gauge symmetry is still present to safeguard the consistency of the theory. The Higgs mechanism elegantly addresses both problems simultaneously: The Higgs field obtains a vacuum expectation value which spontaneously breaks weak isospin and generates a mass for the associated

[2]As we will see, an important exception to this rule occurs when the spin 1 particles are composite particles.

gauge bosons. At the same time, the goldstone modes associated with the spontaneous symmetry breaking ensure the existence of non-linear realization of the gauge symmetry, hence rescuing unitarity. In more mundane terms, the goldstone modes will play the role of the longitudinal polarizations of the gauge bosons and do so in precisely the right way as to prevent unphysical degrees of freedom from contributing to the scattering amplitudes. The Higgs particle is then simply a byproduct of this arrangement: the simplest representation under weak isospin consists out of 4 real degrees of freedom of which only 3 are taken up by the goldstone modes. The remaining degree of freedom is the Higgs boson.

1.2 A Hierarchy problem for spin 0 particles

Aside from any theoretical prejudice that we may have regarding the Higgs mechanism, there is already strong experimental evidence that the new particle is indeed a spin 0 particle. An obvious observation is that it must be a boson, since it decays to two other bosons. Moreover spin 1 particles cannot decay to two massless spin 1 states [6, 7], and therefore the hypothesis of a new spin 1 state is immediately ruled out by the existence of a decay mode to two photons. Finally, the phase space distribution of the final states clearly favors a spin 0 particle over a spin 2 state (figure 1.4).

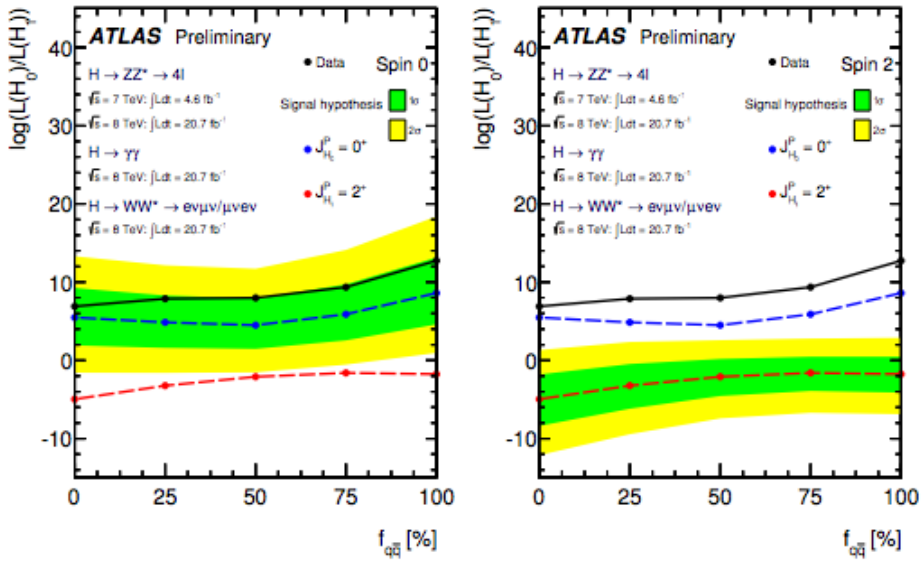

Figure 1.4: The spin 2 hypothesis is disfavored at 99% confidence level, while the spin 0 hypothesis is compatible with the data [8].

Aside from the role they can play in the Higgs mechanism, there is a second reason as to why spin 0 particles are special. In a quantum field theory, spin zero fields are most sensitive to the *most massive* states they interacts with. Concretely, the mass of the spin zero field receives corrections proportional to the mass of these extra states. For our universe, the highest energies at which we certainly expect new states is the Planck scale, at which gravity becomes an important player. This means that the mass of our freshly discovered scalar particle would get corrected as

$$\delta m^2 \sim \frac{1}{16\pi^2} M_{pl}^2 + \cdots \tag{1.3}$$

This lead to an obvious paradox in the sense that the mass of the new particle is measured to be $\sim$ 126 GeV, which is of course much less than the 10^{16} GeV that is suggested by (1.3). This paradox is trivially avoided by invoking some unknown physics at the Planck scale which somehow neutralizes these type of large corrections. However doing so leads to an even more serious problem, since it implies the breakdown of the principle of separation of scales. This empirical principle states that phenomena are governed by physical laws applicable at the natural scale[3] of the problem. For instance, if we would want to compute the orbit of Jupiter, the local weather patterns in New Jersey are totally irrelevant and can be neglected. Obviously, this fact has been one of the cornerstones in the predictive success of physics on all scales that we currently can probe. However from our previous discussion it thus appears that this principle breaks down for spin zero particles: In order to say anything about the Higgs boson it appears that we must understand the full details of quantum gravity, an impossible task in the absence of direct experimental handles on the physics taking place at that scale. This paradox is usually referred to as the *hierarchy problem*.

There is a short list of possible resolutions to the hierarchy problem

1. **We do not fully understand perturbative quantum field theory and the quadratic sensitivity is not really present.** While this is a logical possibility, it is a little hard to imagine. While non-perturbative quantum field theory remains quite mysterious, we achieved astonishing quantitative successes with perturbative

[3]Resonance effects are a notable exception.

calculations. Occasionally radical ideas have been proposed in this direction, but none have gained wide support in the community.

2. **The Higgs boson is composite particle.** If the Higgs boson is a composite particle, its description in terms of a spin zero particle is only valid up to the scale at which its constituents are resolved. Concretely this means that it is inconsistent to extrapolate the estimate in (1.3) all the way up to the Planck scale. In its most simple form this scenario is however ruled out by the LHC already. For a generic composite Higgs one would expect large Higgs self interactions, which in turn lead to a mass and width incompatible with those observed for the Higgs boson.

3. **There are cancellation in (1.3) and they are due to an accident.** This idea makes most sense in the context of a multiverse, where the parameters in the Higgs potential are randomly sampled over the various universes. Our universe would then simply correspond to a choice of parameters for which life can exist. While such an anthropic argument is a priori self consistent, it to some extend eliminates our ability to make predictions about the Higgs boson, at least if we refrain from making untestable assumptions on the nature of the multiverse.

4. **There are cancellation in (1.3) and they are due to a conspiracy, also know as a symmetry.** This final possibility asserts that there are indeed cancellations to keep the Higgs boson light, but that they are there for a specific reason rather than due a multiverse-type accident. This is the avenue that has attracted most attention over the years, especially because it generically leads to the prediction of new particles that may be observable relatively soon. Specifically, one needs to assume the existence of a symmetry to forbid uncontrolled corrections to the Higgs mass operator

$$m^2 h^\dagger h. \tag{1.4}$$

   The exhaustive list of possibilities is again short:

   (a) **Supersymmetry:** Supersymmetry relates the Higgs boson a fermionic partner as follows

$$h \to \epsilon\psi \tag{1.5}$$

where ϵ is the infinitesimal parameter that controls the symmetry transformation. Once supersymmetry has been established, corrections to (1.4) are controlled by the chiral symmetry associated with the fermionic partner of the Higgs, which is then transplanted in to the Higgs itself by the existence of supersymmetry. In order for supersymmetry to work, every standard model particle must have its own, fairly light partner, which makes supersymmetry the ideal hunting ground for collider physicists searching for new signatures at the LHC. Except for the following few paragraphs, this thesis is written entirely within the framework of supersymmetry.

(b) **Shift symmetry:** The action may be invariant under a shift of the Higgs field as follows

$$h \to h + \epsilon. \tag{1.6}$$

This scenario is realized if the Higgs boson is pseudo-goldstone boson of a spontaneously broken global symmetry. Typically the Higgs is a composite particle in this sort of model, very much like pions are the pseudo-goldstone bosons of spontaneous chiral symmetry breaking by the strong dynamics of QCD. The additional global symmetry that is needed for this mechanism predicts the existence of new (colored) particles, analogous to the superpartners in supersymmetry.

(c) **Gauge symmetry:** The Higgs mass may be protected by a gauge symmetry

$$h \to \epsilon^{\mu} A_{\mu}. \tag{1.7}$$

This sort of arrangement may arise in solutions involving extra dimensions. Concretely, the Higgs boson may be provided by the component of the weak gauge fields along a 5th, compactified dimension. Also this case predicts the presence of extra particles near the weak scale from the Kaluza-Klein towers of the compactified extra dimension(s).

(d) **Scaling symmetry:** Large corrections to the Higgs mass could be forbidden by the requirement of scale invariance

$$h \to \epsilon h. \tag{1.8}$$

This scenario requires a consistent embedding of the standard model into an IR fixed point of the renormalization group. This is very challenging due to the upwards running of the hypercharge in the UV and no fully consistent, non-supersymmetric examples are known. The various problems with this scenario are discussed in [9].

Of these four possibilities, supersymmetry is the only one that is fully consistent for energies all the way up to the Planck scale.

1.3 Supersymmetry

Since its introduction in the early seventies, supersymmetry has occupied a central role in theoretical high energy physics. It has directly let to unprecedented developments in our understanding of string theory and the non-perturbative aspects quantum field theory. On the more phenomenological end of the spectrum, the idea of supersymmetry has been equally tantalizing, although somewhat less convincing due to the experimental challenges associated with most of its realizations. A convincing discovery of the principle of weak scale supersymmetry would require the observation of a number of superpartners at a large collider experiment like the LHC, and technical complexities of such an undertaking can hardly be overestimated. At the time of completion of this thesis, the LHC has finalized its first round of data taking, which has blessed us with the tremendously exciting discovery of a weakly coupled Higgs boson. On the other hand, the LHC has not yet uncovered any signs of beyond the standard model physics and none of the traditional signatures related to supersymmetry appear to be present in the 8 TeV data set. This puts us in a interesting limbo, as already supersymmetry is being constrained in interesting ways, while the most important part of the LHC data has yet to be collected. Since I have no crystal ball at my disposal, this thesis is entirely focused on the implications of the 8 TeV data on weak scale supersymmetry, with special attention to properties the newly discovered Higgs boson. As I write it in early 2014, most of its content will be outdated in several years from now, which I do not see as a misfortune, but rather as a very exciting prospect for our field. This section is therefore not intended to be an exhaustive overview of the impact of the 8

TeV data on weak scale supersymmetry nor to provide a pedagogical introduction to the subject. For the latter I gladly refer the interested reader to the classic review by Steve Martin [10], while a more advanced reader can learn the former from the soon-to-be-classic review by Nathaniel Craig [11].

Whereas in the more formal side of high energy physics the importance of supersymmetry is now elevated beyond any discussion, the same is not true for the phenomenological implementations of this idea near the scale of electroweak symmetry breaking. In the end, this is a question that can only be settled decisively by experiment, but in the meantime it is useful to keep the score by listing both the virtues and challenges associated with weak scale supersymmetry.

The main motivation for introducing weak scale supersymmetry is the hierarchy problem, as was discussed in the previous section. In unbroken supersymmetry, all superparticles would have the same masses as their standard model counterparts, an idea which is clearly not phenomenologically viable. However the main virtues of supersymmetry are preserved if supersymmetry is broken spontaneously. For simplicity, let us consider a toy example where all superpartners have the same mass as the supersymmetric top, which was conveniently named ‘ stop’. At energies above well above the stop mass, the mass splitting between the superparticles and the standard model counterparts is neglegible and the theory is very close to a theory with unbroken supersymmetry. An important property of an exactly supersymmetric theory is that the various contributions from particles and sparticles in (1.3) cancel exactly, and the sensitivity to arbitrary high mass scales is therefore removed. If we were to collide particles at energies below the stop mass, there is not enough energy available to produce the superpartners, and they effectively decouple from the theory. Here the theory appears non-supersymmetric and the quadratic sensitivity from (1.3) is reintroduced. The crucial difference is however that now the Higgs boson is quadratically sensitive *to the transition point to the supersymmetric phase* (the stop mass in our toy example), rather than to the Planck scale. If the stop mass is roughly around a TeV, we have successfully traded the large hierarchy problem for a little hierarchy problem. This means that the Higgs mass is now predicted by degrees of freedom that are potentially within reach of our colliders, rather than by physics at the elusive Planck scale.

In addition to ameliorating the hierarchy problem, supersymmetry has a few other compelling features:

- In its most minimal realizations, supersymmetry significantly improves on **gauge coupling unification** in comparison with the standard model (see figure 1.5). Interestingly, the gauge couplings now unify rather precisely, while the same unification in the standard model is only very approximate.

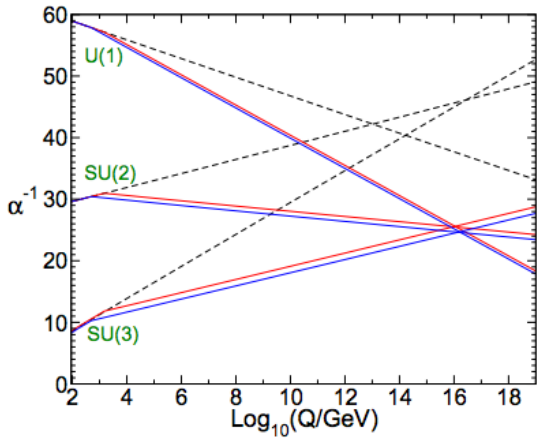

Figure 1.5: Two-loop renormalization group evolution of the inverse gauge couplings $\alpha^{-1}(Q)$ in the Standard Model (dashed lines) and the MSSM (solid lines). In the MSSM case, the sparticle masses are treated as a common threshold varied between 500 GeV and 1.5 TeV, and $\alpha_3(m_Z)$ is varied between 0.117 and 0.121. (Taken from [10].)

- Supersymmetry naturally provides a stable, uncharged particle which in some circumstances can serve as candidate for the **dark matter**. In my opinion, this is perhaps the least compelling element in the list. The mere prediction of a stable, uncharged particle is easily achieved in a wide class of models of beyond the standard model physics, and as such it is not a strong argument in favor of supersymmetry. On the other hand, in some part of its parameter space, the dark matter candidate provided by weak scale supersymmetry is charged under the electroweak force and naturally qualifies as weakly interacting massive particle (WIMP) dark matter, which implies that its annihilation cross section in the early universe is in the right ballpark to give us the correct dark matter abundance today. At the time of this writing, the WIMP paradigm is under stress by null observations in various dark matter direct detection experiments, of which the LUX experiment [12] has been the most powerful so far.

Aside from its assets as listed above, supersymmetry also suffers from a number of challenges, some of which are theoretical, while others are related to (the lack of) certain experimental observations. The latter category is typically shared by other solutions to the hierarchy problem in one way or another.

- A first and important challenge that any model for beyond the standard model physics must confront is the **flavor problem**. Precision flavor experiments have put the scale of generic new physics several orders of magnitude higher than the weak scale, at which one expects new degrees of freedom which address the hierarchy problem. For weak scale supersymmetry this implies that whatever mechanism spontaneously breaks supersymmetry, must do so without introducing large flavor violation. Concretely, all supersymmetry breaking masses and interactions must be approximately diagonal in flavor space. Similar considerations can be made with regards to CP-violation. Fortunately such a spectrum is easily achieved if the effects of supersymmetry breaking are communicated to the supersymmetric standard model by standard model gauge interactions only, which are necessarily flavor conserving. This framework is called **gauge mediated supersymmetry breaking** or simply **gauge mediation**. A gauge mediation model typically consists out of a **hidden sector** which spontaneously breaks supersymmetry, and **messenger sector**. The latter by itself is fully supersymmetric, but its feels the effects of supersymmetry breaking from the hidden sector through a perturbative coupling of some sort. It is important that the messenger sector contains some fields that are charged under the standard model gauge groups. This way the effects of supersymmetry breaking get communicated down to the minimal supersymmetric standard model (MSSM) through loop corrections involving the standard model gauge fields. This setup is shown schematically in figure 1.6 and has the advantage that it is insensitive to the details of the physics which determines the flavor structure of the yukawa matrices, provided that the latter takes place at energies above the typical mass scale of the messenger sector.

- A second challenge for the MSSM is related to the manner in which electroweak symmetry is broken. To see this, we must account for the fact that the MSSM has

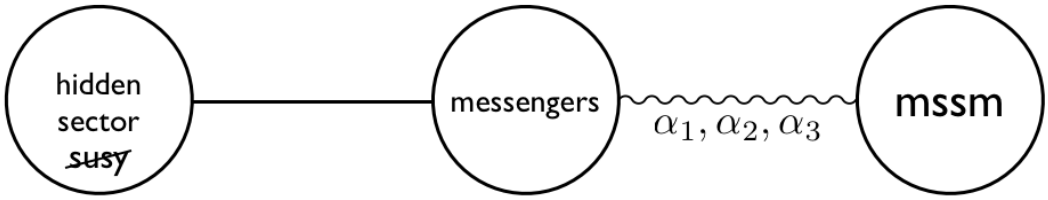

Figure 1.6: Schematic picture of gauge mediated supersymmetry breaking. Supersymmetry is broken spontaneously in the hidden sector and communicated down to the MSSM through loop corrections involving the MSSM gauge fields as well as the messenger fields.

a slightly more complex Higgs sector than the standard model, in the sense that it contains not one but two Higgs doublets, which are usually denoted by H_u and H_d. The Lagrangian for the MSSM Higgs sector looks as follows

$$\begin{aligned}\mathcal{L} \subset &(|\mu|^2 + m_{H_u}^2)|H_u^0|^2 + (|\mu|^2 + m_{H_d}^2)|H_d^0|^2 - (B_\mu H_u^0 H_d^0 + c.c.) \\ &+ \frac{1}{8}(g^2 + g'^2)(|H_u^0|^2 - |H_d^0|^2)^2\end{aligned} \tag{1.9}$$

where I dropped the charged components of the Higgs doublets, since they are not relevant for our discussion here. The symbol μ stands for the mass of the Higgsinos, which are the superpartners of the Higgses (also suppressed in (1.9)). $m_{H_u}^2$, $m_{H_d}^2$ and B_μ are supersymmetry breaking contributions to the masses of the Higgs fields. g and g' are the weak isospin and hypercharge gauge couplings respectively. The Lagrangian in (1.9) is the MSSM equivalent of the famous 'mexican hat' potential of the Higgs field in the standard model. For this model to produce viable electroweak symmetry breaking, a number of conditions must be satisfied:

1. The potential must be bounded from below.
2. The potential must have a minimum for a non-zero value for one or both of the Higgs fields.

Imposing these conditions leads to a set of consistency requirements on the relative sizes of μ, $m_{H_u}^2$, $m_{H_d}^2$ and B_μ. The exact conditions are not particularly illuminating for the qualitative discussion in this introduction and it suffices to know that they are generally satisfied when μ, $m_{H_u}^2$, $m_{H_d}^2$ and B_μ are all in the same ballpark, or more

precisely

$$\mu^2 \sim m_{H_u}^2 \sim m_{H_d}^2 \gtrsim B_\mu. \tag{1.10}$$

This relation is certainly reasonable if all arise through the same mechanism of supersymmetry breaking. However there is one important caveat in the sense that a priori the μ parameter is not related to supersymmetry breaking. Certainly one could choose to adjust it by hand to right size, after which supersymmetry would prevent it from getting large quantum corrections through the mechanism sketched out earlier in this section. However such an ad hoc solution is somewhat unsatisfying, and one would like to have a dynamical mechanism such that μ *automatically* comes out with the correct size. Unfortunately, such a setup is not possible with the standard model gauge interactions alone[4].

Gauge mediation must therefore be supplemented with another mechanism for mediating supersymmetry breaking. Typically this is done by allowing for yukawa interactions between the MSSM Higgs sector and some of the fields in the messenger sector. Although in the literature this idea is occasionally lumped together with gauge mediation, I will here and onwards refer to it as **'Higgs mediated supersymmetry breaking'** or simply **'Higgs Mediation'**. Although Higgs mediation can generate $\mu^2 \sim m_{H_u}^2 \sim m_{H_d}^2$ quite trivially, generic models will also generate the detrimental relation

$$B_\mu \sim 16\pi^2 |\mu|^2 \tag{1.11}$$

which is a violation of the consistency condition in (1.10). This is known as the $\mu/\mathbf{B}_\mu$ **problem**. There are handful solutions known to this problem, some of which will be discussed in the later chapters of this thesis.

- A final nagging problem that plagues supersymmetry (as well as all other symmetry-based solutions to the hierarchy problem) is the lack of experimental evidence for the extra particles it predicts. Of particular interest in supersymmetry are the stops, and to lesser extend the Higgsino's and the gluino (the superpartner of the gluon), as

[4]The technical reason for this is that the mechanism responsible for supersymmetry breaking must also break the Peccei-Quin (PQ) symmetry which protects the μ term. Since gauge interactions preserve PQ symmetries, such a mechanism can not be realized with the standard model gauge interactions alone.

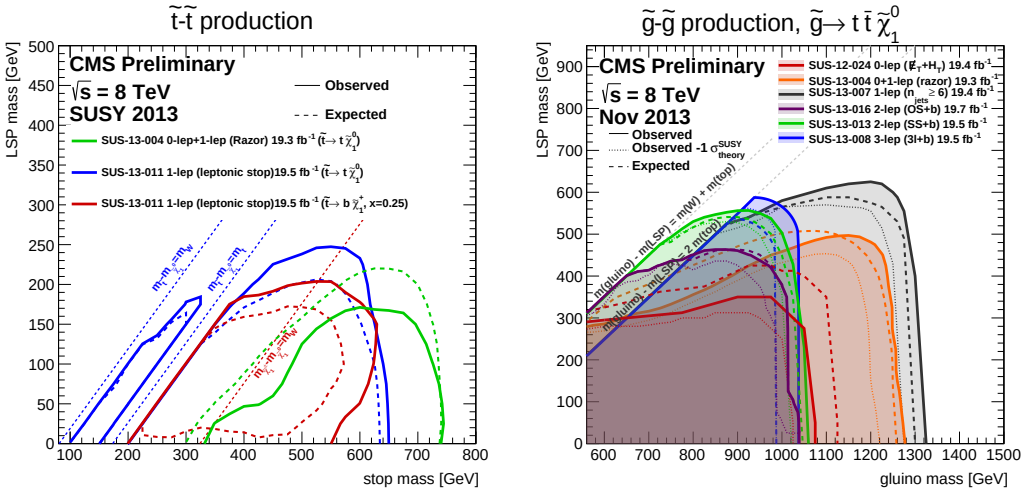

Figure 1.7: Limits set by the CMS collaboration on direct $\tilde{t}\tilde{t}$ production [13, 14] (left) and $\tilde{g}\tilde{g}$ pair production with a cascade decay through stops to a top anti-top pair plus neutralino [15] (right). Similar limits exist from the ATLAS collaboration.

their masses determine the extend to which the model is a successful solution to the hierarchy problem. A complete overview of the limits set by the 8 TeV LHC is beyond the scope of this short introduction, but can be found in [11]. It is however instructive to briefly comment on the limits on the stops and the gluino. In the simplest scenario (with all other superparticles decoupled), the stop now must be heavier than roughly 750 GeV and the gluino heavier than roughly 1300 GeV (see figure 1.7). As always, there is a large amount of caveats associated with these limits, and one can easily construct scenarios in which these limits either strengthen or weaken. However the general take-home point should be that both a light stop and a light gluino with a mass of a few hundred GeV are now firmly excluded, up to a few pathological cases. Although this is certainly somewhat unfortunate from the point of view of naturalness, it is perfectly compatible with the observation of a SM-like Higgs boson with a mass around 126 GeV, as we will discuss in the next section.

1.4 A Higgs Boson at 125 GeV

Now that a Higgs boson has been discovered and its mass measured reasonably well (recall figure 1.1), one can ask the question what implications this measurement has on various models of beyond the standard model physics, in particular supersymmetry. As in the

standard model, the mass of the particle that we associate with the Higgs boson is determined by the product of the vacuum expectation value v and the quartic interaction in its potential:

$$m_h^2 = \lambda v^2 \tag{1.12}$$

In the standard model, the quartic λ is free parameter, and as such the mass of the Higgs boson is a priori not a prediction of the model, aside from an upper bound provided by unitarity. This is in sharp contrast with the MSSM, where the quartic couplings originates the from the equations of motion of the D-terms in the electroweak sector. In more mundane terms, this means that the quartic is fixed by the gauge couplings of the electroweak sector, as can be seen already in equation (1.9). Since the vacuum expectation value is known through our measurements of the masses of the W and Z boson, this results in a prediction for the mass of the lightest CP-even Higgs boson, at least at tree-level:

$$m_h^2 = \cos^2 2\beta \; m_Z^2 \tag{1.13}$$

where $\tan\beta$ is the ratio of the vacuum expectation values of the H_u and H_d fields and m_Z the mass of the Z boson. This implies that the MSSM would have been invalidated at LEP, if it were not for radiative corrections which may increase the mass of the Higgs. At one loop these corrections take the form

$$m_h^2 = \cos^2 2\beta \; m_Z^2 + \frac{3v^2}{4\pi^2}\left(|y_t|^4 \log\frac{M_S^2}{m_t^2} + \frac{A_t^2}{M_S^2}\left(|y_t|^2 - \frac{A_t^2}{12M_S^2}\right)\right) \tag{1.14}$$

with v the total vacuum expectation value of the Higgs fields and m_t is the top mass. $M_S = \sqrt{m_{\tilde{t}_1} m_{\tilde{t}_2}}$. $m_{\tilde{t}_1}$ and $m_{\tilde{t}_2}$ are the masses of the stop mass eigenstates and A_t is an additional supersymmetry breaking Higgs-stop-stop interaction. Specifically, A_t is defined by the operator

$$\mathcal{L} \supset A_t H_u \tilde{Q}_3 \tilde{U}_3 \tag{1.15}$$

in the MSSM Lagrangian, with $\tilde{Q}_3$ and $\tilde{U}_3$ the third generation[5], respectively left and right-handed, superpartners of the quarks, in other words the left and right handed stops.

[5]Note the subtle difference in notation between $\tilde{Q}_3$ and $\tilde{U}_3$ on the one hand and $\tilde{t}_1$ and $\tilde{t}_2$ on the other hand. The former indicates the squark fields in a basis where the gauge interactions are diagonal, while the latter indicates the basis where the mass matrix is diagonal. While this difference is very important when performing accurate calculations, we do not have to pay close attention to it for the qualitative discussion in this introduction.

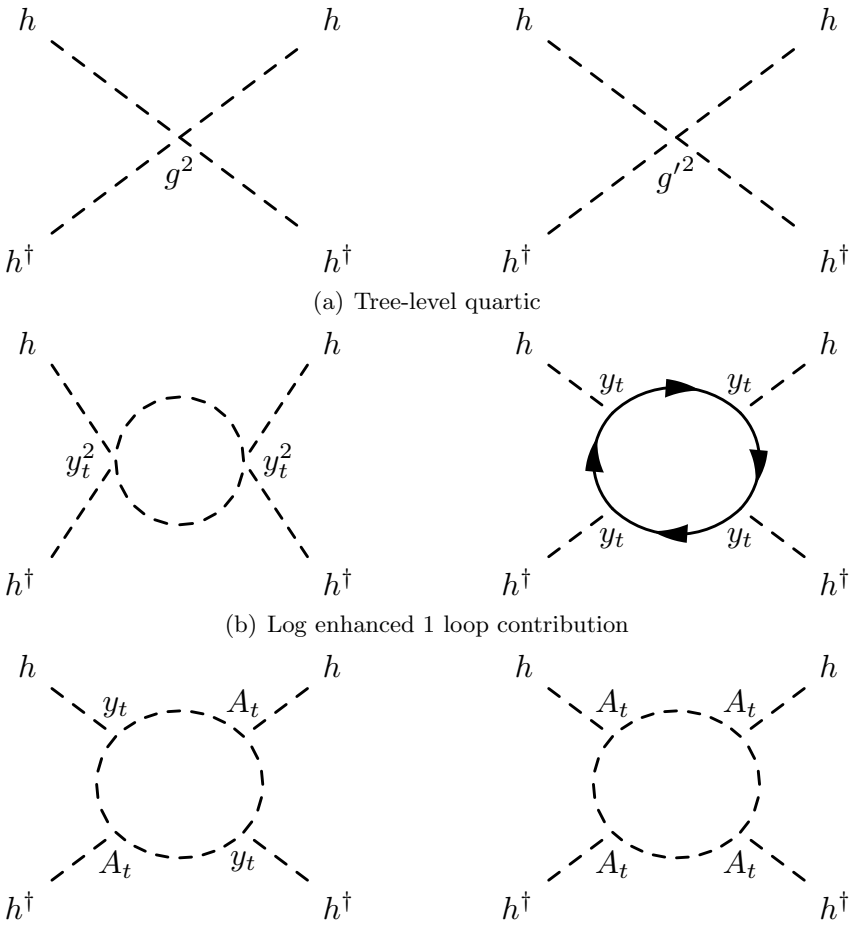

Figure 1.8: Leading diagrams involving (s)tops that contribute to the Higgs quartic in the MSSM.

Note that the interaction term in (1.15) breaks supersymmetry since there is no fermionic analogue for it. For lack of a better name, this type of coupling is usually referred to as an 'A-term'. Similar A-terms may also exist of the other superpartners, however they are irrelevant for the Higgs mass.

Example diagrams for the various contributions in (1.14) are shown in figure 1.8. From (1.14) we see that there are 3 ways by which one could increase the prediction of the Higgs mass to match its measured value.

- Add extra tree-level contributions to the quartic of the type in figure 1.8(a). This necessarily implies adding extra structure to MSSM. The presence of extra fields may boost the tree-level quartic, but necessarily increase the complexity of the model.

Popular incarnations of this mechanism are to extend the MSSM with an extra $U(1)$ gauge symmetry or an extra singlet which comes with a yukawa interaction with Higgs fields. The latter is known as the Next-to-Minimal Supersymmetry Standard model (NMSSM) and will be discussed extensively in chapter 2.

- Staying within the MSSM, one could increase the quartic by relying on the logarithm in the second term in equation (1.14). This corresponds to the contributions from the diagrams in figure 1.8(b). Because of the logarithmic form of this term, this method of increasing the Higgs mass is not very efficient and the stops must be very heavy (between 5 and 10 TeV) to reach the measured value of 125 GeV. In this scenario the stops are unobservable at the LHC.

- Again within the MSSM, the third contribution in (1.14) may be maximized if $\frac{A_t}{M_S} \approx \sqrt{6}$. This corresponds to maximizing the contribution from the diagrams in figure 1.8(c). In this case it suffices to take $M_S \approx 1$ TeV which yields a potentially observable stop signal at the LHC. For historical reasons, this case is known as the 'maximal stop mixing' scenario, since a large A_t may also induce a large left-right mixing in the stop mass eigenstates. Typically it is non-trivial to obtain a large enough A_t from a realistic UV completion of the MSSM.

Although all scenarios are both plausible and interesting, in this thesis I only focus on the large A-term scenario. There are several reasons for this. In contrary to the heavy stop case, it gives us hope of observing stops at the 14 TeV run at the LHC, and in this sense there is a large extend to which this idea is falsifiable in the very short term future. Moreover as we will see, the possible UV completions are very strongly constrained by flavor observables and electroweak symmetry breaking, to the extend that we can hope to systematically map out all the possibilities, something which is much less clear once we deviate from the simplicity of the MSSM.

1.5 Generating A-terms

As I mentioned earlier, the strong constraints on flavor observables naturally push the model builder towards a gauge mediation scenario, as flavor constraints in this case are

automatically and elegantly evaded. Unfortunately, in gauge mediation all A-terms are parametrically small at the typical mass scale of the messenger fields, which I will further refer to as the 'messenger scale'. Specifically, in pure gauge mediation the A-terms at the messenger scale are by far insufficient to realize the desired 'maximal mixing' story where $\frac{A_t}{M_S} \approx \sqrt{6}$. There are however several ways to remediate this problem, each which comes with its own challenges and constraints.

1.5.1 Through RG-running

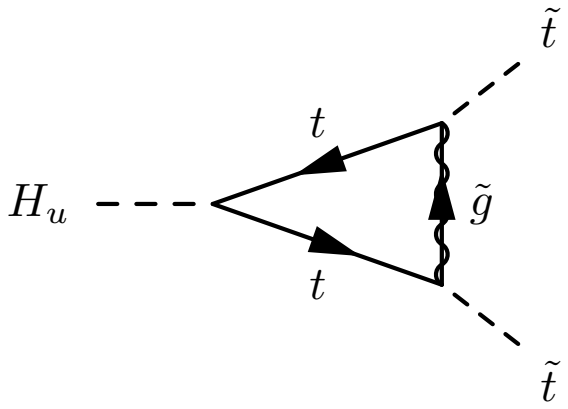

Figure 1.9: Leading diagram that renormalizes the A-term. This diagram may generate a large A-term in the RG running if the gluino mass is sufficiently large.

The most minimal option is to remain within the framework of gauge mediation and to once again rely on radiative corrections to save the day. In particular, the A-terms are sensitive to the gluino in the renormalization group flow between the messenger scale and the weak scale (see figure 1.9). For a sufficiently large messenger scale and/or gluino mass, it is possible to radiatively generate a large weak scale A_t, even if the A-terms start out parametrically small at the messenger scale [16]. This is illustrated by the green lines in figure 1.10. Since we did not deviate from gauge mediation, flavor constraints are not a concern, however this scenario is instead strongly constrained by electroweak symmetry breaking. In particular, the stops receive a positive correction from the gluino as well and even more so than A_t. In order to maintain TeV scale stops at the weak scale, one must arrange the stop masses to start out negative at the messenger scale. While it is certainly possible to build a model dat does this, such negative boundary conditions have

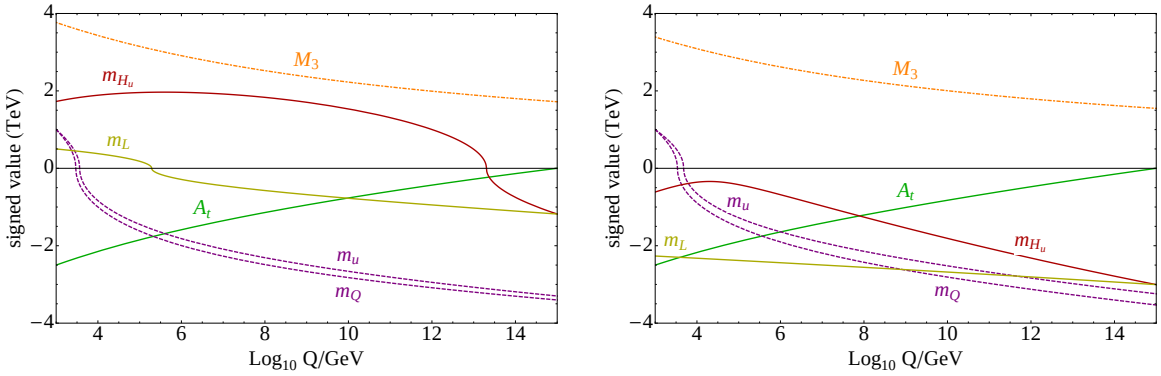

Figure 1.10: Examples of gauge mediation spectra where a large A-term is generated radiatively. If both stops are light at the weak scale, typically electroweak symmetry is restored radiatively (left panel) or the left handed slepton remains tachyonic in the IR (right panel). Both features invalidate the spectrum.

big implications on the rest of the spectrum. Specifically, the negative boundary conditions for the stops (purple lines) induce an upward pull on m_{H_u} (red line), which may jeopardize electroweak symmetry breaking at the weak scale (left panel of figure 1.10). This can be avoided by a negative boundary condition for the Higgs fields at the messenger scale, however in gauge mediation this typically has detrimental consequences to the left handed slepton, as it fails to run positive before hitting the weak scale (right panel of 1.10). The combination of both constraints implies that the 'sweet spot' of the maximal mixing scenario where

$$\frac{A_t}{M_S} \approx \sqrt{6} \quad \text{and} \quad M_S \approx 1 \text{ TeV} \tag{1.16}$$

is firmly ruled out in pure gauge mediation [17].

1.5.2 Through flavored gauge mediation

Since generating A-terms radiatively is rather challenging, one may attempt to generate them through a threshold correction from integrating out the messenger sector, which necessarily requires one to go beyond pure gauge mediation. When doing so, one must proceed with great care. The reason is that in general A-terms are matrices in flavor space, and a large entry for one of the first two generations will typically cause problems with precision flavor tests. The easiest way to guarantee a flavor-safe spectrum is to generate the A-term matrix in the 'minimal flavor violation' ansatz (MFV). Concretely, this implies that actual

A-term is proportional to the standard model yukawa matrix

$$A_{ij} = y_{ij} A_u. \tag{1.17}$$

Because the standard model yukawa couplings for the first two generations are much smaller than the top yukawa, the MFV ansatz naturally suppresses the dangerous entries of the A-term matrix, while keeping the desirable $A_t \equiv A_{33}$ entry large. When working in the MFV ansatz, if is often convenient to deal with the quantity A_u rather than with the real A-term A_t, and I will do so in the later chapters of this thesis. A_u is defined from (1.17), and historically is often called 'A-term' as well. The difference between both is usually clear from the context, and in any case A_t and A_u are equal up to an order one number, which is the top yukawa.

On a qualitative level, the effect of messenger scale threshold corrections is most conveniently seen in the 'effective Kähler potential' formalism, where we have integrated out the fields in the messenger sector. This then yields the following operators

$$X^\dagger H_u^\dagger H_u, \quad X^\dagger Q_i^\dagger Q_j, \quad X^\dagger U_i^\dagger U_j. \tag{1.18}$$

where X is the field responsible for spontaneous supersymmetry breaking, Q_i and U_i are superfields containing the MSSM quark and squark fields, where the indices are flavor indices. For the qualitative discussion in this introduction it suffices to know that the 'superfields' mentioned earlier are just a convenient way to package the standard model fields with their superpartner, in a way that makes supersymmetry manifest. Along the same lines, the 'effective Kähler potential' is nothing more than the supersymmetric version of the effective action. While superfield and Kähler potential techniques are extremely powerful when it comes to concrete computations, we do not need any of this detailed technology in the rest of our discussion in this introduction[6].

The first operator in (1.18) is manifestly MVF, since it carries no flavor indices. The second and third are not MFV and in general a reason for concern. The most straightforward manner to generate this sort of operators is to allow for additional marginal interactions between the messenger fields and the MSSM matter fields. Such interactions can either

[6] A detailed introduction to the subject can be found in for instance [18].

consist out of messenger-messenger-MSSM or messenger-MSSM-MSSM couplings and may or may not be MFV. The MFV case is achieved automatically if the MSSM fields participating in the interaction belong to the Higgs sector only. This case is the main subject of this thesis and is further discussed in the next section. The non-MFV case, sometimes referred to as 'flavored gauge mediation' has been studied in detail elsewhere [19–21]. For each of the operators in (1.18), a generic model will generate a large contribution to the corresponding soft mass operator

$$XX^\dagger H_u^\dagger H_u, \quad XX^\dagger Q_i^\dagger Q_j, \quad XX^\dagger U_i^\dagger U_j. \tag{1.19}$$

As will be discussed in detail in chapter 2, this feature is most detrimental for the first operator, as it may lead to a violation of the consistency condition in (1.10). Even if electroweak symmetry remains possible, this type of contribution tends to severely increase the fine tuning of the model. This is somewhat less of an issue for the operators involving the squarks, however in this case the model builder must provide a detailed explanation for the absence of anomalies in precision flavor experiments.

1.5.3 Through Higgs mediation

As I already mentioned, the first operator in (1.18) is manifestly MFV, and as such it deserves special attention, since it allows us to elegantly bypass various flavor considerations. Concretely, we equip gauge mediation with extra interactions of the form

$$\lambda_u \mathcal{O}_u H_u + \lambda_d \mathcal{O}_d H_d + \lambda_s \mathcal{O}_s H_u H_d \tag{1.20}$$

where the $\mathcal{O}_u$, $\mathcal{O}_d$ and $\mathcal{O}_s$ are operators composed out of fields in the messenger sector. As was mentioned earlier, such interactions are already desirable to facilitate a solution to the μ/B_μ problem [22, 23] and as such they are well motivated regardless the need for large A-terms. The singlet operator $\mathcal{O}_s$ leads to parametrically suppressed A-terms, but the $\mathcal{O}_u$ is capable of generating an A-term of the correct size [23].

Despite its elegance in sidestepping flavor problems, interactions of the form (1.20) are severely constrained by the requirement of electroweak symmetry breaking at the weak scale. In particular, we will show that the first operator in (1.20) will always induce a

contribution to $m^2_{H_u}$, which generically tends to dominated over the soft mass from gauge mediation. In particular there exist a 'A/m_H problem' and a 'little A/m_H problem', where the former is precisely analogous to the better known μ/B_μ problem and can be evaded in certain special cases, as discussed extensively in chapter 2. The little A/m_H problem on the other hand is specific to weakly coupled models and may not invalid the spectrum, but tends to severely enhance the tuning of the model.

This thesis is organized as follows: In chapter 2 we will define the A/m_H problem and a little A/m_H problem precisely and present an example of a fully weakly coupled solution to the former. In chapter 3 we develop a formalism that allows for a very general treatment of models that make use of (1.20). This formalism will then enable us then present a partially strongly coupled set of solutions to both the A/m_H problem and a little A/m_H problem in chapter 4. Chapter 5 contains a brief conclusion and outlook.

Chapter 2

A complete model of low scale Gauge Mediation

With N. Craig, D. Shih and Y. Zhao

Appeared in JHEP 1303 (2013) 154, arXiv:1206.4086

General context of this chapter

As discussed in the introduction, the recent observation of a Higgs boson with mass around 126 GeV motivates the existence of large Higgs-stop-stop couplings (A-terms) in the MSSM. Generating such A-terms presents a special challenge for gauge mediation, which by itself predicts vanishing A-terms at the messenger scale. In this chapter, we extend gauge mediation with messenger-Higgs interactions, which enable us to generate sizable A-terms without introducing problems with precision flavor tests. Realistic models are however non-trivial, and we clearly demonstrate the existence of an 'A/m_H problem' which generically arises in this class of models, and present a mechanism to overcome this problem. Using this mechanism, we construct the first full model of low scale gauge mediation with TeV-scale stops and a Higgs boson with mass of 126 GeV. Specifically we demonstrate that this type of models is compatible with existing solutions to the μ/B_μ-problem. Our models are simple, economical, and complete realizations of supersymmetry at the weak scale, however we show that they nevertheless still suffer from a 'little A/m_H problem', which greatly increases the fine tuning.

2.1 Introduction

The latest results from ATLAS and CMS exclude the Standard Model (SM) Higgs except in the narrow range of $m_h \sim 122-127$ GeV, and show intriguing hints of an excess at $m_h \approx 125$ GeV [24, 25]. A Standard Model-like Higgs in this range renews the urgency of the hierarchy problem, for which supersymmetry (SUSY) remains the best solution available. Numerous

studies have focused on the implications for the MSSM in general (including e.g. [26–29, 16, 30–33]), with the result that $m_h = 125$ GeV in the MSSM translates to a lower bound on a combination of the A-terms and the stop mass. For zero stop mixing, the stops must be heavier than ~ 10 TeV, and for maximal mixing they must be heavier than ~ 1 TeV. In the former case there is little reason to hope for meaningful signs of supersymmetry at the LHC, and the naturalness problem of the MSSM is greatly exacerbated. We will focus on the latter, more conventional scenario in this paper.

Accurately modeling the Higgs sector is especially challenging in low-scale SUSY-breaking scenarios such as gauge mediation (GMSB; for a review and original references, see e.g. [34]). There are two reasons for this. The first is omnipresent and pervasive, but is less directly tied to a Higgs at 125 GeV: the well-known μ - B_μ problem. Gauge mediation does not generate the parameters μ or B_μ at the messenger scale. Extending gauge mediation to include new interactions in the Higgs sector that generate μ tends to produce a B_μ-term that is too large for viable electroweak symmetry breaking (EWSB).

The second reason why the Higgs sector is challenging in gauge mediation is a direct consequence of $m_h = 125$ GeV. This is the failure of gauge mediation to generate A-terms at the messenger scale, in addition to μ and B_μ. The A-terms are instead generated through the renormalization group equations of the MSSM, driven predominantly by the gluino mass. If there is no other source of trilinear soft terms, then in order to generate A-terms of sufficient size to explain the Higgs mass, the messenger scale must be extremely high ($M_{\rm mess} \gtrsim 10^{10}$ GeV), and the gluinos must be extremely heavy ($M_{\rm gluino} \gtrsim 3$ TeV) [16]. Absent additional interactions, this would seem to greatly constrain low-scale supersymmetry breaking.

The purpose of this paper will be to address all of these difficulties in a simple, economical, and calculable setting. To this end, we will construct perturbative spurion-messenger models that generate the A, μ, and B_μ-terms of the right parametric size at the messenger scale. Since vanilla GMSB can generate large A-terms through RG evolution from high messenger scales, in this paper we will focus exclusively on low messenger scales ($M \sim 10^5 - 10^6$ GeV) where the problem of the Higgs mass is most acute. The models presented here are complete and fully calculable effective theories below the messenger scale; generate all the required couplings of the Higgs sector; and are consistent with collider limits and a Higgs

at $m_h = 125$ GeV.

The starting point for our model-building is the introduction of marginal superpotential interactions between the Higgses and messengers.[1] As we will review in the next section, if new Higgs-messenger interactions are introduced, the principal challenge is to generate one-loop A-terms at the messenger scale while not generating too large (one-loop) m_H^2 soft masses. Indeed, just as there is a μ - B_μ problem, there is a completely analogous A - m_H^2 problem. If anything, the A - m_H^2 problem is more serious, because m_H^2 is a singlet under all global symmetries.

Fortunately, the A - m_H^2 problem can be solved by adapting a well-known fact: if the sole source of messenger mass is a single SUSY-breaking spurion X as in minimal gauge mediation (MGM) [42–44], then even in the presence of direct couplings to the messengers, one-loop contributions to scalar mass-squareds vanish to leading order in SUSY-breaking.[2] That is, we may avoid the A - m_H^2 problem provided the superpotential takes the form

$$W = X\, \phi_i \cdot \tilde{\phi}_i + \lambda_{uij} H_u \cdot \phi_i \cdot \tilde{\phi}_j \tag{2.1}$$

with $\langle X \rangle = M + \theta^2 F$ and i, j summed over all the messengers (in irreducible representations of $SU(3) \times SU(2) \times U(1)$) of the theory. Here and below, the dots will be used to denote contraction of gauge indices. In order to avoid generating B_μ at one loop in this model, we must take the analogous coupling for H_d to be zero (or at least extremely small, $\lesssim 10^{-3}$). This can be ensured with an appropriate global symmetry, or by appealing to technical naturalness *a la* the SM Yukawa couplings.

As a mechanism for generating large A-terms, this was first described in a broader context in [41]. Very recently, it was used in [48] to construct models with an eye specifically towards $m_h = 125$ GeV. Here, we will reanalyze these models with one crucial difference: we will take into account a one-loop, negative, F/M^2-suppressed contribution to $m_{H_u}^2$ that was neglected in [48]. Since $F/M \sim 100$ TeV is fixed by the scale of soft masses, this new contribution is important only when the messenger scale is low – within a factor of $\sim$ (a

[1] Alternatives to this would be to consider Higgs-messenger mass mixing [35–39]; interactions between MSSM matter fields and messengers [40, 41, 20, 39]; or perhaps even MSSM matter-messenger mass mixing. Some of these approaches are strongly constrained by precision flavor, for which more intricate model building is required.

[2] This phenomenon was first noticed in the early literature on gauge mediation [22, 40]. An understanding in terms of the symmetries special to MGM can be found in [45–47].

few) $\times$ 100 TeV. In this regime, the one-loop contribution opens a qualitatively new region of parameter space for EWSB that is unavailable at higher scales.

Our models for the MSSM (or those of [48]) may be viewed as a "module" for generating large A-terms in gauge mediation. One can imagine attaching this module to theories involving a successful solution of the μ - B_μ problem without new light degrees of freedom, such as [47, 23, 49]. However, in this paper we explore an alternative and more economical route, one that is all but inexorably suggested by the form of the superpotential (2.1). Namely, if we extend the MSSM to the NMSSM, and couple the NMSSM singlet N to the same MGM messengers, we may simultaneously solve the μ - B_μ problem and the A - m_H^2 problem! Not only that, but in the NMSSM there is also a need for a negative soft mass and large trilinears in the singlet potential in order to achieve viable EWSB and avoid ultra-light pseudoscalars [50].[3] This is a serious problem in conventional GMSB, since the singlet soft mass-squared m_N^2 only arises at three loops and A-terms are again small. To a large extent, this has discouraged the pursuit of NMSSM-like models of GMSB, despite the evident suitability of an additional light singlet for addressing the μ - B_μ problem. Our extended model with Higgs-messenger and singlet-messenger interactions automatically solves this A - m_N^2 problem and reconciles the NMSSM and gauge mediation. Much as before, we find that negative, F/M^2-suppressed one-loop contributions to m_N^2 open a qualitatively new region of parameter space in the NMSSM models when the messenger scale is low.

So our complete model for μ, B_μ and large A_t will be:

$$W = X\,(\phi_i\cdot\tilde{\phi}_i+\varphi_i\cdot\tilde{\varphi}_i)+\lambda_{uij}H_u\cdot(\phi_i\cdot\tilde{\phi}_j+\varphi_i\cdot\tilde{\varphi}_j)+\lambda_N N(\phi_i\cdot\tilde{\varphi}_i)+\lambda N H_u\cdot H_d-\frac{1}{3}\kappa N^3 \quad (2.2)$$

again with $\lambda_d = 0$. This superpotential can be made natural under a $U(1)_X\times\mathbb{Z}_3$ symmetry. The doubling of the messenger sector is necessary so that N can couple to a different messenger bilinear than X in order to avoid generating dangerous tadpoles for N, which are threatening since it is a gauge singlet [41, 46].

The addition of singlet-messenger interactions to an NMSSM model in GMSB has been explored previously in [46], for the purpose of generating μ and B_μ. Here the new ingredient is that we combine it with the A-term module in a natural and efficient way in order to

[3] For related approaches to this problem, see [51, 46, 52, 53]. For a review and references of NMSSM phenomenology, see [54].

generate a suitable mass for the Higgs, together with μ and B_μ. This combination is far from trivial; as we will see, large A-terms place interesting constraints on the NMSSM sector. Indeed, they access a qualitatively different region of parameter space – and lower messenger scales – than were available in [46], and they arguably make it easier to achieve viable EWSB. The interplay of all these issues illustrates the utility in constructing a complete effective theory with the full set of interactions required for viable electroweak symmetry breaking and a sizable Higgs mass.

It bears emphasizing that our philosophy is quite different from the typical approach to the Higgs mass in the NMSSM. Rather than trying to lift the Higgs mass using the NMSSM potential – an endeavor that is largely incompatible with perturbativity in the Higgs sector up to the GUT scale – we instead use the MSSM stop mixing to lift the Higgs mass and only employ the NMSSM to generate μ and B_μ. Indeed, in this scenario it's easier to generate $m_h \approx 125$ GeV if the NMSSM is in the "decoupling limit" of λ, $\kappa \to 0$ with large $\tan\beta$. Otherwise, the NMSSM couplings tend to contribute *negatively* to the Higgs mass. In this sense, the Higgs mass and μ, B_μ have separate origins. Ultimately, however, all the infrared parameters emerge from a common mechanism for generating A, m_H^2, μ, B_μ at the messenger scale via interactions with messenger fields.

The low-energy phenomenology of our models is relatively insensitive to the details of the EWSB sector and the choice of messenger representations. To a large extent it resembles that of MGM, due to the key role played by the MGM-like couplings of the messengers to the hidden sector. Concretely, the stops are the lightest colored scalars, and typically the only colored superpartners below 2 TeV. Additional scalars in the EWSB sector are heavy and the Higgs properties are SM-like. Because we are forced to consider larger effective messenger numbers to improve the $A_t/m_{\tilde{t}}$ ratio, the NLSP is typically the lightest stau. Finally, our exclusive focus on low messenger scales in this paper means that the stau NLSP always decays promptly in the detector. The most fruitful channels for discovery are likely to be those with leptons and missing energy, and these spectra readily satisfy current LHC limits [55].

It is interesting that we are essentially led to minimality in the messenger sector because of the need to solve the A - m_H^2 problem. Since colored superpartners are relatively heavy

in MGM, perhaps this explains why we have yet to observe evidence for supersymmetry at the LHC! Of course, while minimality is appealing from an aesthetic point of view, it is not strictly necessary. The mechanisms we discuss here for generating large A-terms without over-large m_H^2, and μ without over-large B_μ, can in principle be added to any general model of gauge mediation [56], e.g. the model of [57] which covers the GGM parameter space. This greatly expands the possible phenomenology.

The outline of our paper is as follows: In section 2.2 we present the general problems of gauge mediation in light of a Higgs at 125 GeV, focusing on the challenges of generating a μ-term without an over-large B_μ-term, and likewise large A-terms without over-large m_H^2 soft masses. As we discuss in section 2.2, these problems share a common solution, through the use of minimal gauge mediation and (in case of μ - B_μ) the NMSSM. We present specific models in section 2.3. These include a module for generating large A-terms in the MSSM, and a complete theory incorporating μ and B_μ in the NMSSM. Various constraints on the models stemming from EWSB and avoidance of tachyons are discussed in detail in section 2.4, and the spectrum and phenomenology of the models are analyzed in section 2.5. We conclude in section 2.6 with a summary and discussion of future directions. Finally, general formulas for soft masses and a discussion of physics above the messenger scale (i.e. Landau poles) are reserved for appendices 2.A and 2.B, respectively.

2.2 Generalities

2.2.1 The μ-B_μ and A-m_H^2 problems

A successful theory of supersymmetry breaking should give rise to gaugino masses and scalar soft masses of the same order, as well as A-terms and a B_μ-term that are of the same order or smaller. In addition, supersymmetry breaking should ideally provide a natural origin for the μ-term,

$$\mathcal{L} \supset \int d^2\theta \, \mu \, H_u H_d \ . \tag{2.3}$$

Although the μ-term is ostensibly supersymmetric and need not originate from supersymmetry breaking, successful electroweak symmetry breaking requires that the scale of μ coincide with that of the other soft masses in the Higgs sector, i.e., $\mu^2 \sim m_{\text{soft}}^2$. This is the origin

of the so-called "μ problem". A glaring coincidence problem may be avoided only if the μ-term is generated by the same dynamics that breaks supersymmetry.

Gauge mediation gives rise to gaugino masses at one loop and sfermion soft masses-squared at two loops, such that $m_{\tilde{g}} \sim m_{\tilde{f}} \sim m_{\text{soft}}$ as desired. However, gauge interactions alone do not generate all possible soft terms at similar orders. In particular, in the most general gauge mediation model, μ and B_μ are not generated to any order in the gauge couplings, as they are protected by $U(1)_{PQ}$ symmetries which rotate H_u and H_d. Meanwhile the A-terms are not generated to leading order in the gauge couplings [56]. They can be generated at higher orders, through the usual MSSM RGEs, but this means that it is quite challenging to make them large enough, especially for $m_h = 125$ GeV [16]. The failure of gauge interactions to generate appropriate contributions to Higgs sector soft parameters suggests that a viable and complete theory of supersymmetry at the weak scale should include both gauge mediation and additional couplings to the Higgs sector.

This may be arranged in gauge mediation by introducing couplings between the Higgs multiplets and messengers such that, below the scale M of the messengers, the theory contains an effective operator of the form

$$\mathcal{L} \supset \int d^4\theta \, \frac{c_\mu}{M} X^\dagger H_u H_d + \text{h.c.} \tag{2.4}$$

Here we are working in the spurion limit, where the effects of supersymmetry breaking are encoded by the expectation values $\langle X \rangle = M + \theta^2 F$ and the dynamics of X may be neglected; we also assume the messenger sector is weakly coupled. The effective operator (2.4) leads to a μ-term of the right size in weakly-coupled models provided the coefficient c_μ arises at one loop.

However, in most models of gauge mediation, whatever Higgs-messenger interactions give rise to (2.4) likewise generate an effective operator contributing to the B_μ-term of the form

$$\mathcal{L} \supset \int d^4\theta \, \frac{c_{B_\mu}}{M^2} X^\dagger X H_u H_d + \text{h.c.} \tag{2.5}$$

at the same loop order. Consequently, one finds $B_\mu/\mu^2 \propto c_{B_\mu}/c_\mu^2 \sim 16\pi^2/\lambda_\mu^2 \gg 1$, where λ_μ represents some set of perturbative Higgs-messenger couplings that collectively break the PQ symmetry. This "μ - B_μ problem" is a disaster for stable electroweak symmetry

breaking, which generally requires $\mu^2 \sim B_\mu$.[4] Considerable attention has been devoted to possible solutions to this problem.

Interestingly, an analogous problem – which has thus far received much less attention – arises between A-terms and Higgs soft masses $m^2_{H_{u,d}}$. An attractive way to generate sizable A-terms aligned with Standard Model Yukawa couplings is to introduce Higgs-messenger couplings that lead to Kähler terms of the form

$$\mathcal{L} \supset \int d^4\theta \, \frac{c_{A_{u,d}}}{M} X H^\dagger_{u,d} H_{u,d} + \text{h.c.} \tag{2.6}$$

Such terms give rise to A-terms after substituting $F^\dagger_{H_{u,d}} \to -y_u Q \bar{u}$ via the MSSM superpotential, and the F-component vev of X.[5] The resulting A-terms are attractive from the perspective of flavor physics, since they are naturally aligned with Standard Model Yukawa couplings. In order for these A-terms to have a meaningful impact on the gauge-mediated soft spectrum, $c_{A_{u,d}}$ should arise at one loop so that $A \sim m_{\text{soft}}$.

However, in complete analogy with μ - B_μ, whatever interactions generate (2.6) also typically give rise to contributions to Higgs soft masses of the form

$$\mathcal{L} \supset \int d^4\theta \, \frac{c_{m_{u,d}}}{M^2} X^\dagger X H^\dagger_{u,d} H_{u,d} \tag{2.7}$$

at the same loop order. If A-terms are generated at one loop, as is necessary for them to have any impact on the mass of the Higgs, this implies a one-loop contribution to Higgs soft masses that seriously imperils electroweak symmetry breaking. This "A - m_H^2 problem" is especially troublesome because the couplings $c_{m_{u,d}}$ are singlets under all possible global symmetries acting on X and $H_{u,d}$, making it difficult to generalize many conventional approaches to the μ - B_μ problem.

In order to understand the solution to the A - m_H^2 problem, it is useful to reexamine the problem more concretely using the most general perturbative model of messengers coupled to a supersymmetry-breaking spurion [61]:

$$W = \lambda_{ij} X \phi_i \cdot \tilde{\phi}_j + m_{ij} \phi_i \cdot \tilde{\phi}_j \ . \tag{2.8}$$

[4] An exception is if $m^2_{H_d}$ is large and positive, in which case the standard EWSB relations in the MSSM allow for $B_\mu \gg \mu^2$. The idea was first proposed in [58], together with a viable messenger model involving multiple spurions. More details were later worked out in [59, 60].

[5] As we will discuss in more detail later, these terms also contribute to $m^2_{H_{u,d}}$, as well as to B_μ if μ is present in the superpotential.

Here as above, $\langle X \rangle = M + \theta^2 F$. If we want one-loop A-terms, we should couple the messengers directly to the Higgs fields:[6]

$$\delta W = \lambda_{uij} H_u \cdot \phi_i \cdot \tilde{\phi}_j + \lambda_{dij} H_d \cdot \phi_i \cdot \tilde{\phi}_j \ . \tag{2.9}$$

Integrating out the messengers leaves a supersymmetric effective theory for X, H_u and H_d described by the effective Kahler potential

$$K_{eff} = Z_u(X, X^\dagger) H_u^\dagger H_u + Z_d(X, X^\dagger) H_d^\dagger H_d + (Z_\mu(X, X^\dagger) H_u H_d + h.c.) + \dots \tag{2.10}$$

where the ellipses denote terms that are higher order in H_u and H_d, and ϵ is a loop-counting parameter. In addition to being functions of X and $X^\dagger$, the wavefunction factors will also depend on other dimensionful parameters. This includes not only m_{ij} from the superpotential, but also a UV cutoff Λ_0 – in general the wavefunctions are UV divergent quantities.

The terms in (2.10) are responsible for generating μ, B_μ, $m_{H_u}^2$, $m_{H_d}^2$, and A_u, A_d. Specifically, we have, to leading order in F/M^2 and to one-loop order:

$$\begin{aligned} \mu = F\, \partial_X Z_\mu^{(1)} \quad &, \quad B_\mu = |F|^2\, \partial_X \partial_{X^\dagger} Z_\mu^{(1)} \\ A_{u,d} = F\, \partial_X Z_{u,d}^{(1)} \quad &, \quad m_{H_{u,d}}^2 = |F|^2\, \partial_X \partial_{X^\dagger} Z_{u,d}^{(1)} \end{aligned} \tag{2.11}$$

where all the X derivatives are evaluated at $X = M$. If the wavefunctions are completely general functions of X, $X^\dagger$, m_{ij} and Λ_0, typically nothing will cause their mixed second derivatives to disappear, and so nothing prevents B_μ, $m_{H_u}^2$, and $m_{H_d}^2$ from appearing at one loop at leading order in F/M^2. Although one might hope to forbid certain terms from appearing in the wavefunction factors using appropriate global symmetries, the soft terms $m_{H_{u,d}}^2$ are especially dangerous, as they are neutral under all global symmetries.

In summary, we see that if μ is generated at one loop, then B_μ also tends to be generated at one loop; there is nothing in the form of (2.11) that distinguishes the loop counting of the two parameters. Similarly, if $A_{u,d}$ is generated at one loop, then $m_{H_{u,d}}^2$ tends to be generated at one loop. So just as there is a μ - B_μ problem, there is an A - m_H^2 problem.

[6] Note that we could also write down interactions involving singlet messengers S of the form $W \supset S H_u H_d$; we will not consider this option in detail here.

2.2.2 A general mechanism for a solution

As is well known (see especially the discussion in [47]), there is one special case for which the mixed derivatives of the wavefunction factors will vanish: minimal gauge mediation [42–44], for which the only source of mass in the messenger sector is the vev of X. In that case, the superpotential is constrained to take the form $W = \lambda_i X \phi_i \tilde{\phi}_i$. In fact, this model is further special: it is endowed with an R-symmetry under which $R(\phi_i) = R(\tilde{\phi}_i) = 0$ and $R(H_u) = R(H_d) = R(X) = 2$. This R-symmetry is broken only by the lowest-component-vev of X. Then by a combination of dimensional analysis and the R-symmetry, the wavefunction renormalization factors are constrained to take the form

$$Z_{u,d} = f\left(\frac{X^\dagger X}{\Lambda_0^2}\right), \qquad Z_\mu = \left(\frac{X^\dagger}{X}\right) g\left(\frac{X^\dagger X}{\Lambda_0^2}\right) . \tag{2.12}$$

At one loop, we can have at most a logarithmic divergence by power counting. So symmetries and dimensional analysis imply $Z_{u,d}^{(1)} = c_{u,d}\lambda_{u,d}^2 \log X^\dagger X/\Lambda_0^2$, in which case the one-loop contributions to $m_{H_{u,d}}^2$ vanish! Of course, we emphasize that this approach only captures the leading-order effects in F/M^2, so that there may be nonzero one-loop soft masses suppressed by powers of F/M^2 that are not problematically large.

Meanwhile, we see from (2.12) that B_μ does not vanish in general at one loop, and typically must be forbidden by imposing additional symmetries. In fact, if g is a nontrivial function, μ and B_μ can in general be UV sensitive. These problems may be avoided if $\lambda_d = 0$ in (2.9), in which case there is an additional PQ symmetry; the one-loop contribution $Z_\mu^{(1)} \propto \lambda_u \lambda_d$ vanishes and neither μ nor B_μ arise at this order. Since we wish to generate A-terms without exacerbating the μ - B_μ problem, in what follows we will exploit this case and take $\lambda_d = 0$. This choice is technically natural, and may be enforced by a global symmetry distinguishing H_u and H_d.

Although this approach leads to sizable A-terms and solves the A - m_H^2 problem, it does not explain the origin of μ and B_μ. While it is possible to address the problem by supplementing the messenger sector with additional interactions and symmetries, there exists a far more economical route. Namely, if we extend the MSSM by a single light singlet field N, and couple N to the same MGM messengers that H_u couples to, then we can simultaneously generate μ, B_μ and A_t! In this paper, we will focus on the simplest scenario,

namely the $\mathbb{Z}_3$ symmetric NMSSM:

$$W \supset \lambda N H_u \cdot H_d - \frac{1}{3}\kappa N^3 \ . \tag{2.13}$$

As is well known, the main obstacle to marrying the NMSSM and gauge mediation is that a viable vacuum requires a sufficiently large, negative soft mass m_N^2 at the weak scale, as well as sizable trilinear couplings A_λ, A_κ – but pure gauge mediation does not generate any of these quantities at the messenger scale [50]. So by the same logic as before, one is confronted with an A - m_N^2 problem in the NMSSM. But again, the same logic tells us that there is a uniform solution of all of these problems – A - m_N^2, A - m_H^2, and μ - B_μ – via the MGM-messenger mechanism described above!

2.2.3 The little A-m_H^2 problem

Thus far our discussion of viable spectra has focused on the loop order at which various soft parameters arise. While a necessary constraint, it is not sufficient on its own to guarantee successful electroweak symmetry breaking; even if they are all the same size, the Higgs sector soft parameters must satisfy various inequalities in order to ensure a nontrivial vacuum. In particular, the soft masses $m_{H_u}^2$ and $m_{\tilde{t}}^2$ receive large corrections at the messenger scale from the Higgs-messenger coupling λ_u, such that radiative electroweak symmetry breaking may no longer be taken for granted. The contributions to $m_{H_u}^2$ are highly generic and particularly troublesome. As mentioned above, whenever A-terms arise via Kähler operators of the form (2.6), there is an irreducible contribution to $m_{H_{u,d}}^2$ given by $A_{u,d}^2$. These arise from putting the auxiliary fields to their equations of motion, e.g.:

$$-V \supset F_{H_u}^\dagger F_{H_u} + \left(A_u H_u F_{H_u}^\dagger + c.c. \right) \to -A_u^2 H_u^\dagger H_u \tag{2.14}$$

Although this increase in $m_{H_u}^2$ does not necessarily spoil electroweak symmetry breaking, it greatly enhances the degree to which the model is tuned. Thus even when the loop-level A - m_H^2 problem is solved, there is a remnant "little A - m_H^2" problem that is universal in models where the A-terms originate from Kähler operators such as (2.6).

The consequences for EWSB depend on the specific choice of messenger representations and couplings. We will first present general models for the MSSM and the NMSSM, and reserve a detailed discussion of electroweak symmetry breaking for section 2.4.

2.3 Models

2.3.1 Warmup: an MSSM module for large A-terms

Let us now analyze an explicit model with the features discussed above. This model was constructed recently in [48], motivated by $m_h = 125$ GeV. Our analysis in this paper will differ crucially in the treatment of one-loop soft masses. As we will show, these can have profound effects on the model at low messenger scales.

Consider a theory with messengers ϕ_i, $\tilde{\phi}_i$ in vector-like irreps of $SU(3) \times SU(2) \times U(1)$; a SUSY-breaking spurion X with $\langle X \rangle = M + F\theta^2$; and superpotential interactions

$$W = X\, \phi_i \cdot \tilde{\phi}_i + \lambda_u\, H_u \cdot \phi_1 \cdot \tilde{\phi}_2 + y_t\, H_u \cdot Q \cdot U + \mu\, H_u \cdot H_d + \dots \tag{2.15}$$

where the ellipses denote other MSSM interactions that are irrelevant for our purposes. Here we are making a number of simplifying assumptions: first, we are assuming that there is only one combination of the messengers, $\phi_1 \cdot \tilde{\phi}_2$, that can be combined with H_u to make a gauge singlet. The generalization to multiple such couplings is straightforward. Second, at this stage we are interested in generating A-terms at one loop, rather than explaining the origin of μ and B_μ, and so we will allow for arbitrary μ and B_μ.[7] In the next subsection, we will extend the model to also generate these parameters. Finally, we are only including the top Yukawa explicitly in (2.15), because its large size means that it will play a role in the later analysis.[8]

The interactions (2.15) comprise the most general renormalizable superpotential consistent with the SM gauge symmetry, together with messenger number (to forbid messenger-matter mixing), and a global $U(1)_X$ symmetry under which the fields carry the following charges:

$$q_X(X, \phi_i, \tilde{\phi}_i, H_u, H_d) = (1, -1/2, -1/2, 1, -1)\ . \tag{2.16}$$

(Charges of MSSM matter fields can always be chosen such that the usual Yukawa terms are allowed.) Messenger number forbids mixing with matter multiplets and renders the lightest messenger stable, though this may be readily broken by higher-dimensional operators [62].

[7] As noted earlier, the Higgs-messenger interactions contribute to B_μ given a supersymmetric μ-term, but we allow arbitrary additional contributions to satisfy EWSB.

[8] The bottom and tau yukawas are unimportant even at large $\tan\beta$ because our Higgs-messenger couplings only involve H_u.

We may readily extend this model to include N_{mess} flavors of messengers, so in general we consider messengers ϕ_{if}, $\tilde{\phi}_{if}$ with $f = 1, \ldots N_{mess}$. To avoid a proliferation of couplings, we will impose a $U(N_{mess})$ flavor symmetry.

The superpotential interactions (2.15) give rise to both conventional gauge-mediated soft masses and new contributions to $m_{H_u}^2$, m_Q^2, m_U^2, and A_t due to the direct Higgs-messenger interaction. The latter are given by:

$$\delta m_{H_u}^2 = -d_H \frac{\alpha_{\lambda_u}}{12\pi} h(\Lambda/M) \left(\frac{\Lambda}{M}\right)^2 \Lambda^2 + \left(d_H(d_H+3)\frac{\alpha_{\lambda_u}^2}{16\pi^2} - d_H C_r \frac{\alpha_r \alpha_{\lambda_u}}{8\pi^2} \right) \Lambda^2 \tag{2.17}$$

$$\delta m_Q^2 = -d_H \frac{\alpha_t \alpha_{\lambda_u}}{16\pi^2} \Lambda^2 \tag{2.18}$$

$$\delta m_U^2 = -d_H \frac{\alpha_t \alpha_{\lambda_u}}{8\pi^2} \Lambda^2 \tag{2.19}$$

$$A_t = -d_H \frac{\alpha_{\lambda_u}}{4\pi} \Lambda \tag{2.20}$$

Here we have introduced

$$\Lambda \equiv F/M \tag{2.21}$$

Also, d_H counts the total number of fields coupled to H through λ_u; and $C_r = c_r^{H_u} + c_r^{\phi_1} + c_r^{\tilde{\phi}_2}$ is the sum of quadratic Casimirs of the fields which participate in the Higgs-messenger-messenger Yukawa coupling. (Concrete examples of d_H and C_r will be given in section 2.3.3.) The little A - m_H^2 problem is manifest in the second term of (2.17), specifically in the contribution proportional to d_H^2.

The first term in $\delta m_{H_u}^2$ is the Λ/M-suppressed one-loop contribution to $m_{H_u}^2$ which cannot be eliminated by the MGM mechanism described in the previous section. The function $h(x)$ is given by:

$$h(x) = \frac{3\Big((x-2)\log(1-x) - (x+2)\log(1+x)\Big)}{x^4} = 1 + \frac{4x^2}{5} + \ldots \tag{2.22}$$

and is such that the one-loop contribution to $m_{H_u}^2$ is always strictly negative. This effect was neglected in [48], and it will be crucial for the discussion in section 2.4.1, when we analyze the viability of these models from the perspective of EWSB. There are, of course, additional Λ/M-suppressed contributions to all the other soft masses [62, 63], but these are always subdominant. The Λ/M-suppressed contribution to $m_{H_u}^2$ (and only $m_{H_u}^2$) is parametrically important because it first arises at one loop.

Once the number and type of messenger representations are specified, the dimensionless parameter space of the MSSM module for large A-terms consists solely of $(\Lambda/M, \lambda_u)$. In addition, there is one dimensionful parameter Λ that sets the overall scale of the soft masses. Since we are interested in a particular Higgs mass, $m_h = 125$ GeV, this completely fixes Λ, given a choice of $(\Lambda/M, \lambda_u)$. We will explore this parameter space in detail in sections 2.4 and 2.5.

We emphasize that the addition of these Higgs-messenger interactions to the MSSM is essentially modular. It leaves unaltered (and unaddressed) whatever physics generates μ and B_μ, and may be incorporated into a variety of solutions to the μ - B_μ problem. In general, new interactions that generate μ and B_μ also contribute to $m^2_{H_u}$, often at two loops. The sign of these contributions to $m^2_{H_u}$ depend on the details of the model, and may either increase or decrease the value of $m^2_{H_u}$ at the messenger scale. Scenarios in which the new contributions are negative [23, 49] will improve the prospects for (radiative) electroweak symmetry breaking.

2.3.2 The complete NMSSM model for A, μ, and B_μ

While the coupling of messengers to H_u in the MSSM provides an avenue for generating A-terms at one loop, it does not explain the origin of μ and B_μ. Indeed, had we allowed analogous couplings to H_d, we would have generated both a μ-term and a B_μ-term at one loop, which would have been disastrous for EWSB. This suggests another source is required for the μ and B_μ-terms. A natural possibility is the addition of a gauge singlet superfield N, which may be coupled to messengers much like H_u [41, 46].

As discussed in the previous section, the addition of a light gauge singlet superfield raises the usual challenges of generating suitable A-terms and m^2_N in the singlet sector. This is again solved by the same MGM mechanism.[9] However, the new challenge is that N, being a gauge singlet, can potentially mix with X, leading to dangerous tadpole terms for N [41, 46]. To forbid these, it suffices to extend the $U(1)_X$ symmetry of (2.16) to include

[9] The same approach was also used recently in [64]. However the EWSB mechanism in this paper is different from ours, as they require the "lopsided" hierarchy $\mu^2 \sim m^2_{H_u} \ll B_\mu \ll m^2_{H_d}$ [58–60].

N so that[10]

$$q_X(N) = 0 \ . \tag{2.23}$$

By itself though, this would forbid any coupling between N and the messengers. So we will follow the approach of [41, 46] and double the messenger sector, $\phi_i \to \phi_i$, φ_i, using the freedom to assign different $U(1)_X$ charges to ϕ_i and φ_i. For instance, we can take the following charge assignment:

$$q_X(X, \phi, \tilde{\phi}, \varphi, \tilde{\varphi}, H_u, H_d, N) = (1, 0, -1, -1, 0, 1, -1, 0) \ . \tag{2.24}$$

With this $U(1)_X$ symmetry, we can have a viable model with the superpotential

$$W = X(\phi_i \cdot \tilde{\phi}_i + \varphi_i \cdot \tilde{\varphi}_i) + \lambda_u H_u \cdot (\phi_1 \cdot \tilde{\phi}_2 + \varphi_1 \cdot \tilde{\varphi}_2) + \lambda_N N \phi_i \cdot \tilde{\varphi}_i + \lambda N H_u \cdot H_d + \dots \tag{2.25}$$

where the ellipses again denote other MSSM interactions that are irrelevant for our purposes.

At this point N is a total singlet and so its interactions can be fully general, for instance those discussed in [54]. Of course, a total singlet with arbitrary interactions is disastrous for many reasons, including the possible reintroduction of UV divergences; typically some set of symmetries must be imposed to ensure that the theory is well-behaved. In this paper, we will for simplicity focus on the usual $\mathbb{Z}_3$-symmetric NMSSM. Because of the N-messenger-messenger couplings, this $\mathbb{Z}_3$ must be extended to act on the messengers as well. A consistent charge assignment is:

$$\mathbb{Z}_3(X, \phi_i, \tilde{\phi}_i, \varphi_i, \tilde{\varphi}_i, H_u, H_d, N) = (0, 1, 2, 2, 1, 0, 2, 1) \ . \tag{2.26}$$

Then the most general superpotential consistent with our choice of $U(1)_X \times \mathbb{Z}_3$ symmetry is:

$$W = X(\phi_i \cdot \tilde{\phi}_i + \varphi_i \cdot \tilde{\varphi}_i) + \lambda_u H_u \cdot (\phi_1 \cdot \tilde{\phi}_2 + \varphi_1 \cdot \tilde{\varphi}_2) + \lambda_N N \phi_i \cdot \tilde{\varphi}_i + \lambda N H_u \cdot H_d - \frac{1}{3}\kappa N^3 + y_t H_u \cdot Q \cdot U + \dots \tag{2.27}$$

This is our complete model of supersymmetry at the messenger scale, which will give rise to all the superpartner masses, large A_t, μ, and B_μ after the messengers are integrated out.

[10] Note that in [41, 46], a $\mathbb{Z}_3$ symmetry was invoked for this purpose. However, their $\mathbb{Z}_3$ symmetry is neither sufficient nor necessary for obtaining a viable model. In particular, it does not forbid direct EOGM [61] mass terms for the messengers.

Note that the model without the H_u-messenger interaction was studied in [46]. We will see that adding this interaction and requiring large A_t for $m_h = 125$ GeV qualitatively changes the model and actually improves its viability.

The contributions to the soft masses from the NMSSM couplings are given by (these should be added to the standard gauge mediation terms and those in (2.17)-(2.20)) :

$$\delta m_{H_u}^2 = \left(d_H \frac{\alpha_{\lambda_N}\alpha_{\lambda_u}}{16\pi^2} - d_N \frac{\alpha_\lambda \alpha_{\lambda_N}}{16\pi^2} \right) \Lambda^2 \tag{2.28}$$

$$\delta m_{H_d}^2 = \left(- d_H \frac{\alpha_\lambda \alpha_{\lambda_u}}{16\pi^2} - d_N \frac{\alpha_\lambda \alpha_{\lambda_N}}{16\pi^2} \right) \Lambda^2 \tag{2.29}$$

$$\begin{aligned} m_N^2 = -d_N \frac{\alpha_{\lambda_N}}{12\pi} h(\Lambda/M) \left(\frac{\Lambda}{M}\right)^2 \Lambda^2 + \Bigg(& d_N(d_N+2)\frac{\alpha_{\lambda_N}^2}{16\pi^2} - d_N \frac{\alpha_{\lambda_N}\alpha_\kappa}{4\pi^2} \\ & - d_H \frac{\alpha_\lambda \alpha_{\lambda_u}}{8\pi^2} - d_N^{ii} c_r^i \frac{\alpha_{\lambda_N}\alpha_r}{4\pi^2} + \left(d_N^{11} d_1^{H2} + d_N^{22} d_2^{H1} \right) \frac{\alpha_{\lambda_u}\alpha_{\lambda_N}}{16\pi^2} \Bigg) \Lambda^2 \end{aligned} \tag{2.30}$$

$$\delta m_Q^2 = \delta m_U^2 = \delta A_t = 0 \tag{2.31}$$

$$A_\lambda = - \left(d_H \frac{\alpha_{\lambda_u}}{4\pi} + d_N \frac{\alpha_{\lambda_N}}{4\pi} \right) \Lambda \tag{2.32}$$

$$A_\kappa = -3 d_N \frac{\alpha_{\lambda_N}}{4\pi} \Lambda \tag{2.33}$$

where again, $\Lambda \equiv F/M$; d_H is as above; and d_N similarly counts the total number of fields coupling to N via λ_N. We also have d_N^{ii} counting the number of fields of type ϕ_i (or φ_i) coupling to N (and so $d_N = \sum_i d_N^{ii}$). The numbers d_1^{H2} and d_2^{H1} count the number of fields coupling to ϕ_1 and ϕ_2 respectively through the λ_u Yukawa coupling. Finally, c_r^i is the quadratic casimir of ϕ_i in the rth gauge group. Concrete examples of all of these parameters are given in section 2.3.3.

The full NMSSM model introduces three new parameters $(\lambda, \kappa, \lambda_N)$ relative to the MSSM module; as we will discuss in detail in section 2.4.2, EWSB fixes two of the extra parameters (say κ and λ_N) in terms of the third (λ) and the other Higgs sector parameters. So for fixed messenger content, the full parameter space of the theory is Λ, M, and λ_u (the MSSM parameters), plus λ. Restricting our attention to $m_h = 125$ GeV, the full parameter space may be specified by $\Lambda/M, \lambda_u$, and λ. As with the MSSM, it is no longer obvious that EWSB is viable due to new contributions to the Higgs soft mass; we reserve a detailed study for section 2.4.

2.3.3 Examples

Here we will illustrate the use of the general formulas above with two specific examples for messenger representations. These examples effectively exhaust the possibilities for low-scale GMSB consistent with genuine perturbative gauge coupling unification. The only additional possibility which we are not considering here is a **24** of $SU(5)$, as it is incompatible with the messenger doubling needed for the complete NMSSM model.

- The first example is where the messengers fill out $\mathbf{5} \oplus \overline{\mathbf{5}}$ representations of $SU(5)$ (plus the necessary gauge singlets to form the H_u Yukawa coupling). In more detail, we take the $SU(3) \times SU(2) \times U(1)$ representations of the fields in (2.15) and (2.27) to be

$$(\phi_1, \phi_2, \phi_3) = ((\mathbf{1}, \mathbf{1}, 0), (\mathbf{1}, \mathbf{2}, 1/2), (\mathbf{3}, \mathbf{1}, -1/3)) \tag{2.34}$$

  Note that the first field is a pure gauge singlet, and the third is purely a spectator in the MSSM case from the perspective of generating A-terms, serving only to complete the GUT multiplet and communicate SUSY breaking to colored fields via gauge interactions.

  In this model, the quantities needed to fully specify the MSSM and NMSSM soft masses are given by

$$\begin{aligned} &d_H = N_{mess}, \quad d_1^{H2} = 2, \quad d_2^{H1} = 1 \\ &d_N = 3N_{mess}, \quad d_N^{11} = \frac{1}{2}N_{mess}, \quad d_N^{22} = N_{mess}, \quad d_N^{33} = \frac{3}{2}N_{mess} \\ &c_r^1 = (0,0,0), \quad c_r^2 = (0, 3/4, 3/20), \quad c_r^3 = (4/3, 0, 1/15) \end{aligned} \tag{2.35}$$

  Note that for NMSSM models, N_{mess} must be even due to the doubling of the messenger sector.

- Our second example is where the messengers fill out a $\mathbf{10} \oplus \overline{\mathbf{10}}$ of $SU(5)$. So here we also have three messengers (up to an overall multiplicity N_{mess})

$$(\phi_1, \phi_2, \phi_3) = ((\mathbf{3}, \mathbf{1}, 2/3),\ (\mathbf{3}, \mathbf{2}, 1/6),\ (\mathbf{1}, \mathbf{1}, 1)) \tag{2.36}$$

  Note that ϕ is actually *not* a **10** of $SU(5)$. Rather, ϕ plus the conjugate $\tilde{\phi}$ fill out a $\mathbf{10} \oplus \overline{\mathbf{10}}$ of $SU(5)$; this choice is merely a notational convenience that makes manifest

the global symmetries of the theory. The key difference relative to the $\mathbf{5}+\overline{\mathbf{5}}$ case is that the messengers coupling to the Higgs are now charged under $SU(3)$. As was shown in [48], this has interesting consequences for the viable parameter space of the theory due to negative contributions to $m_{H_u}^2$ proportional to $\sim \alpha_3\alpha_{\lambda_u}$ in (2.17).

In this model, for N_{mess} pairs of $\mathbf{10}\oplus\overline{\mathbf{10}}$ messengers, the necessary coefficients for soft parameters are given by

$$\begin{aligned} &d_H = 3N_{mess}, \quad d_1^{H2} = 2, \quad d_2^{H1} = 1 \\ &d_N = 5N_{mess}, \quad d_N^{11} = \frac{3}{2}N_{mess}, \quad d_N^{22} = 3N_{mess}, \quad d_N^{33} = \frac{1}{2}N_{mess} \\ &c_r^1 = (4/3, 0, 4/15), \quad c_r^2 = (4/3, 3/4, 1/60), \quad c_r^3 = (0, 0, 3/5) \end{aligned} \tag{2.37}$$

Again, for NMSSM models, N_{mess} must be even.

2.4 EWSB and Other Constraints

It is clear thus far that introducing additional interactions to generate sizable A-terms has repercussions for the rest of the theory via new contributions to various soft masses. These new contributions are typically quite large (since A-terms are large) and may significantly alter the vacuum structure of the theory relative to MGM. Requiring a viable vacuum in which electroweak symmetry is broken but various other Standard Model symmetries are preserved leads to nontrivial constraints on the space of UV parameters. In particular, the challenges of guaranteeing EWSB while avoiding charge- and color-breaking minima are more acute than in MGM and favor particular values of scales and couplings in the effective theory. In this section we will discuss the qualitative challenges imposed by a viable vacuum and study several benchmark points that exemplify the effects on parameter space. These effects will be further manifest in section 2.5, where we perform a comprehensive numerical study on the viable parameter space for explicit models.

2.4.1 EWSB in the MSSM with large A-terms

In the MSSM, minimizing the Higgs potential leads to the relations

$$\mu^2 = \frac{m_{H_d}^2 - m_{H_u}^2 t_\beta^2}{t_\beta^2 - 1} - \frac{1}{2} m_Z^2 \tag{2.38}$$

$$s_{2\beta} = \frac{2B_\mu}{m_{H_d}^2 + m_{H_u}^2 + 2\mu^2} \tag{2.39}$$

between soft parameters and the observables m_Z and $\tan\beta$ at the scale of EWSB. (Here we write $\tan\beta$ and $\sin 2\beta$ as t_β and $s_{2\beta}$ for short. In all the numerical calculations that follow, we will use $\tan\beta = 10$.) These conditions are satisfied at the minimum of the potential, but alone are not sufficient to guarantee a viable vacuum. Rather, the soft parameters must also satisfy the inequalities

$$B_\mu < |\mu|^2 + \frac{1}{2}(m_{H_u}^2 + m_{H_d}^2) \tag{2.40}$$

$$B_\mu^2 > (|\mu|^2 + m_{H_u}^2)(|\mu|^2 + m_{H_d}^2) \tag{2.41}$$

which correspond to the requirements that the quadratic part of the scalar potential is positive along D-flat directions and that the origin is not a stable minimum (in which case the vacuum could preserve electroweak symmetry), respectively.

These conditions are most readily satisfied if $m_{H_u}^2$ is negative at the weak scale. Indeed, renormalization group evolution of soft parameters down to the weak scale typically ensures that this is the case. The most salient feature of the RG evolution of $m_{H_u}^2$ is the negative contribution coming from the large top quark Yukawa, proportional to the third generation soft masses $m_{Q_3}^2, m_{u_3}^2$ and the top A-term. With high messenger scales, the large logarithm is usually sufficient to guarantee that these contributions drive $m_{H_u}^2$ negative. With low messenger scales, as we are focusing on in this paper, the logarithm is not large, so $m_{H_u}^2$ must be negative for other reasons. In GMSB, the soft masses of colored scalars are substantially larger than the messenger-scale soft mass for H_u due to the size of the QCD gauge coupling and the $SU(3)$ Casimir; this suffices to drive $m_{H_u}^2$ negative in only a few decades of running. So even though $m_{H_u}^2$ is positive at the messenger scale, radiative effects drive it negative before the weak scale. Thus radiative electroweak symmetry breaking is a robust prediction of minimal GMSB.

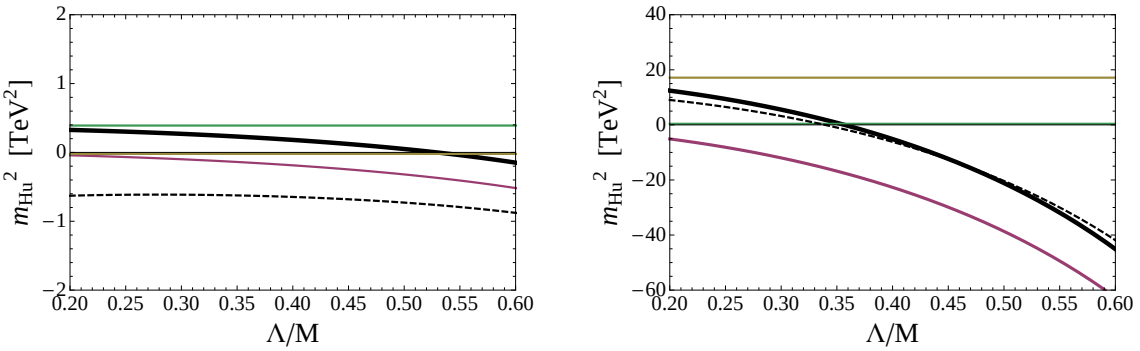

Figure 2.1: Plot of $m^2_{H_u}$ vs Λ/M, for $\Lambda = 110$ TeV, $N_{mess} = 4$, and $\lambda_u = 0.1$ (left panel) and $\lambda_u = 1.1$ (right panel). The total value of $m^2_{H_u}$ in the MSSM at the messenger scale (see (2.15)) is shown in black. The green, red and yellow lines indicate the usual GMSB contribution, the one-loop contribution from λ_u, and the two- loop contribution from λ_u, respectively. Finally, the dashed black line represents the value of $m^2_{H_u}$ RG evolved down to M_{SUSY}. EWSB at large $\tan\beta$ requires $m^2_{H_u} < 0$ at the weak scale. We see that for large λ_u, EWSB is achieved for sufficiently large Λ/M due to the negative 1-loop contribution. For small values of λ_u EWSB is achieved radiatively, as in MGM.

In *any* model (not just GMSB) with sizable contributions to Higgs A-terms at the messenger scale, the success of radiative EWSB is greatly endangered. Even if the A - m^2_H problem is solved at one loop, it is in general impossible to suppress the two-loop contributions to $m^2_{H_u}$. Since generating $m_h \sim 125$ GeV requires A-terms at least as large as the stop masses, and since the A-terms and $m^2_{H_u}$ have a common origin, it is generally the case that $m^2_{H_u} \sim m^2_{stop}$. But then RG contributions from third generation soft masses are no longer sufficient to drive $m^2_{H_u}$ negative when running from a low scale. While A-terms also act to drive $m^2_{H_u}$ negative, they are not parametrically larger than $m^2_{H_u}$ itself. So the success of radiative EWSB now depends sensitively on the messenger scale. All of these features are illustrated concretely in (2.17)-(2.20), but the problem of EWSB is highly generic.

However, all is not lost. In the context of our models, we identify two possibilities for rescuing EWSB:

- If the messenger scale is low ($M \lesssim 10^6$ GeV), then the negative, Λ/M-suppressed one-loop contribution to $m^2_{H_u}$ in (2.17) may be competitive with the unsuppressed two-loop contribution. Partial or complete cancellation between the two terms of different loop order may diminish the value of $m^2_{H_u}$ at the messenger scale or render it

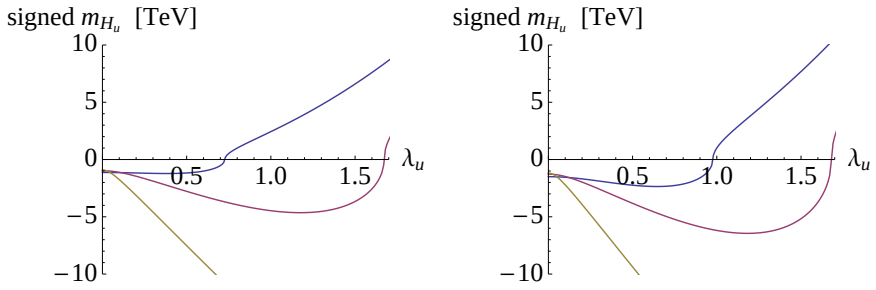

Figure 2.2: Plot of the weak-scale signed mass $m_{H_u}^2/\sqrt{|m_{H_u}^2|}$ vs λ_u, for the $\mathbf{5} \oplus \overline{\mathbf{5}}$ model with $N_{mess} = 4$ (left) and the $\mathbf{10} \oplus \overline{\mathbf{10}}$ model with $N_{mess} = 2$ (right). In both plots, $\Lambda = 110$ TeV. The blue, red and yellow curves correspond to $\Lambda/M = 0.1$, 0.5 and 0.9 respectively. As we will see, $m_h \sim 125$ GeV requires $\lambda_u \sim 1$ for reasonable stop masses. We see that in the $\mathbf{5} \oplus \overline{\mathbf{5}}$ model, $m_{H_u}^2$ becomes positive well below $\lambda_u \sim 1$ for $\Lambda/M = 0.1$, but not for $\Lambda/M = 0.5$ or 0.9. But in the $\mathbf{10} \oplus \overline{\mathbf{10}}$ model, even $\Lambda/M = 0.1$ is possible, because $m_{H_u}^2$ is receiving an additional negative contribution from the colored messengers.

negative. The effect is illustrated in figure 2.1. The 1-loop contribution was neglected in [48], but we will see that it significantly influences theories with low messenger scales; it will also play an additional key role when we turn to the NMSSM.

- Alternatively, there can be a significant reduction of the two-loop contribution itself, if the gauge contribution in (2.17) is large enough to partially or wholly cancel the Yukawa contribution [48]. Since obtaining the physical Higgs mass through stop mixing requires $\lambda_u \gtrsim g_3$, among the Standard Model gauge couplings only g_3 is large enough to result in meaningful cancellation.[11] Thus if any of the messengers ϕ_1, $\tilde{\phi}_1$, ϕ_2, $\tilde{\phi}_2$ are charged under $SU(3)_C$, the two-loop contributions to $m_{H_u}^2$ may largely cancel among themselves for arbitrary messenger scale. Note that this is impossible to arrange when the messengers transform as complete $\mathbf{5} + \overline{\mathbf{5}}$ multiplets, but may occur if they transform as higher-rank representations such as $\mathbf{10} + \overline{\mathbf{10}}$. In this case, $m_{H_u}^2$ is still typically positive at the messenger scale, but is small enough to be driven negative by radiative effects before the weak scale. This effect is illustrated in fig. 2.2.

[11] Also considered in [48] is the possibility that the messengers are charged under a strong hidden sector gauge group.

2.4.2 EWSB in the NMSSM

The discussion of EWSB must be expanded somewhat for the NMSSM due to the additional singlet degree of freedom in the Higgs sector; the introduction of a light singlet changes the vacuum structure of the potential and introduces a number of new parameters into the conditions for electroweak symmetry breaking. Fortunately, it is possible to develop a parametric understanding of the NMSSM vacuum in certain simplifying limits, and that will suffice for our purposes. We will find that the upshot remains largely the same as in the previous subsection – for successful EWSB, we will need large negative m_N^2 at the weak scale, and there is a window of low messenger scales in which the negative, one-loop, Λ/M suppressed contribution to m_N^2 ensures this. In what follows, our discussion will often mirror that of [46], who considered this model without the large A-terms, and without the one-loop correction to m_N^2. We will see that these have vital effects and qualitatively change the behavior of the model.

Upon introducing a singlet, the minimization conditions for the tree-level potential are extended to three equations: (2.38)-(2.39), together with[12]

$$2\frac{\kappa^2}{\lambda^2}\mu^2 - \frac{\kappa}{\lambda}A_\kappa\mu + m_N^2 \;=\; \lambda^2 v^2\left[-1 + \frac{1}{2}s_{2\beta}\left(\frac{B_\mu}{\mu^2} + \frac{\kappa}{\lambda}\right) + \frac{1}{4}s_{2\beta}^2\frac{\lambda^2 v^2}{\mu^2}\right] \ . \qquad (2.42)$$

These equations determine $\mu = \lambda\langle N\rangle$, and B_μ is given by:

$$B_\mu = \frac{\kappa}{\lambda}\mu^2 - A_\lambda\mu - \frac{1}{2}s_{2\beta}\lambda^2 v^2 \ . \qquad (2.43)$$

In general, the solutions to (2.38)–(2.39) and (2.42) are complicated functions of the parameters and couplings. However, things simplify considerably in the case of interest: $v^2 \ll m_{soft}^2$; large $\tan\beta$ (to maximize the tree-level MSSM contributions to the Higgs mass); and $\lambda \ll 1$ (since we are not trying to lift the Higgs mass using the NMSSM quartic). This is a decoupling limit in which the singlet serves largely to fix μ and B_μ and does not mix significantly with the Higgs doublets. Consequently, the constraints on soft parameters imposed by EWSB in the MSSM are largely unchanged, but are supplemented

[12] Of course, these are merely the tree-level equations, which should be dressed with radiative corrections in the full solution. In what follows, we use `NMSSMTools` [65, 66] where necessary to capture the full effects of radiative corrections, but find that the tree-level equations are adequate to understand the parametric behavior of the vacuum.

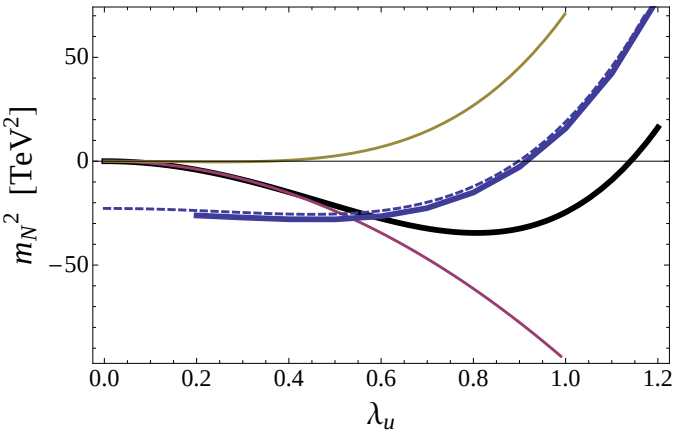

Figure 2.3: Plot of m_N^2 vs. λ_N, for $\Lambda = 110$ TeV, $M = 220$ TeV, $\lambda_u = 1.1$, $N_{mess} = 4$, and κ and λ negligibly small. (At this point, the stops are about 2 TeV and $m_h = 125$ GeV.) The total value of m_N^2 at the messenger scale (2.30) is shown in black; the red and yellow are the one and two loop contributions, respectively. Blue is the required value from EWSB. The dashed curve is given by the tree-level expression from (2.46) at the weak scale, and the solid curve is extracted from `NMSSMTools` at messenger scale. Clearly, both the RG and the weak-scale radiative corrections have negligible effects on m_N^2. The successful EWSB solution lies at where the blue and black curves intersect. We see from this that the one-loop negative contribution to m_N^2 dominates and leads to a successful EWSB solution.

by additional constraints on the singlet sector. In this regime, we find (provided $m_{H_d}^2 + \mu^2$ is not exceptionally large) the approximate relations

$$\mu^2 \approx -m_{H_u}^2 \tag{2.44}$$

$$B_\mu \approx \mu \left(\frac{\kappa}{\lambda}\mu - A_\lambda\right) \approx 0 \tag{2.45}$$

$$m_N^2 \approx A_\lambda(A_\kappa - 2A_\lambda) \tag{2.46}$$

The third equation in particular is a parametrically interesting requirement: although m_N^2 may arise predominantly from either one-loop or two-loop contributions, depending on Λ/M, successful EWSB requires it be the same size as a two-loop contribution. But note that large A_t automatically implies large A_λ according to (2.32), so m_N^2 at the weak scale must in general be quite large and negative for viable EWSB. The only possible exception is if there is some cancellation between A_κ and A_λ, in which case m_N^2 may be smaller and take either sign.

What effects lead to large negative m_N^2 at the weak scale? Since we are focusing on low messenger scales and $\lambda \ll 1$, RG running is generally not sufficient. Instead, we are

led to consider precisely the same mechanism as in the MSSM – with moderate Λ/M, the negative, one-loop, Λ/M-suppressed contribution to m_N^2 in (2.30) cannot be neglected, and can lead to a successful solution to the vacuum conditions. Note that the solution will generally prefer moderate λ_N – if λ_N is too small, then m_N^2 is too small and cannot satisfy (2.46), while if λ_N is too large, the (positive) two-loop term will dominate. The interplay of one- and two-loop contributions to m_N^2 and the requirements for a viable vacuum are illustrated in fig. 2.3 for a particular point in parameter space.

As discussed in section 2.3.2, we can view the NMSSM model as adding three more parameters, $(\lambda, \kappa, \lambda_N)$, to the MSSM module. The requirements for EWSB (2.44)-(2.46) can be used to determine two of these parameters, say (κ, λ_N), in terms of the third (λ) and the other Higgs sector parameters. (In addition, the EWSB equations determine μ.) The nature of this solution is illustrated in fig. 2.4 for one point in parameter space, exemplifying our discussion of the parametric behavior of soft parameters required for EWSB. The red curve can be inferred to good accuracy by solving the approximate tree-level equations (2.44)-(2.46) for κ as a function of λ_N. The black curve meanwhile is flat as a function of κ because when κ is small it has essentially no effect on the dynamics of the model. In general, for fixed $\Lambda, M, \lambda_u, \lambda$, and N_{mess}, each viable solution for EWSB constitutes a similar intersection of curves in the space of κ and λ_N.

2.4.3 Stop and slepton tachyons

In addition to achieving successful EWSB, our models must also have a viable superpartner spectrum. In particular, the squarks and sleptons cannot be tachyonic at the weak scale. Weak-scale tachyons may be induced either by direct contributions to the soft masses at the messenger scale or by RG running. These two effects provide further constraints on the parameter space.

As we can see from (2.18) and (2.19), two-loop cross terms proportional to α_{λ_u} and α_t contribute negatively to the stop masses. Since $y_t \approx 1$ and $\lambda_u \gtrsim g_3$ in order to generate sufficiently large A-terms, this negative contribution is parametrically the same size (or larger!) than the positive gauge-mediated contribution. Further, the large mixing will induce a bigger splitting between two mass eigenvalues in stop mass matrix. These two

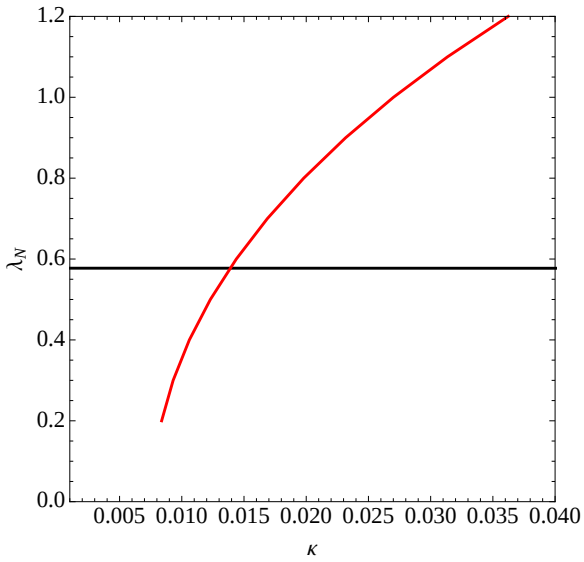

Figure 2.4: Plot showing the EWSB solution in more detail, for the same parameter point as in fig. 2.3. The black line is the contour along which the input value of m_N^2 from the model (2.30) agrees with the value required by EWSB (2.46). It is flat as a function of κ because κ has a negligible effect on m_N^2 when it is small. The red line indicates the agreement between input values and EWSB requirements for κ. The intersection of the two lines gives the consistent EWSB solution for a given value of $\Lambda, M, \lambda_u, N_{mess}$, and λ.

effects lower the stop masses relative to those of other colored scalars. Avoiding prohibitive color-breaking minima therefore leads to an upper bound on λ_u.[13]

A completely different effect may lead to tachyonic sleptons. As discussed in section 2.4.1, EWSB in models with large A-terms and low messenger scales typically entails a large and negative contribution to $m_{H_u}^2$, already at the messenger scale. This can lead to $m_L^2 < 0$ at the weak scale, through the hypercharge trace contribution to one-loop RGEs:

$$2\pi \frac{d}{dt} m_{L_a}^2 = \delta_{a3}\alpha_\tau (m_{L_3}^2 + m_{E_3}^2 + m_{H_d}^2 + A_\tau^2) - \frac{3}{5}\alpha_1 M_1^2 - 3\alpha_2 M_2^2 - \frac{3}{10}\alpha_1 \xi \quad (2.47)$$

where

$$\xi = \mathrm{Tr}[m_Q^2 - 2m_U^2 + m_D^2 - m_L^2 + m_E^2] + m_{H_u}^2 - m_{H_d}^2 \quad (2.48)$$

Since the stau mass eigenvalues are often further separated by mixing and the α_τ contribution to the RGEs, typically the stau is the first state to be driven tachyonic. In any

[13] Were it not for the Higgs mass, which in these models typically require stops above a TeV, this would be an amusing mechanism for generating a natural SUSY spectrum in gauge mediation. Even here, it typically renders the stops several hundred GeV lighter than other colored scalars.

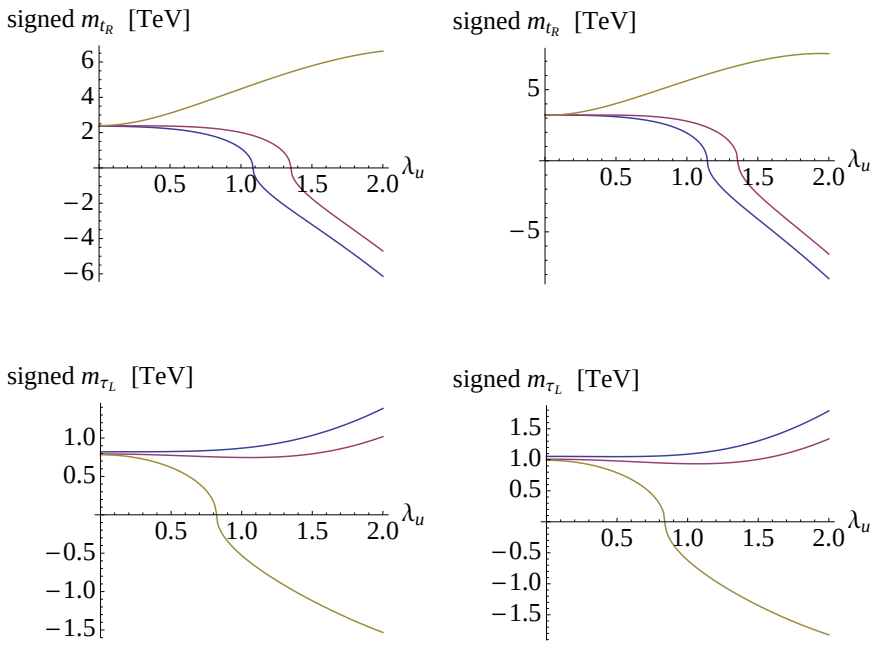

Figure 2.5: Plot of the weak-scale signed masses $m^2_{\tilde{t}_R}/\sqrt{|m^2_{\tilde{t}_R}|}$ and $m^2_{\tilde{\tau}_L}/\sqrt{|m^2_{\tilde{\tau}_L}|}$ vs λ_u, for the $\mathbf{5}\oplus\overline{\mathbf{5}}$ model (left) and the $\mathbf{10}\oplus\overline{\mathbf{10}}$ model (right). The other parameter choices are as in fig. 2.2. We see that in both the $\mathbf{5}\oplus\overline{\mathbf{5}}$ and $\mathbf{10}\oplus\overline{\mathbf{10}}$ models, tachyonic stops are problematic for $\lambda_u \gtrsim 1$, except for larger values of Λ/M. In this regime the stop mass gets pulled *up* during the RG flow by the large negative $m^2_{H_u}$. However, the same effect pushes *down* the left-handed slepton masses, leading to tachyonic sleptons for large Λ/M. Combined with fig. 2.2, we see that for $\lambda_u \sim 1$, a sweet spot exists with moderate Λ/M where all constraints can simultaneously be satisfied.

event, this translates to a requirement that $m^2_{H_u}$ cannot be too large and negative at the messenger scale.

Shown in fig. 2.5 are plots of the stop and slepton masses, illustrating the interplay of all of these effects.

2.4.4 Implications of the constraints

Let us now conclude this section by summarizing briefly its main points and discussing their implications. In the previous subsections we have demonstrated that the soft parameters depend most sensitively on λ_u and Λ/M. To achieve a large enough A-term for $m_h = 125$ GeV, we need $\lambda_u \sim g_3 \sim 1$. Then as we vary Λ/M, a number of issues can arise:

- $m_{H_u}^2$ (and m_N^2) can remain positive at the weak scale even after RG flow, preventing electroweak symmetry breaking. This occurs for low values of Λ/M.

- $m_{H_u}^2$ can be too large and negative already at the messenger scale, resulting in a tachyonic sleptons at the weak scale due to the RG running. This problem arises for large values of Λ/M.

- The stops can be negative at the messenger scale due to the direct contribution from the messenger-Higgs interactions. This effect happens at low to moderate Λ/M and large λ_u.

Clearly a way to address the first two problems is to choose moderate values of the ratio Λ/M. Note that since Λ is usually fixed to be ~ 100 TeV for reasonable superpartner masses, this implies that there is a "sweet spot" of $M \sim$ (a few) $\times$ 100 TeV where the model is viable. In this sense low messenger scales are actually an output of the model.

The third problem is still present at moderate Λ/M, and it is the ultimate limiting factor on the size of A_t. Here the way out is to increase the messenger number – A_t and $m_{\tilde{t}}^2$ are both proportional to N_{mess}, and the relevant quantity for the Higgs mass is $A_t^2/m_{\tilde{t}}^2$. Indeed, for a model with $\mathbf{5} \oplus \overline{\mathbf{5}}$ messengers, we find that for $N_{mess} = 1$, $m_h = 125$ GeV requires extremely heavy stops. But already for $N_{mess} = 2$, $m_h = 125$ GeV is possible for stops as light as 2 TeV. The situation improves somewhat for larger N_{mess}, though the improvement is saturated as the increasing messenger number also raises the gluino mass, which in turn pulls up the stop mass through RG flow. For $\mathbf{10} \oplus \overline{\mathbf{10}}$ messengers, the effective messenger number already starts at three, so this is not an issue in this case. In the following section, we will focus on $N_{mess} = 4$ for the $\mathbf{5} \oplus \overline{\mathbf{5}}$ model and $N_{mess} = 2$ for the $\mathbf{10} \oplus \overline{\mathbf{10}}$ model.

2.5 Spectrum and Phenomenology

In the previous section we discussed qualitatively the challenges and possible solutions for viable models with large A-terms. In this section we will complete our analysis of these models by mapping out the available parameter space and phenomenology of the $\mathbf{5} \oplus \overline{\mathbf{5}}$ and $\mathbf{10} \oplus \overline{\mathbf{10}}$ benchmark models introduced in section 2.3.3. In each case, we may consider either the simple MSSM module for A-terms, or the complete NMSSM theory that also

generates μ and B_μ. As discussed in section 2.4.2, the vacuum structure of the NMSSM is more intricate, which will result in an additional constraint on the parameter space from requiring a nonzero singlet vev. Aside from this additional constraint, the analysis of the MSSM carries over completely to the NMSSM, since we are working in the decoupling limit where $\kappa \to 0$ and $\lambda \to 0$. For numerical exploration of the parameter space, we use a combination of `softsusy v.3.3.0` [67] and `NMSSMTools v.3.1.0` [65, 66].

2.5.1 Models with $\mathbf{5} + \overline{\mathbf{5}}$ messengers

As discussed in section 2.3.1, the parameter space of the MSSM version of this model consists of $\Lambda \equiv F/M$, Λ/M, λ_u, and N_{mess}. Since we are restricting ourselves to low-scale GMSB, we will only consider $N_{mess} \leq 5$ to avoid Landau poles in the gauge couplings. In fig. 2.6 we show contours of the Higgs mass as a function of Λ and λ_u in our "best-case" model ($N_{mess} = 4, \Lambda/M = 0.5$) in the $\mathbf{5} \oplus \overline{\mathbf{5}}$ case; this choice of N_{mess} and Λ/M strikes a favorable balance between large A-terms and viable EWSB. We also show the variation in the lightest stop mass $m_{\tilde{t}_1}$ and the mixing ratio A_t/M_{SUSY} (here $M_{SUSY} \equiv \sqrt{m_{\tilde{t}_1} m_{\tilde{t}_2}}$). The former is controlled mainly by Λ (although as λ_u increases, we see the approaching stop tachyon being reflected in the contours); while the latter is controlled by λ_u. We see that $m_h = 125$ GeV is easily possible, with messenger scales as low as ~ 100 TeV and stops as light as 1500 GeV.

Since we are interested in $m_h = 125$ GeV, it is perhaps more useful to focus on the subspace of parameters for which this is the case. Once we have fixed the Higgs mass and chosen $N_{mess} = 4$, the remaining parameter space of the model is precisely $(\Lambda/M, \lambda_u)$. So contour plots of quantities in this plane provide a complete characterization of the model for a given value of the Higgs mass. In fig. 2.7 we scan over the space of parameters for fixed $m_h = 125$ GeV as a function of Λ/M and λ_u, showing contours of Λ, M_{SUSY}, and A_t/M_{SUSY}. The viable parameter space is bounded by regions with tachyonic superpartner masses or unsuccessful electroweak symmetry breaking, exemplifying our discussion in the previous section.

Generalization from the MSSM module to the full NMSSM model is straightforward. As discussed in sections 2.3.2 and 2.4.2, the NMSSM introduces three new parameters

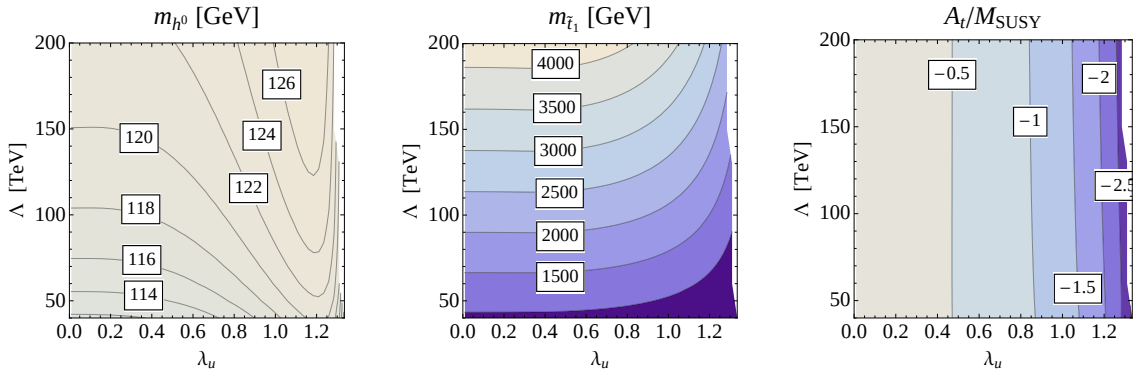

Figure 2.6: Contour plots of m_{h^0}, $m_{\tilde{t}_1}$ and A_t/M_{SUSY} in the Λ vs. λ_u plane, for $N_{mess} = 4$ and $\Lambda/M = 0.5$ (our best-case scenario for the $\mathbf{5} \oplus \overline{\mathbf{5}}$ model).

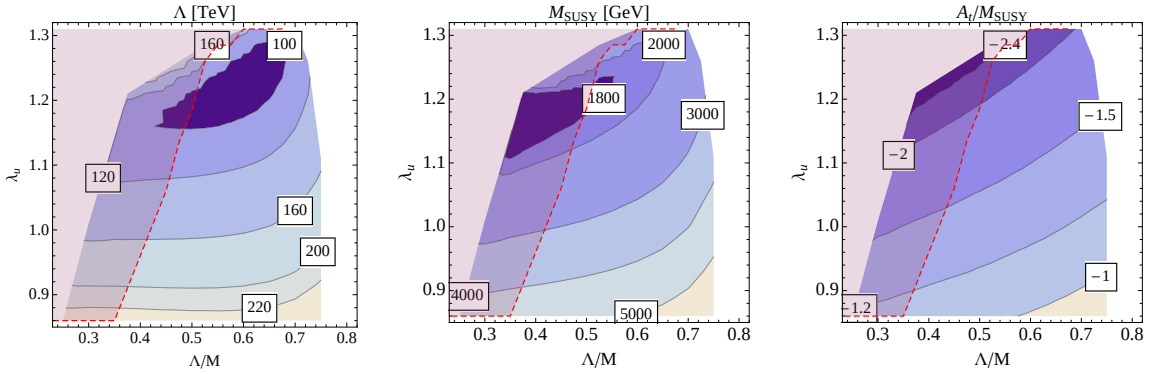

Figure 2.7: Contour plots of the value of Λ required for $m_h = 125$ GeV in the λ_u vs. Λ/M plane for the $\mathbf{5} \oplus \overline{\mathbf{5}}$ model, together with analogous plots for M_{SUSY} and A_t/M_{SUSY}. Here we have fixed $N_{mess} = 4$. The white regions indicate where the spectrum runs afoul of tachyonic color/charge state or electroweak symmetry breaking. Overlaid in red is the region where there does not exist a consistent NMSSM solution with small λ.

$(\lambda, \kappa, \lambda_N)$; we can choose to determine two of the extra parameters, say κ and λ_N, in terms of the third (λ) and the other Higgs sector parameters. So we only need to add one parameter, λ, to the MSSM parameter space. Since our philosophy is to get $m_h = 125$ GeV from stop mixing in the MSSM and μ/B_μ from the NMSSM, it is most favorable to operate in the decoupling limit $\lambda \ll 1$; in the plots below we will take $\lambda = 0.01$ for simplicity.

In section 2.4.2, we also showed that viable EWSB in the NMSSM in the presence of large A_t imposes the additional constraint that m_N^2 should be large and negative at the

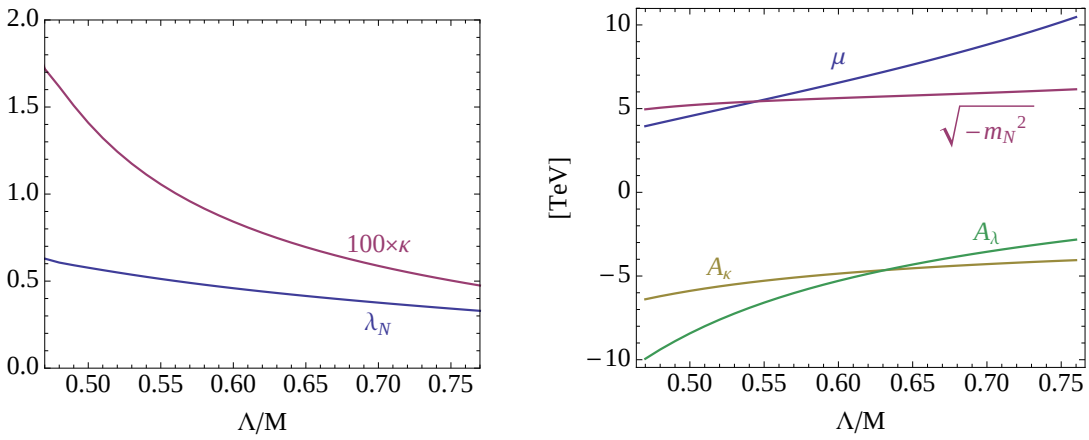

Figure 2.8: A plot showing the dependence of the EWSB solution on Λ/M. The other parameters are as in fig. 2.3. Smaller values of Λ/M are disallowed by $m_{H_u}^2 > 0$ at the weak scale and/or the inability to solve the m_N^2 equation for λ_N; while higher values are disallowed by $m_{\tilde{\tau}}^2 < 0$ at the weak scale.

messenger scale to obtain a satisfactory μ-term. For given values of Λ/M and λ_u, there may not exist a value of λ_N satisfying this constraint, in which case there is no consistent NMSSM solution. For instance, if Λ/M is too small, $m_{H_u}^2 > 0$ as in the MSSM and/or we are unable to find a consistent NMSSM solution; typically the latter condition dominates. Meanwhile at high Λ/M, the stau is driven tachyonic as in the MSSM case. These constraints bound $0.35 \lesssim \Lambda/M \lesssim 0.8.$, and they remove a sizable chunk of the parameter space that is viable for the MSSM module alone. In fig. 2.7 we have overlaid the region in which there is no consistent NMSSM solution at small λ onto the MSSM parameter space. The shape of this boundary in the plane of λ_u and Λ/M is approximately linear due to the conditions for obtaining a sufficiently negative value of m_N^2 in terms of λ_u, λ_N, and Λ/M. While this certainly erodes some of the parameter space viable in the MSSM module, a wide range of possible solutions remains.

Fig. 2.8 exemplifies the discussion of section 2.4, showing the EWSB solution for κ and λ_N as a function of the ratio Λ/M. The figure also shows the values of μ (determined by the vev of N) as a function of Λ/M. We see that as the ratio Λ/M increases, μ likewise increases, because the large negative one-loop contribution to $m_{H_u}^2$ is taking over and must

be cancelled by larger values of μ^2 in order to yield the correct value of the Higgs vev.

Taken together, we see that a consistent model with $m_h = 125$ GeV, a calculable source of μ and B_μ, and a viable superpartner spectrum exists in a window around $\Lambda/M \sim 0.5$ where one-loop soft masses are important but not unreasonably large.

2.5.2 Models with $\mathbf{10} + \overline{\mathbf{10}}$ messengers

For this type of model, the effective messenger number is automatically at least 3, which helps to increase stop mixing. However, the effective messenger number increases rapidly with additional pairs of $\mathbf{10} \oplus \overline{\mathbf{10}}$ messengers; already with two pairs of $\mathbf{10} \oplus \overline{\mathbf{10}}$, we are living dangerously at $M \sim 10^5$ GeV with regard to Landau poles for the Standard Model gauge couplings. In general, enforcing perturbativity up to the GUT scale favors somewhat larger values of M and thus smaller values of Λ/M.

In fig. 2.9 we show contours of the Higgs mass in the plane of Λ and λ_u. The contours of Higgs mass, stop mass, and the ratio A_t/M_{SUSY} are qualitatively similar to the $\mathbf{5} \oplus \bar{\mathbf{5}}$ case. Fig. 2.10 shows the analogous contour plot of Λ values required for $m_h = 125$ GeV in the plane of λ_u and Λ/M. As we discussed in section 2.4.1, the region of viable solutions extends to much smaller values of Λ/M than were allowed for $\mathbf{5} \oplus \bar{\mathbf{5}}$ messengers, since the two-loop correction to $m_{H_u}^2$ is smaller and so the negative one-loop contribution is less important for successful EWSB. Indeed, at small Λ/M there exists a sizable region where the Higgs soft masses are positive at the messenger scale and electroweak symmetry breaking occurs radiatively as in MGM.

As before, we may seamlessly generalize the MSSM module for $\mathbf{10} \oplus \overline{\mathbf{10}}$ messengers to the full NMSSM. The constraint imposed on Λ/M by a viable solution for the NMSSM vacuum is parametrically similar to that in the case of $\mathbf{5} \oplus \bar{\mathbf{5}}$ messengers in terms of the absolute limit, since the numerical details of the solution for NMSSM soft parameters are largely insensitive to the change in messenger representations. However, as shown in fig. 2.10, the NMSSM vacuum constraint precludes the region at small Λ/M that is opened in the $\mathbf{10} \oplus \overline{\mathbf{10}}$ case by reduced two-loop contributions to $m_{H_u}^2$.

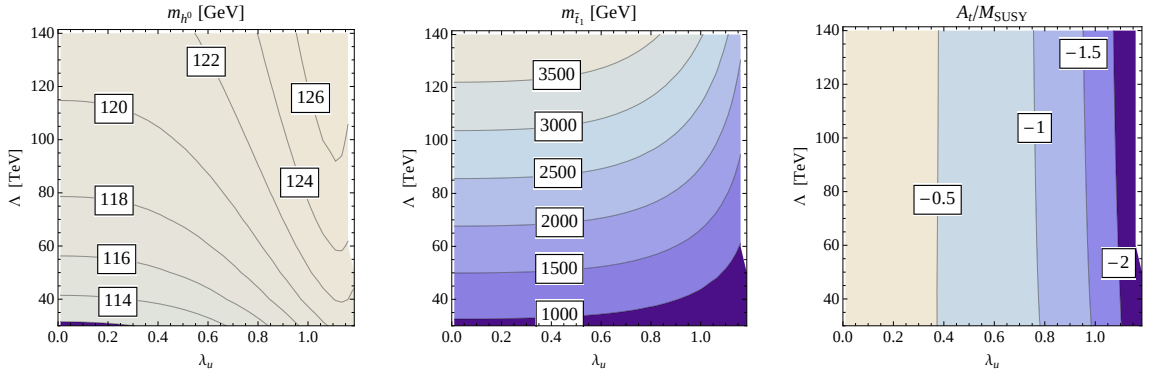

Figure 2.9: Contour plots of m_{h^0}, $m_{\tilde{t}_1}$ and A_t/M_{SUSY} in the Λ vs. λ_u plane, for $N_{mess} = 2$ and $\Lambda/M = 0.3$ (our best-case scenario for the $\mathbf{10} \oplus \overline{\mathbf{10}}$ model).

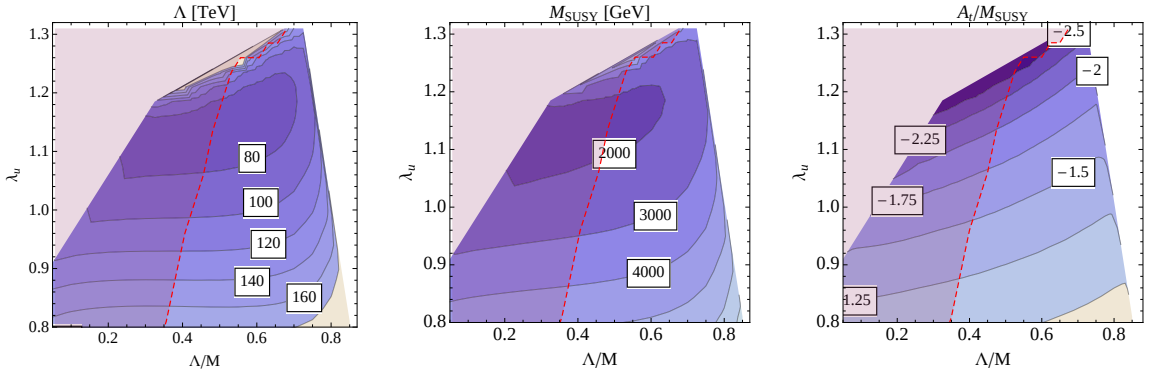

Figure 2.10: Contour plots of the value of Λ required for $m_h = 125$ GeV in the λ_u vs. Λ/M plane for the $\mathbf{10} \oplus \overline{\mathbf{10}}$ model, together with analogous plots for M_{SUSY} and A_t/M_{SUSY}. Here we have fixed $N_{mess} = 2$. Overlaid in red is the region where there does not exist a consistent NMSSM solution with small λ.

2.5.3 Phenomenology

Finally, let us briefly describe the phenomenology of the models considered in the previous sections. The low-energy spectrum does not differ radically between the MSSM and NMSSM cases, since in the NMSSM models the singlet degrees of freedom are heavy and decoupled. Similarly, there are only slight differences between the choice of messenger representations, up to the general effects of changing the effective messenger number. The RG evolution of a representative soft spectrum is shown in fig. 2.11, while the mass spectrum for this point

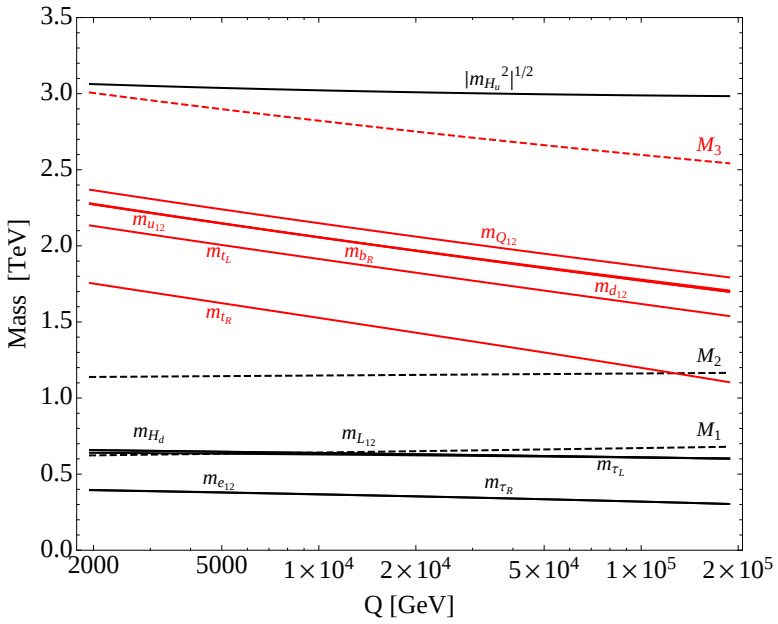

Figure 2.11: Renormalization group evolution of a sample soft spectrum for $N_{mess} = 2$, $\Lambda = 75$ TeV, $\Lambda/M = 0.4$, $\lambda_u = 1$ in the $\mathbf{10} \oplus \overline{\mathbf{10}}$ case (for which $m_h = 125$ GeV). Soft masses for colored superpartners are shown in red, while those for electroweak superpartners are shown in black. Dashed lines denote gaugino masses, solid lines denote scalar masses. Note the H_u soft mass-squared is negative.

is shown in fig. 2.12.

In the colored sector, the stops are typically lighter than in minimal GMSB for the same value of Λ and N_{mess}, due to the additional negative contributions from Higgs-messenger couplings. The large A-term also increases the splitting between the two stop mass eigenvalues, which further lowers the mass of the lighter eigenstate $\tilde{t}_1$. Even so, attaining $m_h = 125$ GeV typically requires stops above ~ 1.5 TeV and gluinos above 2 TeV (and more typically near 3 TeV). Thus the cross section for colored sparticle production is typically quite low, near the limit of observability at the LHC.

In the electroweak sector, the sleptons and electroweakinos are typically at or below a TeV, with the usual MGM splitting between the wino and bino. The sleptons are typically lighter than the wino. The cross section for electroweak sparticle production is also quite low, but nonetheless observable at the LHC.

As we mentioned earlier, we work in the decoupling limit of NMSSM, where both λ and

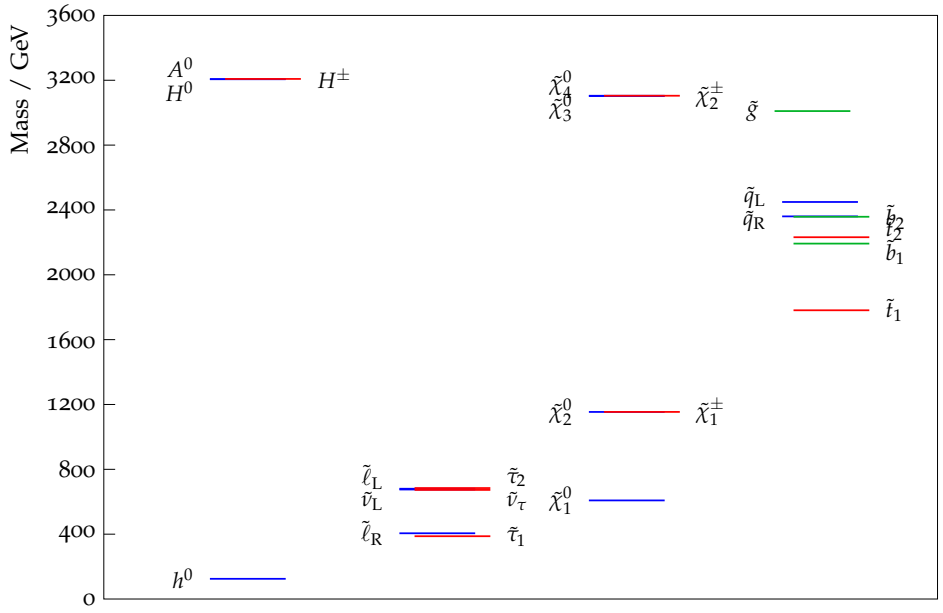

Figure 2.12: The physical mass spectrum, for the same model as in fig.2.11.

κ are small, the gauge singlet component in higgs is negligible and has almost no effects to higgs properties. Although stops have large mixing, they are generically very heavy, so it will not affect the higgs couplings to gluons or photons. Note that the higgsinos and Higgs scalars H^0, A^0, and $H^\pm$ are quite heavy due to the large value of μ necessitated by EWSB, so that the Higgs sector is far into the decoupling limit and the lightest Higgs properties are those of the Standard Model.

The NLSP is almost invariably the stau, except in very small regions of parameter space where it may become a mostly-bino neutralino. The staus are heavily mixed, such that the lightest stau is always lighter than the sneutrino $\tilde{\nu}_\tau$ and there is no co-NLSP. Since the scale of SUSY breaking is low in these scenarios, the NLSP decays promptly in the detector; the most promising search channels for this spectrum are likely to be those involving leptons plus missing transverse energy, such as the H_T/E_T^{miss} binning of the CMS multilepton search [55]. In that paper, limits were set on a GMSB-motivated benchmark model which has degenerate slepton co-NLSPs and specific mass relations among the superpartners. So as such, it is not possible to directly use the CMS search to infer limits on our scenario, which has stau NLSP. It would be interesting to recast the CMS search in terms of our

model; this should be straightforward, since they provide the data for channels where taus are included. Furthermore, we expect that the limits are strictly weaker for stau NLSPs compared to slepton co-NLSPs. For decoupled squarks and gluinos, the CMS limit was $m_{\tilde{\chi}_1^\pm} \gtrsim 600$ GeV, with $m_{\tilde{\ell}_R} = 0.3 m_{\tilde{\chi}_1^\pm}$, $m_{\tilde{\chi}_1^-} = 0.5 m_{\tilde{\chi}_1^\pm}$, and $m_{\tilde{\ell}_L} = 0.8 m_{\tilde{\chi}_1^\pm}$. So we are confident that the existing search does not yet meaningfully encroach on our parameter space. Nevertheless, multilepton searches should ultimately prove sensitive with increased integrated luminosity.

Although ancillary to the phenomenology, we conclude with a few remarks on fine-tuning in the EWSB potential given this characteristic spectrum. As usual, at large $\tan\beta$ the tuning in the potential is governed by a cancellation between μ^2 and $m_{H_u}^2$. In both the MSSM and NMSSM models, the overall tuning (as quantified by the Barbieri-Giudice measure [68]) is typically $10^3 - 10^4$. The tuning in the NMSSM is generically larger than that in the MSSM since the NMSSM has a stronger constraint from EWSB that excludes some of the less tuned points. In section 2.2.3 we introduced the little A - m_H^2 problem, which is essentially the observation that $m_{H_u}^2$ always receives an irreducible, positive contribution from A_u^2. This large contribution must either cancel against a large μ^2-term or against another large term in 2.17 with opposite sign. Either way, such a large cancellation greatly enhances the tuning of the model.

In the MSSM models, the tuning is therefore dominated by λ_u, which controls both A_t and the one- and two-loop contributions to $m_{H_u}^2$. In the NMSSM, the situation is similar, though now the tuning associated with μ is translated to a tuning in λ_N, λ, and κ via (2.42)-(2.43). Amusingly, there is very little tuning associated with the scale of colored superpartners since the threshold contributions to Higgs soft parameters from Higgs-messenger couplings are far more important than radiative corrections from colored scalars. In this sense, the relative heaviness of the gluino and squarks is a red herring for tuning at the weak scale in these models.

2.6 Conclusions

A Higgs boson at 125 GeV poses a challenge for the MSSM in general and in gauge mediation in particular. If colored superpartners lie within reach of the LHC, explaining the

Higgs mass requires large A-terms that are unavailable to pure gauge mediation unless the messenger scale is high [16]. This constraint would appear to challenge the possibility that supersymmetry may be broken and mediated to the MSSM at relatively low scales. Yet low-scale gauge mediation remains an attractive framework due to its distinctive phenomenology, including features such as favorable gravitino cosmology and prompt NLSP decays. This strongly motivates exploring ways in which low-scale gauge mediation might be reconciled with the presumptive mass of the Higgs.

In this work we have constructed simple, economical, and calculable models of low-scale gauge mediation that generate all the necessary parameters in the Higgs sector of the MSSM and readily provide a Higgs at 125 GeV. The key feature is the introduction of Higgs-messenger interactions that lead to large A-terms aligned with the SM flavor structure. This is a natural step in the context of GMSB, since the μ - B_μ problem already suggests that additional interactions are required in the Higgs sector. In general, such interactions lead to an A - m_H^2 problem, which is solved if the only source of mass in the messenger sector is the expectation value of a single SUSY-breaking spurion (i.e. if the messengers are described by minimal gauge mediation). Such models suffice for generating large A-terms and stop mass mixing required for the Higgs, but on their own do not solve the μ - B_μ problem. In this sense they constitute "modules" that may be appended to other solutions to the μ - B_μ problem. One particularly compelling solution is in the context of the NMSSM, where a simple generalization to include singlet-messenger couplings simultaneously ameliorates the problems of the NMSSM in GMSB, and generates viable μ and B_μ. Since the Higgs mass arises primarily due to stop mixing, the singlet sector serves only to generate μ and B_μ, thereby avoiding problematically large singlet-Higgs couplings with Landau poles at low scales. Indeed, these theories remain weakly-coupled up to, and generally well beyond, the messenger scale. It is compelling that a straightforward generalization of low-scale gauge mediation to include perturbative interactions between the Higgs sector and messenger sector – interactions already hinted at by the μ - B_μ problem – naturally accommodates a Higgs at 125 GeV and provides all necessary soft parameters.

Our approach builds on previous works, especially [46] and [48], but the complete combination of interactions for large A-terms and μ/B_μ, and the emphasis on low messenger

scales, are both novel and lead to a qualitatively new model with distinctive features. Chief among these is the crucial role played by one-loop Λ/M-suppressed contributions to $m_{H_u}^2$ in guaranteeing electroweak symmetry breaking, which is otherwise imperiled by large two-loop soft masses that accompany sizable A-terms.

The phenomenology of these models is very similar to that of MGM with high effective messenger number. One notable difference is that the mass of the stop is always significantly lowered relative to the masses of other colored scalars due to the Higgs-messenger interactions, such that the lightest stop is typically several hundred GeV lighter than the remaining squarks. Even so, a Higgs mass at $m_h = 125$ GeV suggests the stop is relatively heavy on LHC scales, above ~ 1.5 TeV, with the gluino above 2 TeV. The NLSP is almost always the stau, though in some cases it may be the lightest neutralino. In either case, NLSP decays to the gravitino are always prompt due to the low messenger scale. Overall, the spectrum is quite consistent with current collider limits and perhaps explains why we have yet to observe evidence for supersymmetry at the LHC.

There are numerous avenues for future study. The models presented here have a potentially large parameter space, of which we have only considered a simplified subspace. It would be interesting, for example, to study the consequences of splitting the messenger multiplets on the low-energy phenomenology. More generally, it should be possible to construct weakly-coupled models with large A-terms that realize the full parameter space allowed by general gauge mediation [56, 57], which would allow for a greater range of NLSP candidates and collider signals. We have also focused exclusively on the decoupling limit of the NMSSM, where $\lambda, \kappa \ll 1$; it may be the case that other parametric regimes are allowed, in which case Higgs signals could deviate from Standard Model expectations. Finally, we have remained agnostic to the origin of the supersymmetry breaking and messenger sectors. Ultimately, it is worth exploring whether our models might be embedded in a complete theory of dynamical supersymmetry breaking in which Higgs-messenger couplings are a natural ingredient.

It bears emphasizing we have limited our focus to weakly-coupled theories with perturbative messenger sectors and decoupled hidden sector interactions. It is plausible that the related problems of μ -B_μ, A - m_H^2, and $m_h = 125$ GeV may alternatively be resolved

in a strongly-coupled hidden sector along the lines of [69–71]. In this case, the details of the hidden sector interactions are crucial to the boundary conditions for soft parameters [72], and it would be interesting to systematically study implications for the Higgs sector in terms of hidden- and messenger-sector correlation functions [49].

Appendices

2.A General Formulas

Whenever SUSY breaking may be parameterized by a single spurion X whose lowest expectation value is responsible for messenger masses, the soft spectrum may be computed to leading order in Λ/M via analytic continuation into superspace [41]. The resulting soft masses and A-terms for arbitrary marginal visible-messenger superpotential interactions linear in the visible sector fields are [35]:[14]

$$\delta m_a^2\Big|_{t=\frac{1}{2}\log|M|^2} = \frac{1}{2}\left[\sum_m \left(\frac{d\gamma_a^+}{d\alpha_m} - \frac{d\gamma_a^-}{d\alpha_m}\right)\partial_t\alpha_m^+ - \frac{d\gamma_a^-}{d\alpha_m}\left(\partial_t\alpha_m^+ - \partial_t\alpha_m^-\right)\right]\Lambda^2\Big|_{t=\frac{1}{2}\log|M|^2} \tag{2.49}$$

$$A_a\Big|_{t=\frac{1}{2}\log|M|^2} = -\sum_m \left(\frac{d\gamma_a^+}{d\alpha_m} - \frac{d\gamma_a^-}{d\alpha_m}\right)\alpha_m^+\Lambda\Big|_{t=\frac{1}{2}\log|M|^2} \tag{2.50}$$

where the δ denotes a correction to the usual GMSB soft masses. The A-term computed here correspond to a specific field label by a, rather than to a coupling. The A-terms corresponding to the couplings y_t, κ, λ, ... are linear combinations of the A-terms computed in (2.50). In what follows i, j, etc. range over messenger fields; and a, b, etc. range over visible sector fields. Repeated indices are summed over, except for the free index a. The A-terms appear in the potential via $V \supset A_a\phi_a\partial_{\phi_a}W(\phi) + \text{h.c.}$. The $\gamma_a^\pm \equiv -\frac{1}{2}\frac{\partial \log Z_a^\pm}{\partial t}$ and $\alpha_m^\pm \equiv \frac{(\lambda_m^\pm)^2}{4\pi}$ are the anomalous dimensions and couplings above and below the messenger threshold, respectively. The sum over m runs over all the couplings in the theory.

We convert (2.49) and (2.50) into more explicit formulas by specifying the anomalous dimensions and the β functions, accounting for couplings between messengers and matter

[14] The conventions for A_a and the anomalous dimensions used in [35] differ slightly from ours. We are using the conventions of [73].

fields but neglecting possible couplings between messengers alone. The anomalous dimensions are then given by

$$\gamma^a = \tfrac{1}{4\pi}\Big(\tfrac{1}{2}d_a^{ij}\alpha_{aij} + \tfrac{1}{2}d_a^{bc}\alpha_{abc} - 2c_r^a\alpha_r\Big) \tag{2.51}$$

$$\gamma^i = \tfrac{1}{4\pi}\Big(d_i^{aj}\alpha_{aij} - 2c_r^i\alpha_r\Big) \tag{2.52}$$

The d_a^{ij} count the number of fields i, j talking to a through the Yukawa vertex (aij). With a slight abuse of notation, we denote the couplings with the messenger sector, the MSSM Yukawa couplings, and the gauge couplings with α_{aij}, α_{abc} and α_r respectively. Similarly, the relevant beta functions are

$$\partial_t\alpha_{abc}^{\pm} = \quad 2\alpha_{abc}(\gamma_a^{\pm} + \gamma_b^{\pm} + \gamma_c^{\pm}) \tag{2.53}$$

$$\partial_t\alpha_{aij}^{\pm} = \quad 2\alpha_{aij}(\gamma_a^{\pm} + \gamma_i^{\pm} + \gamma_j^{\pm}) \tag{2.54}$$

where the $\pm$ subscript again indicates whether α and γ are to be taken above or below the messenger threshold. Substituting these formulas in (2.49) and (2.50) yields

$$\begin{aligned}\delta m_a^2 = \frac{1}{8\pi^2}\Big(&-\frac{1}{2}d_a^{ij}(c_r^a + c_r^i + c_r^j)\alpha_r\alpha_{aij} + \frac{1}{8}\left(d_a^{ij}\alpha_{aij}\right)^2 \\ &+ \frac{1}{2}d_a^{ij}d_i^{bk}\alpha_{bik}\alpha_{aij} - \frac{1}{4}d_a^{bc}d_b^{ij}\alpha_{abc}\alpha_{bij}\Big)\Lambda^2\end{aligned} \tag{2.55}$$

$$A_a = -\frac{1}{8\pi}d_a^{ij}\alpha_{aij}\Lambda\ . \tag{2.56}$$

Now to obtain the formulas (2.17)-(2.20) and (2.28)-(2.33) in the bulk of the text, it suffices to substitute for the correct d_a^{ij}, α_{aij} and α_{abc}. For the MSSM, the indices $a, b, c, \ldots$ run over the fields H_u, Q and U. The indices $i, j, k, \ldots$ run over the messenger fields ϕ_i and $\tilde{\phi}_i$. With this in mind, one can read off the non-zero d's and the couplings from (2.15):

$$d_{H_u}^{\phi_1\tilde{\phi}_2} = d_H, \qquad d_{\phi_1}^{H_u\tilde{\phi}_2} + d_{\tilde{\phi}_2}^{H_u\phi_1} = 3, \qquad \alpha_{H_u\phi_1\tilde{\phi}_2} = \alpha_{\lambda_u}, \qquad \alpha_{H_uQU} = \alpha_t \tag{2.57}$$

with d_H given by (2.35) or (2.37) in the $\mathbf{5}\oplus\overline{\mathbf{5}}$ or $\mathbf{10}\oplus\overline{\mathbf{10}}$ models respectively. The same conventions hold for the NMSSM, with the important difference that the indices $a, b, c, \ldots$ now can take the value H_d and N as well. Moreover several extra couplings must be

accounted for:[15]

$$
\begin{array}{lll}
d_{H_u}^{\phi_1\tilde{\phi}_2} + d_{H_u}^{\varphi_1\tilde{\varphi}_2} = d_H, & d_{\phi_1}^{H_u\tilde{\phi}_2} = d_{\varphi_1}^{H_u\tilde{\varphi}_2} = d_1^{H2}, & d_{\tilde{\phi}_2}^{H_u\phi_1} = d_{\tilde{\varphi}_2}^{H_u\varphi_1} = d_2^{H1}, \\
d_N^{\varphi_1\tilde{\phi}_1} + d_N^{\varphi_2\tilde{\phi}_2} = d_N, & d_{\phi_1}^{N\tilde{\varphi}_1} = d_{\phi_2}^{N\tilde{\varphi}_2} = d_{\tilde{\varphi}_1}^{N\phi_1} = d_{\tilde{\varphi}_2}^{N\phi_2} = 1, & \\
d_N^{H_uH_d} = 2, & d_{H_u}^{NH_d} = 1, & d_N^{NN} = 1, \\
\alpha_{H_u\phi_1\tilde{\phi}_2} = \alpha_{H_u\varphi_1\tilde{\varphi}_2} = \alpha_{\lambda_u}, & \alpha_{N\phi_i\tilde{\varphi}_i} = \alpha_{\lambda_N} & \\
\alpha_{H_uQU} = \alpha_t, & \alpha_{NH_uH_d} = \alpha_\lambda, & \alpha_{NNN} = 4\alpha_\kappa
\end{array}
\tag{2.58}
$$

with d_H, d_N, etc. again given in (2.35) or (2.37). Finally note that equation (2.56) computes the A-terms corresponding to various fields (see (2.11)), instead of couplings. The A-term for the various couplings that are used in the bulk of the draft can be obtained as follows:

$$
\begin{aligned}
A_t &= A_{H_u} \\
A_\lambda &= A_N + A_{H_u} \\
A_\kappa &= 3A_N.
\end{aligned}
\tag{2.59}
$$

2.B Physics Above the Messenger Scale

The models presented in sections 2.5.1 and 2.5.2 are complete and calculable effective theories below the messenger scale. This is the most that one can concretely ask for when treating the hidden sector in the spurion limit, since above the messenger scale the dynamics of the hidden sector and the origin of hidden-messenger couplings are bound to become important. However, one may still wish to study the behavior of the theory above the messenger scale, modulo ignorance of hidden sector dynamics.

Unlike in many realizations of the NMSSM where the singlet contributions to the potential are used to raise the Higgs mass, there is no problem with Landau poles in λ for any of the models we consider. Such Landau poles would be particularly troublesome since they involve all the light degrees of freedom in the EWSB sector. Since we are working in the decoupling limit, λ is always very small at the weak scale, and although it grows in the ultraviolet, it easily remains perturbative all the way to the GUT scale. The same may be

[15] Note the extra factor of 4 in the translation of α_{NNN} to α_κ. This is because of the non-standard NMSSM convention for the normalization of κ.

said of κ, which is likewise small at the weak scale and never runs large below the GUT scale. Thus all the parameters in the NMSSM effective theory below the messenger scale are well-behaved above it as well.

On the other hand, there may conceivably be Landau poles in the gauge couplings and the couplings introduced at the messenger scale. The particular complications are qualitatively different depending on the messenger representations. For MSSM and NMSSM models with $\mathbf{5} \oplus \overline{\mathbf{5}}$ messengers there are no irreducible Landau poles in the Standard Model gauge couplings up to the GUT scale for any value of the messenger scale, since viable models exist with $N_{mess} \leq 4$. For models with $\mathbf{10} \oplus \overline{\mathbf{10}}$ messengers there may be Landau poles in the Standard Model gauge couplings before the GUT scale due to the large effective messenger number if the messenger scale is too low. However, for the most minimal NMSSM model (with effective messenger number 6) we find there are no Landau poles across the range of messenger scales under consideration, as determined by two-loop RG running and one-loop threshold matching. But the Standard Model gauge couplings grow strong as they approach the GUT scale, and perturbation theory is perhaps no longer reliable. Higher values of the effective messenger number, corresponding to more than two pairs of $\mathbf{10} \oplus \overline{\mathbf{10}}$, introduce Landau poles in the gauge couplings below the GUT scale.

The situation is somewhat different with respect to superpotential couplings. In $\mathbf{5} \oplus \overline{\mathbf{5}}$ models λ_u typically reaches a Landau pole before the GUT scale, since its value is necessarily quite large at the messenger scale and its RG evolution is dominated at one loop by λ_u itself and also by y_t. In $\mathbf{10} \oplus \overline{\mathbf{10}}$ models there are also large negative contributions from g_3, which help to control the running. These effects are evident in the β functions, which in the MSSM case are dominated by

$$\beta_{\lambda_u} \sim \frac{\lambda_u}{16\pi^2}\left[(N_{mess}+3)\lambda_u^2 + 3y_t^2 + \dots\right] \qquad \left(\mathbf{5} \oplus \overline{\mathbf{5}} \text{ messengers}\right) \tag{2.60}$$

$$\beta_{\lambda_u} \sim \frac{\lambda_u}{16\pi^2}\left[(3N_{mess}+3)\lambda_u^2 + 3y_t^2 - \frac{16}{3}g_3^2 + \dots\right] \qquad \left(\mathbf{10} \oplus \overline{\mathbf{10}} \text{ messengers}\right) \tag{2.61}$$

For $\mathbf{5} \oplus \overline{\mathbf{5}}$ messengers, there is always a Landau pole below the GUT scale in the range of parameters with $m_h = 125$ GeV. For $\mathbf{10} \oplus \overline{\mathbf{10}}$ messengers there are Landau poles for $\lambda_u > 0.9$, while for $\lambda_u \leq 0.9$ the color contributions lead to an approximate fixed point. This is illustrated clearly in fig. 2.13, which shows the scale of the Landau pole in λ_u

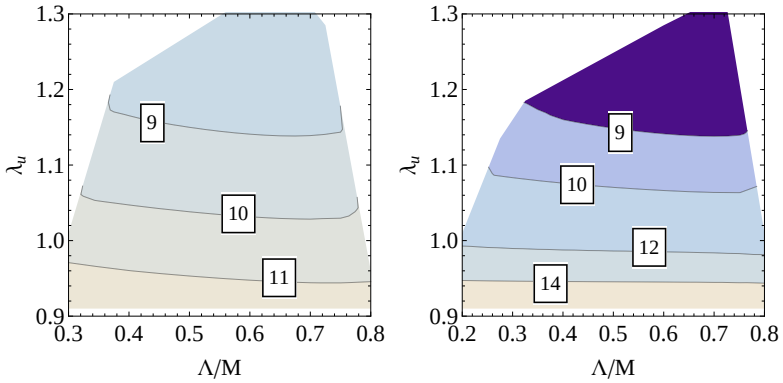

Figure 2.13: Contour plots of $\log_{10}(M_{Landau}/\text{GeV})$ for points with $m_h = 125$ GeV in typical MSSM models of $\mathbf{5} \oplus \overline{\mathbf{5}}$ messengers with $N_{mess} = 4$ (left) and $\mathbf{10} \oplus \overline{\mathbf{10}}$ messengers with $N_{mess} = 2$ (right). The Landau pole is mainly caused by the blow up of λ_u.

across the parameter space with $m_h = 125$ GeV. The occurrence of Landau poles is some sense a different manifestation of the same phenomenon that caused problems with radiative electroweak symmetry breaking: λ_u must be large at the messenger scale to generate sizable A-terms. For $\mathbf{5} \oplus \overline{\mathbf{5}}$ messengers, the only two-loop contributions to $m_{H_u}^2$ and one-loop contributions to β_{λ_u} are large and positive, while for $\mathbf{10} \oplus \overline{\mathbf{10}}$ messengers there is a partial cancellation with color contributions in both the soft mass and beta function.

We emphasize, however, that the apparent Landau pole in λ_u does not doom the models with $\mathbf{5} \oplus \overline{\mathbf{5}}$ messengers. In a complete theory of dynamical supersymmetry breaking, supersymmetry is broken by dimensional transmutation in a hidden sector gauge group. Perhaps the messengers at low scales are actually composites of the strong dynamics (as in theories of direct supersymmetry breaking), or are charged under the hidden sector gauge group and accumulate additional negative contributions to β_{λ_u}. In either case, the unknown strong dynamics naturally control the apparent landau pole in λ_u, whose appearance is simply an artifact of maintaining the spurion limit all the way to the GUT scale. In this respect, fig. 2.13 indicates the scale at which new physics must appear in the hidden sector. Finally, although it is not entirely meaningful given the likely role of hidden sector dynamics, it is at least reassuring that there are models with $\mathbf{10} \oplus \overline{\mathbf{10}}$ messengers and $m_h = 125$ GeV for which all couplings remain perturbative up to the GUT scale.

Chapter 3

General Messenger Higgs Mediation

With N. Craig and D. Shih

Appeared in JHEP 1308 (2013) 118, arXiv:1302.2642

General context of this chapter

In the previous chapter we presented a first, simple example of a model that accommodates the Higgs mass through a combination of Higgs and gauge mediation. Along the way, we identified the 'A/m_H problem' and proposed a simply, weakly coupled solution. In this chapter we attempt to study Higgs mediation in a more general and more systematic way, with a special emphasis on the A/m_H problem. In particular, the solution presented in the previous chapter was rather non-generic, and one would like to know whether other possibilities exist. Moreover our proposed solution still suffered from a 'little A/m_H problem' and it is an interesting question whether solutions to this secondary problem can be constructed.

For this purpose we developed a general formalism for analyzing supersymmetric models where the Higgs sector directly couples to the messengers of supersymmetry breaking. Our framework is applicable to the μ/B_μ problem in addition to the A/m_H problem. Using our formalism, we identify new avenues to solving both these problems through strong dynamics in the messenger sector or hidden sector. Although our formalism is entirely general, we show how it reproduces familiar results in two simplifying limits: one where the hidden sector consists of a single spurion, and the other where it is approximately superconformal. In the latter limit, our formalism generalizes and clarifies the scenario of hidden sector sequestering, which we show can solve both the μ/B_μ and A/m_H^2 problems uniformly.

3.1 Introduction

The recent discovery [1, 2] of a Higgs-like particle with a mass near 125 GeV has profound implications for physics beyond the Standard Model. It renews the urgency of the hierarchy problem, for which supersymmetry (SUSY) remains the best solution. Minimal realizations of weak-scale SUSY such as the MSSM are highly constrained, since the tree-level prediction for the Higgs mass is bounded from above by the mass of the Z boson and must be increased through radiative corrections. As discussed in [26–30, 16], to obtain $m_h = 125$ GeV in the MSSM while minimizing the fine-tuning of the electroweak scale, the A-terms must be large relative to other soft masses and close to maximal mixing [74–76, 33].

There are several options for generating large weak-scale A-terms in calculable models, and each comes with its own challenges. One option is to have $A \approx 0$ at the messenger scale M but generate it through RG running of the MSSM. In [16], it was shown that this places strong constraints on the messenger scale and the gluino mass, requiring both to be very high. Another option is to generate non-zero A-terms already at the messenger scale, by directly coupling H_u and H_d to the messengers.[1] Aside from being richer in terms of model building possibilities, this option is attractive and economical because such couplings are already necessary for solving the μ problem of the MSSM. But here the main challenge, at least in weakly-coupled models, is something called the "A/m_H^2 problem:" A and m_H^2 are typically generated at the same loop order, in direct analogy with the μ/B_μ problem [77]. Such a large m_H^2 would have disastrous effects on electroweak symmetry breaking (EWSB) and fine-tuning.

In [77], the problem of generating large A-terms was studied in the context of weakly-coupled messenger models where SUSY is broken by a spurion X. Here the challenges of the A/m_H^2 problem are perhaps starkest. Integrating out the messengers generates effective operators involving the SUSY-breaking hidden sector and the Higgs fields; the A-terms arise from

$$c_{A_u} \int d^4\theta \, \frac{X^\dagger}{M} H_u^\dagger H_u \to A_u H_u^\dagger F_{H_u} \tag{3.1}$$

[1] We could also consider direct couplings of the quark superfields to the messengers, but these would not be minimally flavor violating.

where we have substituted $\langle X \rangle = \theta^2 F$. In general, $m^2_{H_u}$ is also generated at the same loop order, since the only difference in the effective operator is the non-chiral operator $X^\dagger X$ instead of the chiral hidden sector operator X:

$$c_{m^2_{H_u}} \int d^4\theta \, \frac{X^\dagger X}{M^2} H_u^\dagger H_u \to \hat{m}^2_{H_u} H_u^\dagger H_u \tag{3.2}$$

This is exactly analogous to the more well-known μ/B_μ problem – for which the effective operators are the same as in (3.1) and (3.2), but with $H_u^\dagger H_u$ replaced by $H_u H_d$. In [77], it was argued (following [47]) that only models where the messengers receive all masses and SUSY-breaking from a single spurion (i.e. models of minimal gauge mediation (MGM) [42–44]) can solve the A/m_H^2 problem, by eliminating the one-loop m_H^2 at leading order in F/M^2. (See also [48] for a study of these MGM-based models.) But even in these models, a residual problem – dubbed the "little A/m_H^2 problem" in [77] – remains: $m^2_{H_u}$ always contains an irreducible, positive, two-loop contribution $\propto A_u^2$ coming from integrating out the auxiliary component of H_u in (3.1). Since the A-terms must be large (at least ~ 2 TeV) for maximal stop mixing and $m_h = 125$ GeV, this also presents difficulties for radiative EWSB and for fine tuning.

Motivated by these considerations, in this paper we will broaden the scope of [77] considerably and take a general, model-independent approach to studying the Higgs soft spectrum arising from direct Higgs-messenger couplings. This will include both weakly-coupled spurion models and strongly-coupled models as special cases. Our main tool in this endeavor will be the supersymmetric correlator formalism of [56, 57]. This was first applied to the Higgs sector in [23], assuming the following portals between the Higgs and hidden sectors [56]:

$$W = \lambda_u O_u H_u + \lambda_d O_d H_d \tag{3.3}$$

where the hidden sector operators $O_{u,d}$ are $SU(2)$ doublets.[2] (Singlet couplings were also studied in [23]; in the interest of clarity we will only work out the doublet case in this paper. The extension to the singlet case is straightforward.) We will refer to this framework as

[2]Throughout the paper we will be neglecting potential contributions to soft masses proportional to the MSSM gauge and Yukawa couplings. Note that the presence of hidden sector operators $O_{u,d}$ implies at the minimum some gauge-mediated contributions to the MSSM soft spectrum, but these need not be the leading effect; the interactions in (3.3) may be incorporated into various models of supersymmetry breaking.

"General Higgs Mediation" (GHM), in analogy with [56, 57]. Integrating out the hidden sector generates the Higgs-sector soft Lagrangian:[3]

$$-\delta\mathcal{L} \supset \Big(A_u H_u^\dagger F_{H_u} + A_d H_d^\dagger F_{H_d} + c.c.\Big) - \Big(\hat{m}^2_{H_u} H_u^\dagger H_u + \hat{m}^2_{H_d} H_d^\dagger H_d\Big) \tag{3.4}$$

$$+ \mu\Big(H_u F_{H_d} + H_d F_{H_u} - \psi_{H_u}\psi_{H_d} + c.c.\Big) - \Big(B_\mu H_u H_d + c.c.\Big) \tag{3.5}$$

Note that we have put hats on the dimension-two soft masses in (3.4), in order to distinguish them from the full dimension-two soft masses that are only obtained upon integrating out $F_{H_{u,d}}$:

$$m^2_{H_{u,d}} = \hat{m}^2_{H_{u,d}} + |A_{u,d}|^2, \qquad B_\mu = \hat{B}_\mu + \mu(A_u^* + A_d^*) \tag{3.6}$$

Correlator formulas for the Higgs soft parameters were derived to leading order in $\lambda_{u,d}$ in [23]. No assumption was made in [23] regarding the structure of the hidden sector, thus their results were best suited to the single-sector case where there is no distinction between messenger and SUSY-breaking hidden sectors.

Here we will extend the work of [23] in two ways. First, we will extend their single-sector formulas for the dimension-two soft masses to next-to-leading order in $\lambda_{u,d}$. This is obviously necessary in order to discuss phenomenologically relevant models where $A^2_{u,d} \sim m^2_{H_{u,d}}$ and $B_\mu \sim \mu^2$. Second, we will derive more detailed formulas for models in which the messenger sector is distinct from the SUSY-breaking hidden sector, along the lines of [78]. This factorization is illustrated in fig. 1, and in analogy with [78], we will refer to this framework as "General Messenger Higgs Mediation" (GMHM). We will focus on the superpotential portal of [78]:

$$W = \kappa O_h O_m \tag{3.7}$$

In general, the coupling κ can be dimensionful, and $O_{h,m}$ have dimensions $\Delta_{h,m}$. O_h is a chiral operator that breaks SUSY

$$\langle Q^2 O_h\rangle \equiv F^{\frac{\Delta_h+1}{2}} \tag{3.8}$$

and generalizes the spurion X to possibly nontrivial, interacting hidden sectors. (Without loss of generality, we take F to be real, and we shift O_h so that its lowest component

[3]Here and for the rest of the paper, we are neglecting the "wrong Higgs couplings," as they arise at a higher order in the supersymmetry breaking order parameter [23].

has zero vacuum expectation value.) It would also be interesting to study the Kähler and half-Kähler portals considered in [78], but we will not do so here.

One of the primary virtues of GMHM is that it enables the study of models where the SUSY-breaking scale $\sqrt{F}$ is much smaller than the messenger scale M. When this is the case, there is an additional small parameter F/M^2 to expand in, and the expressions for the soft masses often simplify. More generally, many existing models feature this separation between SUSY-breaking hidden sector and messenger sector, and so GMHM is the ideal framework for studying them collectively.

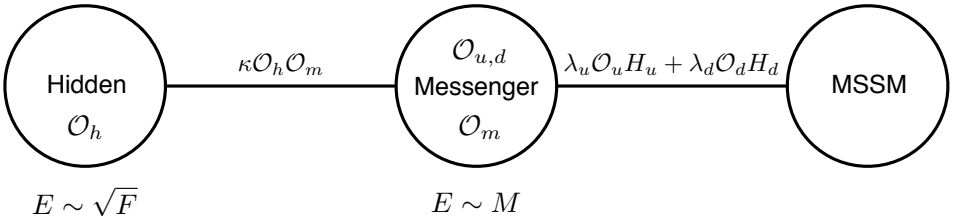

Figure 3.1: The general setup of GMHM, assuming doublet portals connecting the Higgs sector to the messenger sector. The messengers are characterized by a scale M, and they communicate via another perturbative superpotential interaction with the hidden sector, which is characterized by a SUSY-breaking scale $\sqrt{F}$.

Computing soft parameters in the framework of GMHM involves a double expansion in $\lambda_{u,d}$ and κ. Carefully performing this double expansion and manipulating the resulting correlators, we will derive fully general formulas for Higgs soft parameters in any setup of the form in figure:

$$\mu = \lambda_u \lambda_d \kappa^* \langle \bar{Q}^2 O_h^\dagger \rangle_h \int d^4y \, C_\mu(y) \tag{3.9}$$

$$A_{u,d} = |\lambda_{u,d}|^2 \kappa^* \langle \bar{Q}^2 O_h^\dagger \rangle_h \int d^4y \, C_{A_{u,d}}(y) \tag{3.10}$$

$$B_\mu = \lambda_u \lambda_d |\kappa|^2 \int d^4y d^4y' \, \langle Q^4 [O_h^\dagger(y) O_h(y')] \rangle_h C_{B_\mu}(y, y'; \lambda_{u,d}) \tag{3.11}$$

$$m^2_{H_{u,d}} = -|\mu|^2 + |\lambda_{u,d}|^2 |\kappa|^2 \int d^4y d^4y' \, \langle Q^4 [O_h^\dagger(y) O_h(y')] \rangle_h C_{m^2_{H_{u,d}}}(y, y'; \lambda_{u,d}) \tag{3.12}$$

where $Q^4 = Q^2 \bar{Q}^2$. C_μ, etc. are integrated correlation functions of messenger-sector operators; explicit expressions for them will be given in Section 2. Since we have expanded to NLO in $\lambda_{u,d}$, C_{B_μ} and $C_{m^2_{H_{u,d}}}$ contain $\mathcal{O}(|\lambda_{u,d}|^2)$ corrections.

These formulas have broad applicability, as they may be used to compute Higgs soft

parameters for any model with Higgs-messenger couplings in which the messenger sector and SUSY-breaking hidden sector factorize. We will illustrate this in several ways, starting with showing how they reproduce the results of the weakly-coupled spurion models of [77]. In these models, the hidden sector has no dynamics, and so

$$\langle Q^4[O_h^\dagger(y)O_h(y')]\rangle_h \to |\langle Q^2 O_h\rangle|^2 \tag{3.13}$$

We will show how the A/m_H^2 problem is a generic property of the integrated messenger correlators $\int C_{m^2_{H_{u,d}}}$ and $\int C_{A_{u,d}}$, and how the little A/m_H^2 problem (made explicit in (3.6)) arises from the disconnected part of $C_{m^2_{H_{u,d}}}$.

The utility of the GMHM framework extends far beyond spurion-messenger models, however. Such broadening of scope is powerfully motivated by the challenges that weakly-coupled spurion models face in accommodating the Higgs mass. Perhaps the key lies in non-trivial dynamics of the hidden sector, as the considerations that led to the A/m_H^2 problem could be completely avoided at strong coupling. For instance, if the messenger sector is strongly-coupled, the notion of a loop factor might not even apply. Or, as has been suggested before in the context of the μ/B_μ problem [69–71], if the SUSY-breaking hidden sector is strongly coupled, then $O_h^\dagger O_h$ should really be replaced with a general non-chiral operator O_Δ with scaling dimension Δ. If $\Delta > 2\Delta_h$ and $\sqrt{F} \ll M$, then the anomalous dimension of O_Δ could help to sequester B_μ relative to μ^2:

$$\frac{B_\mu}{\mu^2} \sim \left(\frac{\sqrt{F}}{M}\right)^{\Delta-2\Delta_h} \ll 1 \tag{3.14}$$

It is natural to ask whether the same mechanism can help with the A/m_H^2 problem. As we will see, GMHM is ideally suited to addressing such questions. We will show that hidden-sector sequestering is contained within the GMHM framework, and that it can be successfully applied to both the μ/B_μ and the A/m_H^2 problems. In particular, we will demonstrate how dependence on the hidden sector OPE and anomalous dimensions emerges naturally from (3.9).

In the course of generalizing hidden-sector sequestering using GMHM, we will clear up a lingering disagreement regarding the sequestered soft spectrum. In [70, 79], it was claimed

that the result of complete hidden-sector sequestering should be:

$$m^2_{H_{u,d}} \to -\mu^2 \ , \quad B_\mu \to 0 \tag{3.15}$$

In particular, the fully sequestered soft parameters do not depend on the A-terms, nor do they depend on OPE coefficients in the hidden sector. The claim was based on an argument that the A-term and μ-term operators were redundant, in the sense that they could be removed by a field redefinition [79].

Various questions were raised in [72] about the validity of this argument – what if the UV theory is strongly coupled and field redefinitions are not well-defined? If the UV theory is an interacting SCFT, shouldn't the OPE coefficient of $O_h^\dagger O_h \to O_\Delta$ be involved? Using superconformal perturbation theory, [72] argued that the result of hidden sector sequestering, starting from an interacting SCFT in the UV, should really be:

$$m^2_{H_{u,d}} \to -\mathcal{C}_\Delta \mu^2 + (1-\mathcal{C}_\Delta) A^2_{u,d} \ , \quad B_\mu \to (1-\mathcal{C}_\Delta)\mu(A^*_u + A^*_d) \tag{3.16}$$

where $\mathcal{C}_\Delta$ is an OPE coefficient. This obviously differs from (3.15).

These previous studies of nontrivial hidden sector dynamics have all been based on RG evolution in the effective theory below the messenger scale. As we will see, in GMHM we instead work with the full theory and expand systematically in the couplings, expressing everything in terms of integrals over correlation functions. (In this sense GMHM is like a fixed-order calculation vs. the "running and matching" taken in previous works.) This allows for more precise control over the final answer and a clearer understanding of the interplay between different contributions. Using our general GMHM formulas, valid for any SUSY-breaking hidden sector and any messenger sector, we will show that – surprisingly – GMHM reproduces the claims of [70, 79] and (3.15), *even in strongly coupled cases where field redefinitions are not necessarily applicable*. We will reconcile the conformal perturbation theory RGEs derived in [72] with (3.15), vis a vis an approximate sum rule derived from the OPE.

Significantly, applying the GMHM formalism to models of hidden sector sequestering allows us to go beyond simply clarifying existing results. In particular, the case of complete sequestering advocated in [70, 79] is an idealized limit in which $M \gg \sqrt{F}$ and $\Delta \gg 2\Delta_h$.

However, phenomenological considerations [79, 80] and recent bounds on operator dimensions [81] constrain these respective inequalities, so that viable models are only partially sequestered and remain sensitive to the details of the hidden sector. As we will show, the GMHM formalism provides an efficient framework for computing the soft spectrum of such partially sequestered models.

The outline of our paper is as follows: In Section 2 we apply the GMHM formalism to the Higgs sector and obtain general NLO expressions for Higgs soft parameters given the portals (3.3) and (3.7). We demonstrate their power in Section 3 by computing Higgs soft parameters in the spurion limit and the SCFT limit. In Section 4 we connect our GMHM results to previous work on hidden sector sequestering by computing Higgs soft parameters in an effective theory framework. We find perfect agreement between our GMHM results and various methods for computing soft parameters in the effective theory. In the process we reconcile results from superconformal perturbation theory with GMHM through an approximate sum rule derived from the OPE. We reserve various technical details of the GMHM framework for Appendix A. In Appendix B, we describe a check of the superconformal perturbation theory RGEs and the validity of field redefinitions using a perturbative Banks-Zaks fixed point.

3.2 The Higgs in GMHM

3.2.1 General Higgs Mediation at NLO

In this section, we will derive correlator formulas for the Higgs soft parameters in GMHM. The first step is to expand in the direct Higgs-hidden-sector couplings (3.3), assuming a fully general hidden sector. In [23], this was performed to leading order in $\lambda_{u,d}$. Since a successful solution to the μ/B_μ and A/m_H^2 problems will have $B_\mu \lesssim \mu^2$ and $m_{H_u}^2 \lesssim A_u^2$, we must extend the results of [23] by going to NLO for the dimension-two soft masses. We

find:

$$\mu = \lambda_u \lambda_d \langle \mathcal{X}_\mu \rangle \tag{3.17}$$

$$A_{u,d} = |\lambda_{u,d}|^2 \langle \mathcal{X}_{A_{u,d}} \rangle \tag{3.18}$$

$$\hat{B}_\mu = \lambda_u \lambda_d \langle \mathcal{X}_{B_\mu} \rangle \tag{3.19}$$

$$\hat{m}^2_{H_{u,d}} = |\lambda_{u,d}|^2 \langle \mathcal{X}_{m^2_{H_{u,d}}} \rangle \tag{3.20}$$

where we have introduced the following notation for later convenience:[4]

$$\mathcal{X}_\mu = -\int d^4x \; Q^\alpha O_u(x) Q_\alpha O_d(0) \tag{3.21}$$

$$\mathcal{X}_{A_{u,d}} = +\int d^4x \; \bar{Q}^2 \Big[O_{u,d}(x) O^\dagger_{u,d}(0) \Big] \tag{3.22}$$

$$\mathcal{X}_{B_\mu} = -\int d^4x \; Q^2 O_u(x) Q^2 O_d(0) \left(1 + \sum_{i=u,d} |\lambda_i|^2 \int d^4z \, d^4z' Q^2 [O_i H_i(z)] \bar{Q}^2 [O_i^\dagger H_i^\dagger(z')] \right) \tag{3.23}$$

$$\mathcal{X}_{m^2_{H_{u,d}}} = -\int d^4x \; Q^2 \bar{Q}^2 \Big[O_{u,d}(x) O^\dagger_{u,d}(0) \Big] \left(1 + \sum_{i=u,d} |\lambda_i|^2 \int d^4z \, d^4z' Q^2 [O_i H_i(z)] \bar{Q}^2 [O_i^\dagger H_i^\dagger(z')] \right) \tag{3.24}$$

Note that we Wick rotated the formulas from [23] to Euclidean space, to avoid a proliferation of factors of i.

Since we are computing terms in an effective action, all diagrams contributing to (3.17) must be 1PI. This becomes an issue first at NLO order in $\lambda_{u,d}$, where we must contract the extra Higgs fields in the last two lines of (3.21). Shown in figure 3.2 are the different topologies for the diagrams at this order. Each blob is a connected (or if necessary, 1PI) hidden-sector correlator. The bottom two diagrams are interesting, since they involve *disconnected* hidden sector correlators. Let's now discuss these topologies in turn:

[4] A note about our slightly non-standard conventions for the supercharges Q_α and $\bar{Q}_{\dot{\alpha}}$. To avoid cluttering our formulas with irrelevant factors of two, we are normalizing Q and $\bar{Q}$ so that for a WZ model, $-\mathcal{L} = Q^4 K + (Q^2 W + c.c.)$. This differs from the more standard conventions of e.g. Wess and Bagger that would have 1/16 and 1/4 in front of the Kähler potential and superpotential respectively.

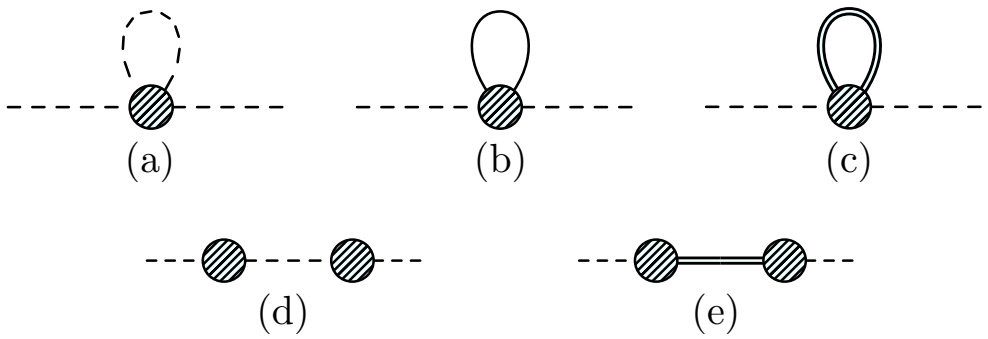

Figure 3.2: Topologies for the NLO expansion of the dimension-two soft parameters. The dashed lines, the solid line and the double lines represent the Higgs scalar, fermion and auxiliary propagators, respectively. The shaded blobs represent connected hidden-sector correlators. The diagrams on the bottom line are not 1PI and therefore do not contribute to $\hat{B}_\mu$ and $\hat{m}^2_{H_{u,d}}$. Note that there is no diagram of this type with an intermediate fermion line, as the individual correlators would have to be Grassmann odd.

1. Clearly, the three topologies[5] (a), (b), and (c) should always be included in the calculation of $m^2_{H_{u,d}}$ and B_μ.

2. The topology (d) should not contribute, since it is not 1PI. Note that these diagrams are always schematically of the form $m_1^2 \times \frac{1}{z^2} \times m_2^2$ where $m^2_{1,2}$ are shorthand for B_μ, $m^2_{H_{u,d}}$. So if the soft masses are further suppressed by an additional small parameter (such as the GMHM portal κ), then this topology will always be higher order in this parameter.

3. Finally, the topology (e) is not 1PI in the theory (3.4) that includes the Higgs auxiliary fields. However, these auxiliary fields must be integrated out, and the full dimension-two soft masses are given by (3.6). This corresponds precisely to adding back in the topology (e) of (3.2). For instance, taking the NLO contribution to $\langle \mathcal{X}_{B_\mu} \rangle$ with $i = u$, contracting the auxiliary Higgs propagators, and disconnecting the correlator, we obtain:

$$\int \delta^{(4)}(z - z') \Big\langle Q^2 O_u(x) Q^2 O_d(0)\, O_u(z) O_u^\dagger(z') \Big\rangle \to \int \Big\langle Q^2 O_u(x) O_u^\dagger(z) \Big\rangle \Big\langle Q^2 O_d(0) O_u(z) \Big\rangle \tag{3.25}$$

[5] An interesting subtlety about diagram (c): since the LO contribution is non-vanishing, the NLO contribution might be scheme dependent. In particular, employing the δ-function from contracting the Higgs F-components in (3.21) collides the operators O_i and $O_i^\dagger$, which can generate a UV divergence.

The integral on the right can be fully factorized using the translation invariance of both correlators and a simple change of variables. After putting back in all the couplings etc., this becomes $A_u^* \mu$. A complete set of such disconnected diagrams is shown in fig. 3. Taking all of these into account exactly reproduces (3.6).

To summarize, when computing the full B_μ and $m^2_{H_{u,d}}$, we should in fact include diagrams of the type (e) in (3.2), despite the fact that they do not appear to be 1PI at first glance. Meanwhile, disconnected correlators connected by a scalar propagator as in topology (d) must still be excluded from the NLO formulas.

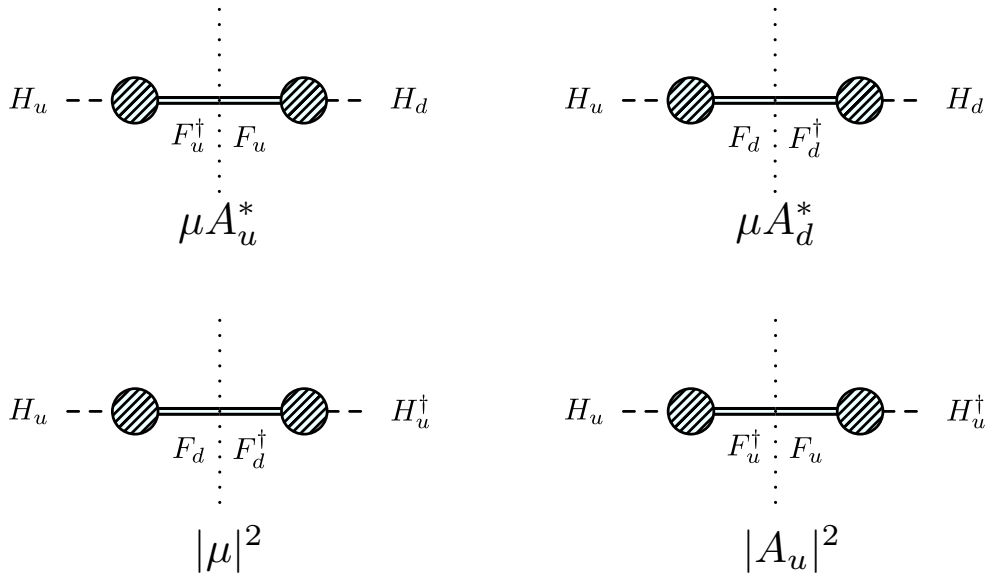

Figure 3.3: The NLO contributions to B_μ (upper two) and $m^2_{H_u}$ (lower two) involving contractions of the auxiliary fields of the Higgs multiplets. The contributions to $m^2_{H_d}$ are identical to $m^2_{H_u}$ upon switching $u \leftrightarrow d$ everywhere. When cut at the dotted line, these diagrams provide the extra contributions in (3.6).

3.2.2 Higgs soft parameters in GMHM

As discussed in the introduction, in the GMHM setup we further divide the overall hidden sector into a separate SUSY-breaking hidden sector and messenger sector, connected by a weakly-coupled portal. (We take the operators O_u and O_d to be in the messenger sector, as shown in (3.1).) Although in [78] more general portals were considered, in this paper we are focusing on the superpotential portal (3.7) for simplicity. We then expand in κ and factorize the correlators (3.17) into separate correlators of the messenger and hidden

sectors. Supersymmetry in the messenger sector then allows us to simplify the resulting expressions.

One general problem that immediately arises is that one typically finds both dimension-one soft masses and B_μ already at $\mathcal{O}(\kappa)$. This would be disastrous for EWSB, as it would imply $B_\mu \sim \mu \times M$, where M is the messenger scale. As we discuss more in Appendix A, a symmetry of the messenger sector that can forbid this while allowing for nonzero μ and $A_{u,d}$ (and gaugino masses) is an R-symmetry under which

$$R(O_m) = 2, \quad R(O_u) + R(O_d) = 4 \tag{3.26}$$

We will assume this R-symmetry throughout the paper.

With this in hand, we find that the GHM expressions (3.17) become, at the leading nonvanishing order in κ:

$$\mu = \lambda_u \lambda_d \kappa^* \langle \bar{Q}^2 O_h^\dagger \rangle_h \int d^4y \left\langle O_m^\dagger(y) \mathcal{X}_\mu \right\rangle_m \tag{3.27}$$

$$A_{u,d} = |\lambda_{u,d}|^2 \kappa^* \langle \bar{Q}^2 O_h^\dagger \rangle_h \int d^4y \left\langle O_m^\dagger(y) \mathcal{X}_{A_{u,d}} \right\rangle_m \tag{3.28}$$

$$\hat{B}_\mu = \lambda_u \lambda_d |\kappa|^2 \int d^4y\, d^4y' \left\langle Q^4 \left[O_h^\dagger(y) O_h(y') \right] \right\rangle_h \left\langle O_m(y) O_m^\dagger(y') \mathcal{X}_{B_\mu} \right\rangle_m \tag{3.29}$$

$$\hat{m}^2_{H_{u,d}} = |\lambda_{u,d}|^2 |\kappa|^2 \int d^4y\, d^4y' \left\langle Q^4 \left[O_h^\dagger(y) O_h(y') \right] \right\rangle_h \left\langle O_m(y) O_m^\dagger(y') \mathcal{X}_{m^2_{H_{u,d}}} \right\rangle_m \tag{3.30}$$

For more details, we refer the reader to Appendix A. Here the m and h subscripts denote correlators evaluated purely in the messenger and SUSY-breaking hidden sector, respectively. The integrated operators $\mathcal{X}_\mu$ etc. were defined in (3.21); now the components of the Higgs fields are understood to be contracted. In the last two lines we see that the answers always organize themselves so that they depend on a single hidden sector correlator, $\left\langle Q^4 \left[O_h^\dagger(y) O_h(y') \right] \right\rangle_h$.

As in the previous subsection, at NLO in $\lambda_{u,d}$, we must again deal with the issue of connected vs. disconnected correlators. The NLO topologies in GMHM are shown in (3.4), in direct analogy with (3.2). As argued in the previous subsection, topology (6) is the contribution (3.6) of integrating out $F_{H_{u,d}}$, so it must be included in the final result for B_μ and $m^2_{H_{u,d}}$. Due to the R-symmetry and supersymmetry, topologies (3) and (5) do not contribute. Finally, the other topologies must clearly be included since they are 1PI.

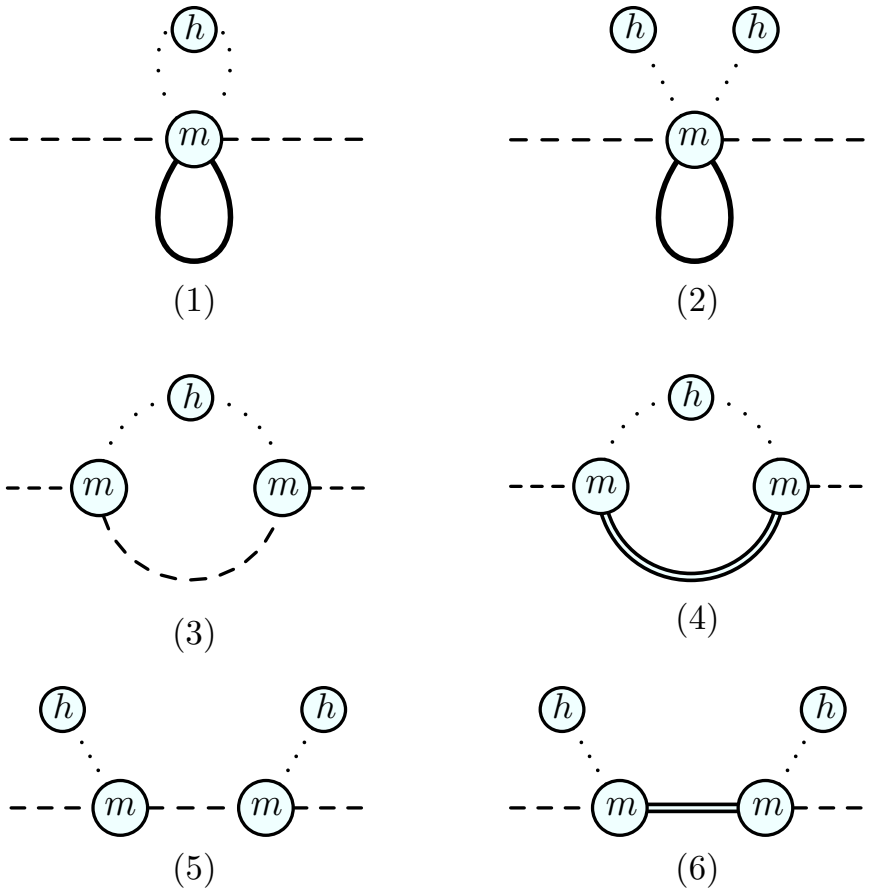

Figure 3.4: Possible topologies for the NLO in $\lambda_{u,d}$ contributions to the dimension-two soft parameters in GMHM. Blobs denoted with m (h) denote messsenger (hidden sector) correlators. The thick solid lines in (1) and (2) represent the sum of scalar, fermionic and auxiliary Higgs propagators.

Therefore, we conclude that *the full B_μ and $m^2_{H_{u,d}}$ are given by the full hidden and messenger correlators, to this order in the GMHM expansion.* The final formulas are thus simply

$$B_\mu = \lambda_u \lambda_d |\kappa|^2 \int d^4y\, d^4y' \left\langle Q^4 \left[O_h^\dagger(y) O_h(y') \right] \right\rangle_{h,full} \left\langle O_m(y) O_m^\dagger(y') \mathcal{X}_{B_\mu} \right\rangle_{m,full} \tag{3.31}$$

$$m^2_{H_{u,d}} = -|\mu|^2 + |\lambda_{u,d}|^2 |\kappa|^2 \int d^4y\, d^4y' \left\langle Q^4 \left[O_h^\dagger(y) O_h(y') \right] \right\rangle_{h,full} \left\langle O_m(y) O_m^\dagger(y') \mathcal{X}_{m^2_{H_{u,d}}} \right\rangle_{m,full} \tag{3.32}$$

where for $m^2_{H_{u,d}}$ we have subtracted out $|\mu|^2$ to adhere to the standard convention for these soft masses. These formulas are valid at $\mathcal{O}(|\kappa|^2)$ and up to $\mathcal{O}(|\lambda_{u,d}|^4)$, i.e. at the same order in the GMHM expansion as our results for μ^2, etc.

Let us conclude this section with one important observation about (3.31) that we will need later: even though the full messenger correlators – including disconnected parts – are

used in (3.31), in fact only the region of integration with $|y - y'| \lesssim 1/M$ contributes to the soft masses. The reason is that the full messenger correlators fall off exponentially at long distance:

$$\left\langle O_m(y) O_m^\dagger(y') \mathcal{X}_{B_\mu, m^2_{H_{u,d}}} \right\rangle_{m,full} \to 0 \;\text{ as }\; |y - y'| \gg 1/M \tag{3.33}$$

since effectively only connected messenger diagrams contribute after integrating out the Higgs auxiliary fields. (For more explicit details, we again refer the reader to Appendix A.) This implies that when $\sqrt{F} \ll M$ – as is generally the case in models of dynamical SUSY breaking – the hidden sector correlator is effectively at short distance and the expressions (3.31) can be further simplified using the OPE in the hidden sector. We will put this observation to work in the next section when we discuss hidden sectors that are approximately superconformal at the scale M.

3.3 Examples

The power of the GMHM formalism becomes apparent upon considering various special cases in which the general expressions (3.27) simplify further. As was shown in [78], illustrative examples include the well-known spurion limit employed in the study of many weakly-coupled models (such as those in [77, 48]); and the SCFT limit used to study hidden sector sequestering [69**?** , 79, 72, 80]. As we will see, the latter idea is especially attractive – although originally proposed for solving the μ/B_μ problem, we will show that it can work equally well for the A/m_H^2 problem. In the following subsections, we will consider these two special limits in turn, and show how they are reproduced in the GMHM framework.

3.3.1 Spurion limit

In the spurion limit, the hidden sector operator O_h has no nontrivial interactions, and all hidden-sector correlators are given by their fully disconnected components. Although it is not necessary for the spurion limit, for simplicity, we will take O_h to have canonical dimension $\Delta_h = 1$ in this subsection. So we have:

$$\langle Q^2 O_h \rangle_h = F\,, \qquad \langle Q^4 \big[O_h(x) O_h^\dagger(0) \big] \rangle_{h,full} = |\langle Q^2 O_h \rangle_h|^2 = |F|^2 \tag{3.34}$$

The formulas for μ and $A_{u,d}$ are identical to those in (3.27). For B_μ and $m^2_{H_{u,d}}$, we saw in the previous section that the fully disconnected contributions (i.e. disconnecting both hidden and messenger correlators) are precisely those of integrating out $F_{H_{u,d}}$ as in (3.6). Thus from (3.31), we have:

$$B_\mu = \mu(A_u^* + A_d^*) + \lambda_u\lambda_d|\kappa|^2|F|^2 \int d^4y\, d^4y' \left\langle O_m(y)O_m^\dagger(y')\mathcal{X}_{B_\mu}\right\rangle_{m,connected} \tag{3.35}$$

$$m^2_{H_{u,d}} = |A_{u,d}|^2 + |\lambda_{u,d}|^2|\kappa|^2|F|^2 \int d^4y\, d^4y' \left\langle O_m(y)O_m^\dagger(y')\mathcal{X}_{m^2_{H_{u,d}}}\right\rangle_{m,connected} \tag{3.36}$$

Here we see that whether there is a μ/B_μ or A/m_H^2 problem depends on the messenger sector in the following manner:

1. If the messenger sector is strongly coupled, then loop counting is not well-defined, and there need not be any problem with μ/B_μ or A/m_H^2. However, there is not much more that we can say about this scenario, since the messenger sector is strongly coupled and typically incalculable, and statements about the parametric form of the soft masses are exhausted by dimensional analysis.

2. If instead the messenger sector is weakly coupled, then the messenger correlators can be computed, and they generally include a loop factor $(1/16\pi^2)$ in addition to dimensional analysis. For generic messenger sectors, the connected correlators in (3.35) are non-zero at one loop, which results in

$$\mu \sim \frac{\lambda_u\lambda_d}{16\pi^2}\frac{F}{M} \qquad B_\mu \sim \frac{\lambda_u\lambda_d}{16\pi^2}\frac{F^2}{M^2} \qquad A_{u,d} \sim \frac{|\lambda_{u,d}|^2}{16\pi^2}\frac{F}{M} \qquad m^2_{H_{u,d}} \sim \frac{|\lambda_{u,d}|^2}{16\pi^2}\frac{F^2}{M^2}. \tag{3.37}$$

   Now the μ/B_μ and A/m_H^2 problems are manifest. So, in contrast to the strongly-coupled case, a weakly coupled messenger sector typically implies the existence of a μ/B_μ and A/m_H^2 problem.

The A/m_H^2 problem is especially manifest in (3.35), since using (3.21) we can rewrite the LO formulas for A and m_H^2 as:

$$A_{u,d} = |\lambda_{u,d}|^2\kappa^* F\partial_{M^*}Z_{u,d}, \qquad (m^2_{H_{u,d}})_{LO} = -|\lambda_{u,d}|^2|\kappa F|^2\partial_M\partial_{M^*}Z_{u,d} \tag{3.38}$$

with $Z_{u,d} \equiv \int d^4x\, \langle O^\dagger_{u,d}(x)O_{u,d}(0)\rangle_m$, where we have imagined deforming the messenger sector by $\delta W = MO_m$. This form of $A_{u,d}$ and $m^2_{H_{u,d}}$ indicates that, to leading order in

$\frac{F}{M^2}$, they generically arise at the same loop order in the messenger sector (when "loop order" is well-defined). This is the GMHM analogue of the argument using field strength renormalization that was presented in [77].

As shown in [77], MGM is the unique solution to the A/m_H^2 problem in the weakly-coupled messenger + spurion limit. In this case, the second derivative in (3.38) vanishes because the correlator in question evaluates to $\log MM^*$. One-loop contributions to m_H^2 still exist, but they are higher order in κ, i.e. they are suppressed by F/M^2. The same solution does not apply to μ/B_μ because the relevant correlator does not generally factorize into terms holomorphic and anti-holomorphic in M, though it may be arranged in more elaborate models with additional scales [47]. In [77], the μ/B_μ problem was avoided by taking $\lambda_d = 0$, while μ and B_μ were then generated using an extension to the NMSSM along the lines of [41, 46].

Finally, let us comment on the "little A/m_H^2 problem." This is manifested by the presence of the $A_{u,d}^2$ term in (3.35). Even if the 1-loop contribution to $m_{H_u}^2$ is dealt with through the MGM mechanism, large A-terms still imply a large 2-loop contribution to $m_{H_u}^2$, which drastically increases the tuning of the model or impedes electroweak symmetry breaking altogether. We emphasize that this is a universal feature of models with SUSY breaking spurions that generate large A-terms through Higgs-messenger couplings. The problem can ultimately be traced back to the relation $\langle Q^4\big[O_h(x)O_h^\dagger(0)\big]\rangle_{h,full} = |\langle Q^2 O_h\rangle_h|^2$, which is a consequence of the triviality of the spurion limit. When hidden sector interactions are accounted for, we may instead have $\langle Q^4\big[O_h(x)O_h^\dagger(0)\big]\rangle_{h,full} \ll |\langle Q^2 O_h\rangle_h|^2$, thus providing a route for solving the little A/m_H^2 problem. This strongly motivates going beyond the spurion limit in the hidden sector, as we consider in the next subsection.

3.3.2 Models with hidden sector SCFTs

In these models we take $\sqrt{F} \ll M$, with the hidden sector described by an approximate SCFT at and above the scale M. Then, as discussed below (3.31), the hidden sector correlator $\langle Q^4[O_h^\dagger(y)O_h(y')]\rangle_{h,full}$ is always pinned by the messenger sector correlator at $|y-y'| \lesssim \frac{1}{M} \ll \frac{1}{\sqrt{F}}$, i.e. at short distance. So we can apply the OPE of the SCFT to it:

$$O_h(y)O_h^\dagger(y') \sim |y-y'|^{-2\Delta_h}\mathbf{1} + \mathcal{C}_\Delta |y-y'|^\gamma O_\Delta(y') + \dots \tag{3.39}$$

where

$$\gamma \equiv \Delta - 2\Delta_h \tag{3.40}$$

Here $\mathbf{1}$ is the unit operator (it drops out under the action of Q^4), and O_Δ (with dimension Δ) is the lowest-dimension scalar operator in the UV fixed point of the hidden sector. The $\ldots$ denotes terms with higher-dimension operators; we neglect them here as they will be further suppressed by F/M^2. Substituting this into (3.31) we obtain

$$B_\mu \approx \lambda_u \lambda_d |\kappa|^2 \mathcal{C}_\Delta \langle Q^4 O_\Delta \rangle_h \int d^4y\, d^4y'\, |y-y'|^\gamma \Big\langle O_m(y) O_m^\dagger(y') \mathcal{X}_{B_\mu} \Big\rangle_{m,full} \tag{3.41}$$

$$m^2_{H_{u,d}} \approx -|\mu|^2 + |\lambda_{u,d}|^2 |\kappa|^2 \mathcal{C}_\Delta \langle Q^4 O_\Delta \rangle_h \int d^4y\, d^4y'\, |y-y'|^\gamma \Big\langle O_m(y) O_m^\dagger(y') \mathcal{X}_{m^2_{H_{u,d}}} \Big\rangle_{m,full} \tag{3.42}$$

As in the spurion limit, the general expressions for μ and $A_{u,d}$ again remain unchanged with respect to (3.27). So if $\gamma > 0$ (i.e. $\Delta > 2\Delta_h$) and $\sqrt{F} \ll M$, the contributions proportional to $\langle Q^4 O_\Delta \rangle_h$ are subleading with respect to those proportional to $|\langle Q^2 O_h \rangle_h|^2$, and they are suppressed relative to μ^2 and $A^2_{u,d}$. This is precisely the phenomenon of hidden-sector sequestering [69–71], as seen from the point of view of GMHM. From (3.41), we note that the $-|\mu|^2$ contribution to $m^2_{H_{u,d}}$ is the only unsequestered contribution to the soft masses; in particular, there is no unsequestered contribution involving the OPE coefficient. We will comment more on the physical interpretation of this fact, and its relation to previous work, in the following section.

The idea of hidden-sector sequestering was originally proposed in order to solve the long-standing μ/B_μ problem. Now with the need for large A-terms forced upon us by a Higgs at 125 GeV, we also have the A/m_H^2 problem to contend with. We see from (3.41) that sequestering has the potential to solve both problems simultaneously. But despite its theoretical elegance, this approach suffers from a number of practical challenges. Foremost, it is difficult to achieve proper electroweak symmetry breaking with the fully sequestered boundary condition $B_\mu \approx 0$ and $m^2_{H_{u,d}} \approx -|\mu|^2$ [79, 80]. Moreover, recent developments in the understanding of 4D SCFT's have resulted in strict upper bounds on the allowed anomalous dimensions [81]. These bounds have made it increasingly difficult to envision a realistic setup where the anomalous dimensions and separation between $\sqrt{F}, M$ are large enough to achieve the desired amount of sequestering.

The GMHM expressions (3.41) point to possible ways out of these difficulties. For example, we see that the sequestered contributions in (3.41) depend on the OPE coefficient $\mathcal{C}_\Delta$. So if this is small for some reason, then we can again overcome the infamous loop factors. This is an entirely separate mechanism for solving the μ/B_μ and A/m_H^2 problems that has not been considered before. Alternatively, one could combine a relatively small OPE coefficient with some realistic amount of sequestering. The expressions in (3.41) provide a calculable setup to further investigate such partially sequestered models [82].

In both of these solutions, the burden of addressing the μ/B_μ and A/m_H^2 problems is shifted towards the hidden sector. This is in contrast to spurion-based models, where the messenger sector does all the legwork. From (3.41) we can see another important difference with the spurion limit, as *both* the 1-loop and the 2-loop contributions are susceptible to sequestering and the smallness of the OPE coefficient. Therefore a solution to the μ/B_μ and A/m_H^2 problems through sequestering, a small OPE coefficient, or some combination of the two, automatically implies a solution to the little A/m_H^2 problem.

3.4 Comparison with effective theory

Previous studies of hidden sector dynamics have worked in terms of the effective theory below the messenger scale M, in which the Higgs sector and hidden sector are coupled through irrelevant operators in the Kähler potential [69–71, 79, 72]. Furthermore, these studies have relied on using the RG to evolve down to the SUSY-breaking scale $\sqrt{F} \ll M$ in order to extract the physical soft parameters. In this section we re-visit the effective theory approach and show how its results can be matched to the GMHM calculation presented in Section 2 (which is more analogous to a fixed-order calculation in a full theory).

The hidden sector may or may not be strongly coupled at the scale M. Either way, we will assume for simplicity that it is approximately superconformal, i.e. that M is well-separated from all the other mass scales in the hidden sector. So we are in the SCFT limit of GMHM described in the previous subsection. Upon integrating out the messenger sector,

the effective theory at the scale M is of the form

$$\mathcal{L}_{eff} \supset \int d^4\theta \sum_i \left[\frac{c_\mu(M)}{M^{\Delta_h}} O_h^\dagger H_u H_d + \frac{c_{B_\mu,i}(M)}{M^{\Delta_i}} O_{\Delta_i} H_u H_d + \text{h.c.} \right.$$
$$\left. + \frac{c_{A_{u,d}}(M)}{M^{\Delta_h}} O_h^\dagger H_{u,d}^\dagger H_{u,d} + \text{h.c.} + \frac{c_{m_{u,d},i}(M)}{M^{\Delta_i}} O_{\Delta_i} H_{u,d}^\dagger H_{u,d} \right] \quad (3.43)$$

where O_h is a hidden-sector chiral operator with an F-term expectation value, while the O_{Δ_i} are non-chiral operators that appear in the OPE (3.39) of $O_h^\dagger$ and O_h. Previous approaches have only focused on the leading operator appearing in the OPE, but in general there are many such operators germane to the effective theory. For example, in Appendix B we construct an explicit Banks-Zaks example with two nontrivial O_{Δ_i}. Unlike in the GMHM calculation, it will be important to keep track of all the operators in the OPE, because of the potentially unsequestered contributions in (3.16)

The numerical values of the coefficients $c_\mu, c_{B_\mu,i}, c_{A_{u,d}}, c_{m_{u,d},i}$ at the scale M depend on the details of the hidden sector and messenger sector, and they are fixed by matching to the full theory. With this effective theory in hand, the Higgs sector soft parameters may be computed in three equivalent ways: (1) by direct calculation in the effective theory with cutoff M; (2) by RG evolution of the coefficients c_i to a lower scale E satisfying $\sqrt{F} \ll E < M$ followed by calculation in the effective theory (still assumed to be superconformal) with cutoff E; and (3) RG evolving down to a scale $E \ll \sqrt{F}$ and "freezing-out" the SCFT dynamics by just substituting operator vevs, i.e. transitioning to the spurion limit where there are no nontrivial correlation functions. (Keep in mind that operator dimensions need not be canonical in the spurion limit.) The third approach has been taken by previous works, with the further assumption that the transition to the spurion limit happens abruptly at $\sqrt{F}$. But it is very instructive to perform the calculation all three ways and compare with the predictions from GMHM. We can also compare the GMHM and direct effective theory results to arguments from field redefinitions when the hidden sector starts at a UV free fixed point.

3.4.1 Direct calculation in the effective theory with cutoff M

To compute the Higgs sector soft parameters directly in the effective theory, we imagine performing the path integral over the effective theory with the momentum of hidden sector

fields and loops of Higgs doublets restricted to lie below the Wilsonian cutoff M. The leading contributions from operators involving the O_{Δ_i} are trivially computed by treating $H_{u,d}$ as background fields. There are also contributions to soft parameters quadratic in c_μ and $c_{A_{u,d}}$; these correspond to NLO contributions to the GMHM result coming from disconnected messenger correlators.

The calculation of the full soft mass proceeds entirely in parallel to the GMHM calculation. For simplicity we will focus on the scalar masses $m^2_{H_{u,d}}$; the calculation for B_μ is analogous. The linear O_{Δ_i} contributions are straightforward; working in the effective theory (3.43) to leading order in $c_{m_{u,d},i}$, we simply have:

$$m^2_{H_{u,d}}\Big|_{linear} = -\sum_i \frac{c_{m_{u,d},i}(M)}{M^{\Delta_i}} \langle Q^4 O_{\Delta_i}\rangle_M \tag{3.44}$$

Here and below, the subscript M will denote correlation functions evaluated in the effective theory with cutoff M. Turning now to the contributions quadratic in c_μ and $c_{A_{u,d}}$, after some manipulations we have for example

$$m^2_{H_{u,d}}\Big|_{quadratic} \supset \frac{|c_{A_{u,d}}(M)|^2}{M^{2\Delta_h}} \int d^4x \left\langle Q^4[O_h^\dagger(x) O_h(0)]\right\rangle_M \partial^2 \langle H^\dagger_{u,d}(x) H_{u,d}(0)\rangle_M \tag{3.45}$$

At this stage, simply substituting a free propagator for the Higgs correlator in (3.45) is evidently problematic; integrating over x would give rise to a pure contact term. This reflects the fact that the contribution being computed here is only sensitive to physics above the cutoff. Indeed, this agrees with the GMHM result – as discussed at the end of Section 2, the hidden sector correlator for disconnected contributions is pinned by the messenger correlators at distances $\lesssim 1/M$, and so it does not accumulate any significant contributions from below the scale M.

We can regulate the contact term in (3.45) any number of ways; different choices correspond to different prescriptions for matching with the full GMHM calculation. One useful regulator is to replace the delta function at $x = 0$ with a (radial) delta function at $|x| = 1/M$. As we will see below, this has the useful advantage of respecting both the physical cutoff at M and the assumed abrupt transition to the spurion limit when the sliding cutoff is taken to $\sqrt{F}$. As such, we can apply this scheme uniformly to the various effective theory cases of interest and absorb all scheme-dependence into a single set of matching conditions at M.

Substituting the general OPE (3.39) and applying the regulator to (3.45), we obtain

$$m^2_{H_{u,d}}\Big|_{quadratic} \supset \sum_i \frac{|c_{A_{u,d}}(M)|^2}{M^{\Delta_i}} \mathcal{C}_{\Delta_i} \langle Q^4 O_{\Delta_i} \rangle_M \tag{3.46}$$

where $\mathcal{C}_{\Delta_i}$ and γ_i are defined as in (3.39). The calculation of the $|c_\mu|^2$ contribution is entirely analogous, although here we must remember to subtract out the fully disconnected contribution $|\mu|^2$, since this is conventionally not included in the definition of $m^2_{H_{u,d}}$. Repeating the same procedure for B_μ and combining the various contributions, the general effective theory result is

$$B_\mu = -\sum_i \left(\frac{c_{B_\mu,i}(M) - \mathcal{C}_{\Delta_i} c_\mu(M)(c^*_{A_u}(M) + c^*_{A_d}(M))}{M^{\Delta_i}} \right) \langle Q^4 O_{\Delta_i} \rangle_M \tag{3.47}$$

$$m^2_{H_{u,d}} = -|\mu|^2 - \sum_i \left(\frac{c_{m_{u,d},i}(M) - \mathcal{C}_{\Delta_i}(|c_{A_{u,d}}(M)|^2 + |c_\mu(M)|^2)}{M^{\Delta_i}} \right) \langle Q^4 O_{\Delta_i} \rangle_M \tag{3.48}$$

The dependence of the soft terms only on the composite vevs $\langle Q^4 O_{\Delta_i} \rangle$, and not on $|\langle Q^2 O_h \rangle|^2$, is in complete agreement with the result (3.41) from GMHM in the SCFT limit. The specific linear combinations of coefficients appearing in (3.47) may be used to fix the matching of $c_{m_{u,d},i}, c_{B_\mu,i}$ with the $\mathcal{O}(\lambda^4)$ terms in the GMHM result for $m^2_{H_{u,d}}$ and B_μ.

3.4.2 Effective theory with cutoff $\sqrt{F} \ll E < M$: testing the RGEs

Alternately, we may compute the soft parameters in a different effective theory with a cutoff $E < M$ by evolving the coefficients $c_i(M)$ to the scale E via RG running and repeating the direct calculation of scalar masses in the new effective theory. The scalar masses should, of course, agree with the result obtained in the theory with cutoff M. This procedure is completely straightforward in effective theories with cutoff $E \gg \sqrt{F}$, where the hidden sector is still an SCFT at the cutoff and the regularization scheme can be maintained. We refer the reader to [72, 83] for the details of computing beta functions using superconformal perturbation theory. One thing to keep in mind is that to preserve the result for the soft masses, it is crucial to use the same regulator and scheme as in (3.46). The result for the

beta functions between M and $\sqrt{F}$ is:

$$\beta_{c_\mu} = \Delta_h c_\mu \tag{3.49}$$

$$\beta_{c_{A_{u,d}}} = \Delta_h c_{A_{u,d}} \tag{3.50}$$

$$\beta_{c_{m_{u,d},i}} = \Delta_i c_{m_{u,d},i} - \gamma_i \mathcal{C}_{\Delta_i}(|c_\mu|^2 + |c_{A_{u,d}}|^2) \tag{3.51}$$

$$\beta_{c_{B_\mu,i}} = \Delta_i c_{B_\mu,i} - \gamma_i \mathcal{C}_{\Delta_i} c_\mu (c^*_{A_u} + c_\mu c^*_{A_d}) \tag{3.52}$$

In general, integrating the beta functions from M to E yields

$$|c_\mu(E)|^2 = |c_\mu(M)|^2 \left(\frac{E}{M}\right)^{2\Delta_h} \qquad |c_{A_{u,d}}(E)|^2 = |c_{A_{u,d}}(M)|^2 \left(\frac{E}{M}\right)^{2\Delta_h} \tag{3.53}$$

$$c_{m_{u,d},i}(E) = c_{m_{u,d},i}(M) \left(\frac{E}{M}\right)^{\Delta_i} - \mathcal{C}_{\Delta_i}\left(|c_\mu(M)|^2 + |c_{A_{u,d}}(M)|^2\right)\left[\left(\frac{E}{M}\right)^{\Delta_i} - \left(\frac{E}{M}\right)^{2\Delta_h}\right] \tag{3.54}$$

$$c_{B_\mu,i}(E) = c_{B_\mu,i}(M) \left(\frac{E}{M}\right)^{\Delta_i} - \mathcal{C}_{\Delta_i} c_\mu(M)\left(c^*_{A_u}(M) + c^*_{A_d}(M)\right)\left[\left(\frac{E}{M}\right)^{\Delta_i} - \left(\frac{E}{M}\right)^{2\Delta_h}\right] \tag{3.55}$$

The calculation of soft masses in the theory with cutoff E proceeds in the SCFT limit precisely as above, with the replacement $M \to E$:

$$B_\mu = -\sum_i \left(\frac{c_{B_\mu,i}(E) - \mathcal{C}_{\Delta_i} c_\mu(E)(c^*_{A_u}(E) + c^*_{A_d}(E))}{E^{\Delta_i}}\right)\langle Q^4 O_{\Delta_i}\rangle_E \tag{3.56}$$

$$m^2_{H_{u,d}} = -|\mu|^2 - \sum_i \left(\frac{c_{m_{u,d},i}(E) - \mathcal{C}_{\Delta_i}(|c_{A_{u,d}}(E)|^2 + |c_\mu(E)|^2)}{E^{\Delta_i}}\right)\langle Q^4 O_{\Delta_i}\rangle_E \tag{3.57}$$

Note that at a superconformal fixed point, operator wavefunction renormalization is trivial, and so $\langle Q^4 O_{\Delta_i}\rangle$ does not change between M and E. Substituting the integrated couplings (3.53) into (3.56), we again obtain (3.47). Of course, the fact that running alone yields agreement between the two calculations is not surprising, since there are no physical thresholds between M and E. This serves as an check of the RGEs that were derived independently using superconformal perturbation theory in [72].

3.4.3 Effective theory below $\sqrt{F}$

Finally, we come to the most commonly considered case in the literature: RG evolving down to the scale $\sqrt{F}$ and "freezing-out" the SCFT dynamics by just substituting operator

vevs – in other words, transitioning abruptly to the spurion limit. We imagine that just above the scale $\sqrt{F}$, some unspecified relevant operator in the SCFT turns on and drives it very quickly to a SUSY-breaking vacuum. Then right above $\sqrt{F}$, the couplings (3.53) obtained using the superconformal RGEs should be valid, while right below $\sqrt{F}$, the hidden sector is gapped and we should be in the spurion limit. Computing the dimension-two soft parameters in the spurion theory, we find:

$$m^2_{H_{u,d}} = -|\mu|^2 - \sum_i \frac{c_{m_{u,d},i}(\sqrt{F})}{(\sqrt{F})^{\Delta_i}} \langle Q^4 O_{\Delta_i} \rangle_{\sqrt{F}} + \frac{|c_\mu(\sqrt{F})|^2 + |c_{A_{u,d}}(\sqrt{F})|^2}{(\sqrt{F})^{2\Delta_h}} |\langle Q^2 O_h \rangle_{\sqrt{F}}|^2 \tag{3.58}$$

$$B_\mu = -\sum_i \frac{c_{B_\mu,i}(\sqrt{F})}{(\sqrt{F})^{\Delta_i}} \langle Q^4 O_{\Delta_i} \rangle_{\sqrt{F}} + \frac{c_\mu(\sqrt{F})(c^*_{A_u}(\sqrt{F}) + c^*_{A_d}(\sqrt{F}))}{(\sqrt{F})^{2\Delta_h}} |\langle Q^2 O_h \rangle_{\sqrt{F}}|^2 \tag{3.59}$$

Substituting (3.53) into (3.58) with $E \to \sqrt{F}$, we have

$$\begin{aligned} m^2_{H_{u,d}} = -|\mu|^2 &- \sum_i \left(\frac{c_{m_{u,d},i}(M) - \mathcal{C}_{\Delta_i} \left(|c_\mu(M)|^2 + |c_{A_{u,d}}(M)|^2 \right)}{M^{\Delta_i}} \right) \langle Q^4 O_{\Delta_i} \rangle_{\sqrt{F}} \\ &+ \frac{|c_\mu(M)|^2 + |c_{A_{u,d}}(M)|^2}{M^{2\Delta_h}} \Delta S \end{aligned} \tag{3.60}$$

$$\begin{aligned} B_\mu = -\sum_i &\frac{c_{B_\mu,i}(M) - \mathcal{C}_{\Delta_i} c_\mu(M) \left(c^*_{A_u}(M) + c^*_{A_d}(M) \right)}{M^{\Delta_i}} \langle Q^4 O_{\Delta_i} \rangle_{\sqrt{F}} \\ &+ \frac{c_\mu(M)(c^*_{A_u}(M) + c^*_{A_d}(M))}{M^{2\Delta_h}} \Delta S \end{aligned} \tag{3.61}$$

where

$$\Delta S \equiv |\langle Q^2 O_h \rangle_{\sqrt{F}}|^2 - \sum_i \mathcal{C}_{\Delta_i} (\sqrt{F})^{-\gamma_i} \langle Q^4 O_{\Delta_i} \rangle_{\sqrt{F}} \tag{3.62}$$

Comparing this with (3.47), we see that there is an apparent disagreement. In particular, the answer in the spurion theory seems to have "unsequestered" contributions $\propto (\sqrt{F}/M)^{2\Delta_h}$. This result illustrates the fact that, in general, threshold corrections to the couplings $c_{B_\mu,i}$ and $c_{m_{u,d},i}$ at the scale $\sqrt{F}$ cannot be neglected.

At the same time, it is also true that our regularization scheme (see the discussion around (3.45)) minimizes these threshold corrections. The key ingredient here is the continuity of the OPE. If the theory transitions abruptly to the spurion limit at a scale $\sqrt{F}$, then

continuity of the OPE demands:

$$|\langle Q^2 O_h\rangle_{\sqrt{F}}|^2 \approx \langle Q^4[O_h(x)O_h(0)]\rangle_{\sqrt{F}}\big|_{|x|=1/\sqrt{F}} \approx \sum_i \mathcal{C}_{\Delta_i}(\sqrt{F})^{-\gamma_i}\langle Q^4 O_{\Delta_i}\rangle_{\sqrt{F}} \tag{3.63}$$

Substituting this into (3.60), we find that the threshold corrections are minimized, and the result is brought into agreement with previous effective theory calculations and the GMHM expectation. In the limit $\Delta_i \gg 2\Delta_h$, the $\langle Q^4 O_{\Delta_i}\rangle$ terms are negligible, and we indeed find

$$m^2_{H_{u,d}} \approx -|\mu|^2, \qquad B_\mu \approx 0 \tag{3.64}$$

as claimed in [70, 79].

Had we chosen a different regularization scheme in (3.45), e.g. a smoother regulator that smears out the integrand in (3.45) around the cutoff, then the second term in ΔS would have been correspondingly smeared. Then the OPE sum rule (3.63) would not have accounted for ΔS, and additional threshold corrections to the couplings would have been required.[6] In a sense, our choice of radial delta function regularization is particularly appropriate in that it is abrupt and localized at the cutoff, in the same way that our transition to the spurion limit is taken to be abrupt. This allows us to maintain the same regularization scheme in effective theories above and below $\sqrt{F}$ and smoothly absorb all scheme dependence into matching at the scale M.

3.4.4 Field redefinitions

Finally, we can compare both results to the soft parameter predictions obtained via field redefinition at a UV free fixed point as in [79]. If the hidden sector is weakly interacting at the scale M, and O_h is a dimension-one elementary field, then the only nontrivial operator in the OPE is $O_{\Delta_1} \sim O_h^\dagger O_h$ and the terms linear in O_h in (3.43) are redundant, i.e., may be eliminated by field redefinitions. Such UV free theories are only a restricted subset of models amenable to treatment by our formalism, but they provide a useful check.

In this case, the terms proportional to $c_{A_{u,d}}$ may be eliminated by the redefinition

$$H_{u,d} \to \tilde{H}_{u,d} = H_{u,d}(1 + c_{A_{u,d}} O_h^\dagger/M) \tag{3.65}$$

[6] Even in this case, one can check that in the limit $\gamma_i \ll 1$, the beta functions and soft masses become scheme independent to leading order in γ_i and the matching procedure at $\sqrt{F}$ is likewise insensitive to the details of exiting the SCFT.

which leads to an equivalent effective theory at the scale M

$$\mathcal{L} \supset \int d^4\theta \left[\frac{c_\mu}{M} O_h^\dagger \tilde{H}_u \tilde{H}_d + \frac{c_{B_\mu} - c_\mu (c_{A_u}^* + c_{A_d}^*)}{M^2} O_h^\dagger O_h \tilde{H}_u \tilde{H}_d + \text{h.c.} \right. \tag{3.66}$$

$$\left. + \frac{c_{m_{u,d}} - |c_{A_{u,d}}|^2}{M^2} O_h^\dagger O_h \tilde{H}_{u,d}^\dagger \tilde{H}_{u,d} + \dots \right] \tag{3.67}$$

where the ellipses denote terms of cubic order or higher in hidden sector fields (i.e., higher order in κ in the GMHM approach). In this effective theory there are no additional contributions to Higgs soft masses proportional to $|c_{A_{u,d}}|^2$.

To compute the physical mass of the scalar doublet $\tilde{H}_u$, we may treat it as a background field, keeping $\tilde{H}_d, O_h$ as dynamical fields and performing the field redefinition

$$\tilde{H}_d \to \tilde{H}_d' = \tilde{H}_d + \frac{c_\mu^*}{M} O_h \tilde{H}_u^\dagger \tag{3.68}$$

where the apparently non-holomorphic field redefinition preserves supersymmetry because $\tilde{H}_u$ is simply a background field. Now there are also no additional contributions proportional to $|c_\mu|^2$, and the calculation of soft masses is straightforward. In this theory the physical mass of the scalar $\tilde{H}_u$ is simply

$$m_{\tilde{H}_u}^2 = -|\mu|^2 - \frac{c_{m_u}(M) - |c_{A_u}(M)|^2 - |c_\mu(M)|^2}{M^2} \langle Q^4 (O_h^\dagger O_h) \rangle_M \tag{3.69}$$

From this we can infer the soft mass, and it is in complete agreement with the results from GMHM and the effective theory. Analogous arguments hold for the calculation of $m_{H_d}^2$ and B_μ. Note that here $\langle Q^4 (O_h^\dagger O_h) \rangle_M \neq |F|^2$, since by assumption the hidden sector is asymptotically free and the operator vev reflects sequestering due to nontrivial dynamics below the scale M.

To summarize, we have found agreement between the Higgs sector soft parameters as computed in GMHM and the soft parameters computed by a variety of approaches in the effective theory below the messenger scale: directly in the effective theory defined at the scale M; in effective theories with cutoffs above and below $\sqrt{F}$; and via field redefinition in the effective theory when the hidden sector is weakly coupled at the scale M. The key to reconciling the weakly-coupled results of [70, 79] with the superconformal perturbation theory result of [72] is the approximate operator vev sum rule (3.63) imposed by the OPE.

Of course, thus far our discussion has remained fairly abstract. We validate certain features of our analysis by comparison with explicit perturbative calculations in a toy Banks-Zaks model, the details of which we reserve for Appendix B.

3.5 Conclusions and future directions

The discovery of a Higgs near 125 GeV poses significant challenges for minimal supersymmetry. If electroweak symmetry breaking is natural, either the Higgs sector must be extended – often at the expense of other attractive features of the MSSM such as perturbative gauge coupling unification – or A-terms must be large. While this latter option is attractive, it poses a particular challenge for calculable models where intrinsic A terms are naturally small. Introducing new interactions to generate A terms results in the A/m_H^2 problem, i.e., unwanted contributions to other soft terms that threaten EWSB and supersymmetric naturalness.

Yet the A/m_H^2 problem is but one symptom of a broader sickness in the Higgs sector of calculable models. Beyond confronting the A/m_H^2 problem to accommodate the observed Higgs mass, calculable models must also confront the more familiar μ/B_μ problem to achieve EWSB. In addition, we see from (3.6) that such models also potentially suffer from the little A/m_H^2 problem, even if the one loop contribution to $m_{H_u}^2$ vanishes. The ubiquity and tenaciousness of these problems in calculable models with weakly-coupled hidden sectors strongly favors hidden sectors with non-trivial dynamics. In this case, powerful tools are required in order to make concrete predictions for the physical spectrum.

In this work, we have developed a framework for computing the soft spectrum arising from general Higgs-messenger interactions in theories where the SUSY-breaking dynamics factorizes into arbitrary messenger and hidden sectors. We compute soft parameters in a supersymmetric correlator formalism through a double expansion in the portals connecting the Higgs, messenger, and hidden sectors. This approach allows us to identify general solutions to the μ/B_μ and A/m_H^2 problems. An essential key is that while μ and $A_{u,d}$ depend on the one-point function $\langle Q^2 O_h \rangle_h$ in the hidden sector, B_μ and $m_{H_{u,d}}^2$ depend on the two-point function $\langle Q^4 (O_h^\dagger(y) O_h(y')) \rangle_h$. Although in spurion models these two are trivially related, more generally they need not have anything to do with one another.

Although our results are quite general, we demonstrate their power by using them to compute the soft spectrum for hidden sectors in the spurion and SCFT limits. In the SCFT limit, we make contact with previous approaches to hidden sector sequestering [69–71, 79, 72]. In particular, we resolve a long-standing disagreement between different approaches to hidden-sector sequestering, validating the results obtained via field redefinitions and reconciling previously conflicting results from superconformal perturbation theory using an approximate sum rule derived from the OPE. However, our general formalism allows us to go beyond the case of full sequestering considered in previous works and compute the soft spectrum in the case of partial sequestering, where hidden sector anomalous dimensions conspire with details of the hidden sector to yield potentially viable phenomenology. This is particularly attractive since the idealized limit of full sequestering appears increasingly unrealistic due to both limits on operator dimensions [81] and tightly constrained parametrics [79, 80]. In partially sequestered scenarios, SCFT data (such as OPE coefficients and operator dimensions), operator vevs, and numerical coefficients all play important roles in solving the μ/B_μ and A/m_H^2 problems. Interestingly, in contrast with the spurion limit, a solution to the A/m_H^2 problem in this context automatically guarantees a solution to the little A/m_H^2 problem. Moreover these models have much more parametric freedom compared to the fully sequestered case, and exhibit novel phenomenology that we will explore in detail in future work [82].

Let us conclude by highlighting a variety of interesting future directions:

1. Much as GGM delineated the full parametric freedom available in gauge mediation, our formalism delineates the full parametric freedom available to models with Higgs-messenger interactions. It would be particularly useful to determine whether this full parameter space may be spanned by weakly coupled models, along the lines of what was done for GGM in [57, 84].

2. In this work we have applied our formalism to two simplified cases, the spurion limit and the SCFT limit. However, the formalism may be applied to any theory in which the overall hidden sector factorizes into separate messenger and SUSY-breaking hidden sectors, and there are likely many other well-motivated cases amenable to detailed

study. For example, it may be used to compute corrections to the spurion limit in weakly-interacting hidden sectors whose IR physics are described by O'Raifeartaigh models.

3. We have restricted our attention to superpotential portals connecting the messenger and hidden sectors. It would be interesting to analyze Kähler portals to determine whether there are other qualitatively new features or new approaches to the μ/B_μ and A/m_H^2 problems. Along similar lines, we have focused on SUSY-breaking due to a chiral operator in the hidden sector; it would be interesting to consider more general operators as well.

4. Considerable attention has recently been devoted to the NMSSM in light of the observed Higgs mass, and calculable models for the NMSSM soft spectrum must confront challenges analogous to the A/m_H^2 problem. It would therefore be fruitful to extend our formalism to cover the NMSSM and related models involving additional degrees of freedom at the weak scale.

5. In partially sequestered scenarios, SCFT data such as operator dimensions and OPE coefficients play a key role in determining the Higgs soft spectrum. While considerable effort has recently been devoted to developing general bounds on operator dimensions in 4D SCFTs [81], it would be particularly useful to extend general bounds on OPE coefficients beyond those considered in [81]. This in turn should increase the predictiveness of viable partially-sequestered models.

Appendices

3.A Details on the factorization of the correlators

In this appendix, we provide some more details about the required R-symmetry in the messenger sector and show explicitly how the correlators for the dimension-two soft parameters in (3.27) factorize into a hidden sector correlator and a messenger sector correlator.

3.A.1 $\mathcal{O}(\kappa)$ expansion and R-symmetry

With the $\mathcal{X}$ defined in (3.21), the formulas for the soft parameters to leading order in κ are given by

$$\mu = \lambda_u\lambda_d\kappa^*\langle\bar{Q}^2 O_h^\dagger\rangle_h \int d^4y\ \langle O_m^\dagger(y)\mathcal{X}_\mu\rangle_m\ + \lambda_u\lambda_d\kappa\langle Q^2 O_h\rangle_h \int d^4y\ \langle O_m(y)\mathcal{X}_\mu\rangle_m \quad (3.70)$$

$$A_{u,d} = |\lambda_{u,d}|^2\kappa^*\langle\bar{Q}^2 O_h^\dagger\rangle \int d^4y\ \langle O_m^\dagger(y)\mathcal{X}_{A_{u,d}}\rangle_m \quad (3.71)$$

$$\hat{B}_\mu = \lambda_u\lambda_d\kappa\langle Q^2 O_h\rangle_h \int d^4y\ \langle O_m(y)\mathcal{X}_{B_\mu}\rangle_m \quad (3.72)$$

$$\hat{m}^2_{H_{u,d}} = \mathcal{O}(\kappa^2) \quad (3.73)$$

All other possibilities are forbidden by the supersymmetry Ward identities on the messenger correlator. This can be most easily understood from the observation that $\mathcal{X}_{A_{u,d}}$, $\mathcal{X}_{B_\mu}$ and $\mathcal{X}_{m^2_{H_{u,d}}}$ in (3.21) can be written as

$$\mathcal{X}_{A_{u,d}} = \bar{Q}^2\big[\cdots\big], \quad \mathcal{X}_{B_\mu} = Q^2\big[\cdots\big], \quad \mathcal{X}_{m^2_{H_{u,d}}} = Q^4\big[\cdots\big] \quad (3.74)$$

where the $\cdots$ are integrated operators built out of supercharges, $O_{u,d}$ and $H_{u,d}$ operators. To understand the formula for μ, one should additionally keep in mind that we have shifted the vev of the lowest component of O_h to zero, as explained in the introduction.

The $\mathcal{O}(\kappa)$ contribution to B_μ in (3.70) is allowed by supersymmetry and results in the parametric behavior $B_\mu \sim M\mu$, which is disastrous for electroweak symmetry breaking. We therefore wish to impose a suitable symmetry on the messenger sector that forbids the correlator contributing to B_μ, while preserving an $\mathcal{O}(\kappa)$ contribution to both μ and $A_{u,d}$. From (3.70) one can easily see that the only symmetries satisfying these criteria are R-symmetries with charge assignments

$$R[O_m] = 2 \quad R[O_u] + R[O_d] = 4 \quad (3.75)$$

or

$$R[O_m] = 2 \quad R[O_u] + R[O_d] = 0 \quad (3.76)$$

(3.75) and (3.76) respectively preserve the first and second correlator contributing to μ. All known models in the literature adhere to the first charge assignment, and this is why we have assumed (3.75) throughout this paper. It would of course be interesting to explore the

other R-charge assignment, but we will not do so here. We emphasize that the presence of an R-symmetry in the messenger sector is a generic feature of all models that attempt to generate both μ and $A_{u,d}$ through the same set of Higgs-Messenger interactions.

3.A.2 $\mathcal{O}(\kappa^2)$ expansion

Since the $\mathcal{O}(\kappa)$ contribution is assumed to vanish by virtue of the R-symmetry that we imposed in the previous section, we now proceed to the derivation for the $\mathcal{O}(\kappa^2)$ contribution to $\hat{B}_\mu$. The derivation for $\hat{m}^2_{H_{u,d}}$ is completely analogous. The only contribution compatible with the R-symmetry in (3.75) is

$$\hat{B}_\mu = \lambda_u \lambda_d |\kappa|^2 \int d^4y\, d^4y' \left\langle Q^2 \left[O_h O_m(y) \right] \bar{Q}^2 \left[O_h^\dagger O_m^\dagger(y') \right] \mathcal{X}_{B_\mu} \right\rangle_{m+h} \tag{3.77}$$

Using (3.74), we can write (3.77) as

$$\hat{B}_\mu = \lambda_u \lambda_d |\kappa|^2 \int d^4y\, d^4y' \left\langle Q^2 \bar{Q}^2 \left[O_h O_m(y) O_h^\dagger O_m^\dagger(y') \mathcal{X}_{B_\mu} \right] \right\rangle_{m+h} \tag{3.78}$$

where we dropped total derivatives. Now we redistribute the supercharges over the combinations $O_h O_h^\dagger$ and $O_m O_m^\dagger \mathcal{X}_{B_\mu}$ and factorize the correlators. The unbroken supersymmetry of the messenger correlator kills all terms except the term where all the supercharges are inside the hidden sector correlator:

$$\hat{B}_\mu = \lambda_u \lambda_d |\kappa|^2 \int d^4y\, d^4y' \left\langle Q^2 \bar{Q}^2 \left[O_h(y) O_h^\dagger(y') \right] \right\rangle_h \left\langle O_m(y) O_m^\dagger(y') \mathcal{X}_{B_\mu} \right\rangle_m \tag{3.79}$$

The result has now arranged itself such that all the contributions from the hidden sector are packaged in a single hidden sector two-point function.

3.A.3 Short distance dominance of the messenger correlator

Finally, let us explicitly verify that the disconnected components of the messenger correlators for B_μ and $m^2_{H_{u,d}}$ indeed fall off at long distance as claimed in (3.33), and that they integrate to give the auxiliary field contributions in (3.6), as claimed in (3.31).

As an example, consider the $\mathcal{O}(\kappa^2, \lambda_u\lambda_d|\lambda_u|^2)$ messenger correlator for B_μ

$$\left\langle O_m(y)O_m^\dagger(y')\mathcal{X}_{B_\mu}\right\rangle_m \tag{3.80}$$

$$\supset |\lambda_u|^2 \int d^4x d^4z d^4z' \,\langle O_m(y)O_m^\dagger(y')Q^2O_u(x)Q^2O_d(0)Q^2\big[O_uH_u\big](z)\bar{Q}^2\big[O_u^\dagger H_u^\dagger\big](z')\rangle_m \tag{3.81}$$

$$= |\lambda_u|^2 \int d^4x d^4z d^4z' \,\langle Q^2O_m(y)O_m^\dagger(y')Q^2O_u(x)Q^2O_d(0)O_uH_u(z)\bar{Q}^2\big[O_u^\dagger H_u^\dagger\big](z')\rangle_m \tag{3.82}$$

where in the second line we used the supersymmetry Ward identity, dropping any total derivatives. In order to enable a contraction between the H_u operators, the $\bar{Q}^2$ must act on $O_u^\dagger(z')$:

$$\left\langle O_m(y)O_m^\dagger(y')\mathcal{X}_{B_\mu}\right\rangle_m \tag{3.83}$$

$$\supset |\lambda_u|^2 \int d^4x d^4z d^4z' \,\frac{1}{4\pi^2}\frac{1}{(z-z')^2}\langle Q^2O_m(y)O_m^\dagger(y')Q^2O_u(x)Q^2O_d(0)O_u(z)\bar{Q}^2O_u^\dagger(z')\rangle_m \tag{3.84}$$

Now we want to factorize this into two separate correlators. All one-point functions are assumed to vanish, and one can easily check that there is no factorization into a product of two- and four-point functions consistent with the symmetries. This leaves a product of three-point functions, and here the only non-vanishing factorization consistent with all the symmetries is

$$\left\langle O_m(y)O_m^\dagger(y')\mathcal{X}_{B_\mu}\right\rangle_m \tag{3.85}$$

$$\supset |\lambda_u|^2 \int d^4x d^4z d^4z' \,\frac{1}{4\pi^2}\frac{1}{(z-z')^2}\langle Q^2O_m(y)Q^2O_u(x)\bar{Q}^2O_u^\dagger(z')\rangle_m\langle O_m^\dagger(y')Q^2O_d(0)O_u(z)\rangle_m \tag{3.86}$$

Moving the supercharges around in the first correlator produces a $\partial_{z'}^2$, and after integrating by parts we are left with a $\delta^{(4)}(z-z')$. So the answer becomes:

$$\left\langle O_m(y)O_m^\dagger(y')\mathcal{X}_{B_\mu}\right\rangle_m \tag{3.87}$$

$$\supset |\lambda_u|^2 \int d^4x d^4z \,\langle O_m(y)Q^2O_u(x)O_u^\dagger(z)\rangle_m\langle O_m^\dagger(y')Q^2O_d(0)O_u(z)\rangle_m \tag{3.88}$$

This is the desired result: the delta function ensures that, to this order in perturbation theory, the messenger correlator always falls off exponentially for $M|y-y'| \to \infty$, despite

the fact that it is disconnected. Furthermore, substituting (3.87) back into (3.79) but now using the disconnected component of the hidden sector correlator, the result becomes precisely μA_u^*. The argument is analoguous for $m^2_{H_{u,d}}$ and the $\mathcal{O}(\kappa^2, \lambda_u\lambda_d|\lambda_d|^2)$ contribution to B_μ, and in this way we reproduce the contributions from integrating out the F-terms in (3.6).

3.B A Banks-Zaks model of hidden sector renormalization

3.B.1 Setup

In this appendix we study a toy example of a weakly-coupled interacting SCFT containing a chiral gauge singlet operator X that will serve as a proxy for the supersymmetry breaking operator O_h. The goal is to validate the beta functions in (3.49), obtained through superconformal perturbation theory, against a direct calculation of the beta functions through Feynman diagrams. In the process, we are also equipped to confirm the validity of the field redefinition argument in our weakly coupled example. This provides an explicit check of the various approaches to hidden sector sequestering in an effective theory framework.

Our toy model is the same one as in [83]: a Banks-Zaks model coupled to X via the superpotential

$$W = \frac{1}{2\pi}\lambda X \mathrm{Tr}\, Q\tilde{Q} \ . \tag{3.89}$$

Here Q and $\tilde{Q}$ are N_f flavors charged under an $SU(N_c)$ gauge group with $N_f = 3N_c/(1+\epsilon)$, and the trace is over all colors and flavors.[7] Before the deformation (3.89), the only coupling in the theory is the gauge coupling, g; for $N_f, N_c \gg 1$, this undeformed theory flows to the perturbative BZ fixed point at which $\beta_g = 0$. Deforming this BZ model by the addition of (3.89) induces a flow to a new fixed point at which $\beta_\lambda = \beta_g = 0$, with [83]

$$\hat{g}_* = \left(\epsilon + \mathcal{O}(\epsilon^2)\right) + \frac{5}{3N_c^2}\left(\epsilon + \mathcal{O}(\epsilon^2)\right) \tag{3.90}$$

$$\hat{\lambda}_* = \frac{2}{3}\epsilon(1+\epsilon) + \mathcal{O}\left(\frac{\epsilon^2}{N_c^2}\right) \tag{3.91}$$

where $\hat{g} = N_c g^2/8\pi^2, \hat{\lambda} = N_c^2\lambda^2/8\pi^2$ are the generalized 't Hooft couplings.

[7] In what follows, we work with the conventions in [83]. In particular, we take Q and $\tilde{Q}$ to be canonically normalized, and X to be CFT-canonically normalized.

We would like to study hidden sector renormalization at the fixed point in which Kähler operators linear in X renormalize Kähler operators linear in O_{Δ_i}, where O_{Δ_i} are scaling operators that appear in the OPE of $X^\dagger X$. In a perturbative SCFT, we expect the dimensions of such operators O_{Δ_i} to be close to two. This singlet-deformed BZ theory possesses two such candidate operators:

$$L = \frac{4\pi^2}{\sqrt{2N_f N_c}}\mathrm{Tr}(Q^\dagger Q + \tilde{Q}^\dagger \tilde{Q}) \tag{3.92}$$

$$J^X = X^\dagger X \ . \tag{3.93}$$

Here these operators are CFT-canonically normalized to leading order in the undeformed theory, i.e., using free field contractions. These operators are easiest to work with from the point of view of computing Feynman diagrams. But due to mixing in the beta functions, they are not scaling operators at the deformed BZ fixed point. Rather, they are related to scaling operators O_{Δ_1} and O_{Δ_2} via a linear transformation:

$$\begin{pmatrix} O_{\Delta_1} \\ O_{\Delta_2} \end{pmatrix} = \begin{pmatrix} S_{11} & S_{12} \\ S_{21} & S_{22} \end{pmatrix} \begin{pmatrix} L \\ J^X \end{pmatrix} \ . \tag{3.94}$$

This change of basis is related to the diagonalization of the matrix of anomalous dimensions Γ; we refer the reader to [83] for details. Although explicit formulas for S can be derived, we will not actually need them.

3.B.2 Beta functions

Here we will verify the renormalization of the couplings $c_{B_\mu,i}$ and $c_{m_{u,d},i}$ due to $c_\mu, c_{A_{u,d}}$. To do so, we compute this result at the fixed point using superconformal perturbation theory and compare with data computed perturbatively at the free fixed point.

Neglecting visible-sector interactions due to H_u, H_d, for the couplings $c_{m_{u,d},i}, c_{B_\mu,i}$ we

apply the superconformal perturbation theory results of Section 4 to find

$$\frac{d}{d\log\Lambda}\begin{pmatrix} c_{m_{u,d},1} \\ c_{m_{u,d},2}\end{pmatrix} = \begin{pmatrix}\Delta_1 & 0 \\ 0 & \Delta_2\end{pmatrix}\begin{pmatrix} c_{m_{u,d},1} \\ c_{m_{u,d},2}\end{pmatrix} - \begin{pmatrix}\mathcal{C}_{\Delta_1}\gamma_1(1+\dots) \\ \mathcal{C}_{\Delta_2}\gamma_2(1+\dots)\end{pmatrix}(|c_\mu|^2 + |c_{A_{u,d}}|^2) \tag{3.95}$$

$$\frac{d}{d\log\Lambda}\begin{pmatrix} c_{B_\mu,1} \\ c_{B_\mu,2}\end{pmatrix} = \begin{pmatrix}\Delta_1 & 0 \\ 0 & \Delta_2\end{pmatrix}\begin{pmatrix} c_{B_\mu,1} \\ c_{B_\mu,2}\end{pmatrix} - \begin{pmatrix}\mathcal{C}_{\Delta_1}\gamma_1(1+\dots) \\ \mathcal{C}_{\Delta_2}\gamma_2(1+\dots)\end{pmatrix}(c_\mu c^*_{A_u} + c_\mu c^*_{A_d}) \ . \tag{3.96}$$

where again $\gamma_i \equiv \Delta_i - 2\Delta_X$. The $\dots$ are higher order corrections in $\gamma_{1,2}$ that are scheme-dependent. For comparison with the direct calculation of RGEs, we need to compute the coefficients $\mathcal{C}_{\Delta_1}\gamma_1$ and $\mathcal{C}_{\Delta_2}\gamma_2$. While we could compute the OPE coefficients and anomalous dimensions separately, it suffices to merely extract the combinations $\mathcal{C}_{\Delta_i}\gamma_i$ from three-point functions in the hidden sector. The form of the three-point functions is dictated by conformal invariance up to the OPE coefficients $\mathcal{C}_{\Delta_1}$, C_{Δ_2}; expanding in powers of ϵ and $1/N_c$ yields

$$\langle X^\dagger(x_1)X(x_2)O_1(x_3)\rangle = \frac{\mathcal{C}_{\Delta_1}}{x_{13}^2 x_{23}^2}\left(1+\gamma_1\log x_{12} - \nu_1\log(x_{13}x_{23})\right) + \dots \tag{3.97}$$

$$\langle X^\dagger(x_1)X(x_2)O_2(x_3)\rangle = \frac{\mathcal{C}_{\Delta_2}}{x_{13}^2 x_{23}^2}\left(1+\gamma_2\log x_{12} - \nu_2\log(x_{13}x_{23})\right) + \dots \tag{3.98}$$

Working around the free fixed point, we have access to the $X^\dagger - X - L$ and the $X^\dagger - X - J^X$ three point functions, shown diagrammatically at one loop in fig. 5. We can compute $\mathcal{C}_{\Delta_i}\gamma_i$ by isolating the $\log x_{12}$ terms in the perturbative three-point functions and rotating to the basis of scaling operators using (3.94).

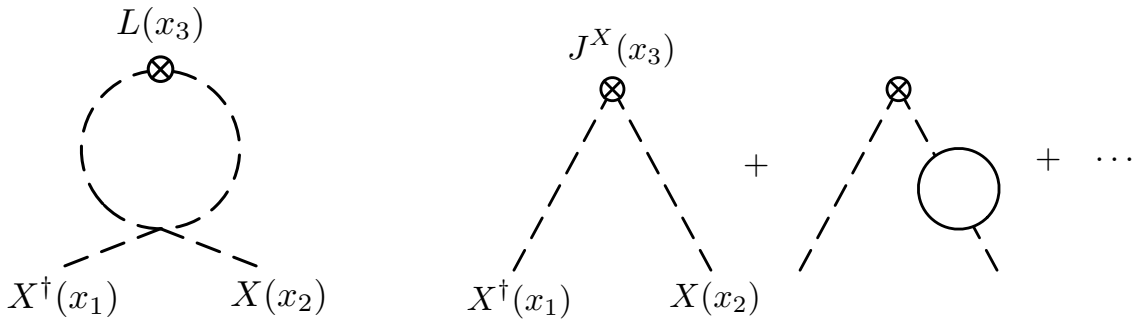

Figure 3.5: The leading perturbative contributions to the $X^\dagger - X - L$ and $X^\dagger - X - J^X$ three point functions.

Therefore we have at one loop

$$\begin{pmatrix} \mathcal{C}_{\Delta_1}\gamma_1 \\ \mathcal{C}_{\Delta_2}\gamma_2 \end{pmatrix} = S \begin{pmatrix} b_L \\ b_{J^X} \end{pmatrix} \tag{3.99}$$

where b_L, b_{J^X} are the coefficients of the $\log x_{12}$ terms appearing in the $X^\dagger - X - L$ and $X^\dagger - X - J^X$ three point functions, respectively. Diagrammatically, it is clear that $b_{J^X} = 0$ at one loop, since the loops in $X^\dagger - X - J^X$ are functions only of x_{13} or x_{23}. However, the loop in $X^\dagger - X - L$ is sensitive to x_{12}, and so b_L should be nonzero at one loop. An explicit calculation of the diagrams in)(3.5) yields $b_L = 2\sqrt{\frac{2}{3}}\frac{\epsilon}{N_c}$ and $b_{J^X} = 0$.

Now we can compare the superconformal perturbation theory result with standard pertubation theory around the free fixed point. As before, the calculation around the free fixed point in terms of L, J^X is related to the scaling operators by the transformation (3.94). Thus we need only verify that

$$\frac{d}{d\log\Lambda}\begin{pmatrix} c_{m_{u,d},L} \\ c_{m_{u,d},J^X} \end{pmatrix} \supset -\begin{pmatrix} b_L \\ b_{J^X} \end{pmatrix}(|c_\mu|^2 + |c_{A_{u,d}}|^2) \tag{3.100}$$

$$\frac{d}{d\log\Lambda}\begin{pmatrix} c_{B_\mu,L} \\ c_{B_\mu,J^X} \end{pmatrix} \supset -\begin{pmatrix} b_L \\ b_{J^X} \end{pmatrix}(c_\mu c^*_{A_u} + c_\mu c^*_{A_d}) \tag{3.101}$$

by a standard one-loop calculation of beta functions around the free fixed point.

In perturbation theory, the renormalization of $c_{m_{u,d},L}$ proportional to $|c_\mu|^2$ or $|c_{A_{u,d}}|^2$ arises at one loop and $\mathcal{O}(\epsilon/N_c)$. We may compute these loop diagrams in components using a suitably clever choice of external lines. Focusing on $c_{m_{u,d},L}Q^\dagger Q F^\dagger_{H_{u,d}} F_{H_{u,d}}$, for example, there is one diagram proportional to $|c_\mu|^2$, corresponding to the first diagram shown in figure 3.6. Similarly, for $c_{m_{u,d},L}F^\dagger_Q Q H^\dagger_{u,d} F_{H_{u,d}}$ there is one diagram proportional to $|c_{A_{u,d}}|^2$, corresponding to the second diagram in figure 3.6 . In contrast, the renormalization of $c_{m_{u,d},J^X}$ first arises at two loops and $\mathcal{O}(\epsilon^2/N_c^2)$. Similarly, the renormalization of $c_{B_\mu,L}$ proportional to $c_\mu(c^*_{A_u} + c^*_{A_d})$ arises at one loop and $\mathcal{O}(\epsilon/N_c)$. For the external components $c_{B_\mu,L}F^\dagger_Q Q F_{H_u} H_d$ there is one diagram proportional to $c_\mu c^*_{A_u}$, corresponding to the third diagram in figure 3.6 , while for $c_{B_\mu,L}F^\dagger_Q Q F_{H_d} H_u$ there is an analogous diagram proportional to $c_\mu c^*_{A_d}$. As was the case for $c_{m_{u,d},J^X}$, the renormalization of c_{B_μ,J^X} first arises at two loops and $\mathcal{O}(\epsilon^2/N_c^2)$, and we do not consider it here.

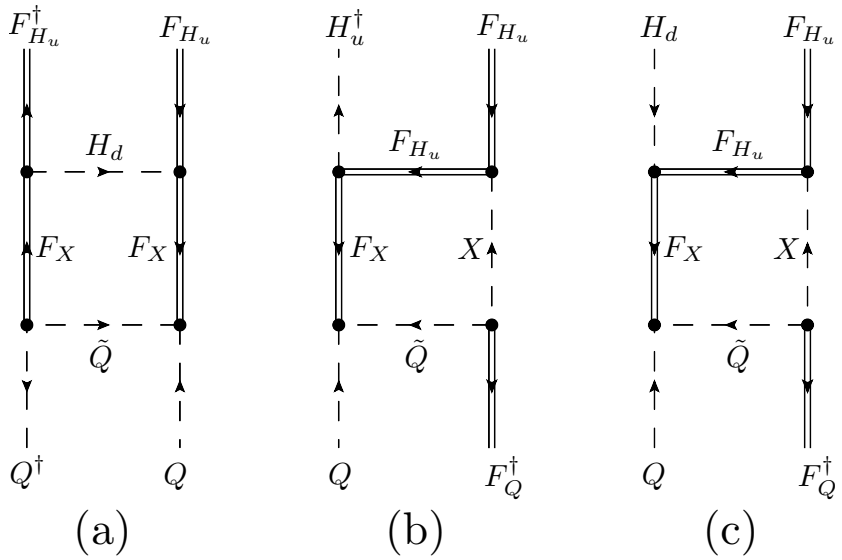

Figure 3.6: Component diagrams for the one-loop renormalization of (a) $c_{m_u,L}$ proportional to $|c_\mu|^2$, (b) $c_{m_u,L}$ proportional to $|c_{A_u}|^2$, and (c) $c_{B_\mu,L}$ proportional to $c_\mu c^*_{A_u}$.

Computing these one-loop diagrams in $\overline{MS}$, the counterterms cancelling UV divergences associated with the one-loop diagrams renormalizing $c_{m_{u,d},L}$ and $c_{B_\mu,L}$ yield contributions to the beta functions of the form

$$\frac{dc_{m_{u,d},L}}{d\log\Lambda} \supset -2\sqrt{\frac{2}{3}}\frac{\epsilon}{N_c}(|c_\mu|^2 + |c_{A_{u,d}}|^2) + \dots \tag{3.102}$$

$$\frac{dc_{B_\mu,L}}{d\log\Lambda} \supset -2\sqrt{\frac{2}{3}}\frac{\epsilon}{N_c}(c_\mu c^*_{A_u} + c_\mu c^*_{A_d}) + \dots \tag{3.103}$$

in agreement with (3.100). This directly confirms the hidden sector renormalization calculated using superconformal perturbation theory in (3.95) via standard perturbation theory to one loop at the free fixed point.

3.B.3 Confirming the field redefinition argument

It is also straightforward to see that this toy model is also consistent with the results expected from field redefinitions in the UV. The validity of the field redefinition argument

requires the beta functions to take the form

$$\frac{d}{d\log\Lambda}\begin{pmatrix} c_{m_{u,d},L} \\ c_{m_{u,d},J^X} \end{pmatrix} \approx \Gamma \begin{pmatrix} c_{m_{u,d},L} \\ c_{m_{u,d},J^X} \end{pmatrix} - (\Gamma - 2\Delta_X \times \mathbf{1}) \begin{pmatrix} 0 \\ ! \\ 1 \end{pmatrix} (|c_\mu|^2 + |c_{A_{u,d}}|^2) \tag{3.104}$$

$$\frac{d}{d\log\Lambda}\begin{pmatrix} c_{B_\mu,L} \\ c_{B_\mu,J^X} \end{pmatrix} \approx \Gamma \begin{pmatrix} c_{B_\mu,L} \\ c_{B_\mu,J^X} \end{pmatrix} - (\Gamma - 2\Delta_X \times \mathbf{1}) \begin{pmatrix} 0 \\ 1 \end{pmatrix} (c_\mu c^*_{A_u} + c_\mu c^*_{A_d}) \tag{3.105}$$

This field redefinition prediction agrees with the result from superconformal perturbation theory provided

$$S^{-1}\begin{pmatrix} \mathcal{C}_{\Delta_1} \\ \mathcal{C}_{\Delta_2} \end{pmatrix} = \begin{pmatrix} 0 \\ 1 \end{pmatrix} \tag{3.106}$$

We can check this directly in our toy model since (3.106) is precisely what is computed by the non-log-enhanced terms in the $X^\dagger - X - L$ and $X^\dagger - X - J^X$ three point functions. These terms are scheme-dependent starting at $\mathcal{O}(\epsilon)$, so the only scheme-independent contributions come from tree-level diagrams in (3.5); these yield 0 for $c_{m_{u,d},L}, c_{B_\mu,L}$ and 1 for $c_{m_{u,d},J^X}, c_{B_\mu,J^X}$. Thus (3.106) is trivially satisfied, rendering explicit agreement between the expectations from superconformal perturbation theory, direct perturbative calculation, and field redefinitions in the UV.

Chapter 4

Higgs Mediation with Strong Hidden Sector Dynamics

With D. Shih

Submitted to JHEP, appeared on arXiv:1206.4086

General context of this chapter

In the previous chapter we developed a general formalism to study Higgs-messenger interactions, and showed that strong hidden sector dynamics could provide a possible solution to both the μ/B_μ and A/m_H^2 problems. Now we provide an existence proof for this idea in the form of a fully worked out example.

Concretely, we present a simple model that achieves $m_h \approx 126$ GeV in the MSSM with large A-terms and TeV-scale stops through a combination of gauge mediation and Higgs-messenger interactions. The μ/B_μ and A/m_H^2 problems are both solved by a common mechanism – partial sequestering from strong hidden sector dynamics. Using the framework of the previous chapter, we explicitly calculate the soft masses in terms of the vacuum expectation values, operator dimensions and OPE coefficients of the strongly-coupled hidden sector. Along the way, we also present a general analysis of the various constraints on sequestered Higgs mediation models. The phenomenology of such models is similar to gaugino mediation, but with large A-terms. The next-to lightest supersymmetric particle (NLSP) is always long-lived and is either the lightest stau or the Higgsino. The colored states are typically out of reach of the 8 TeV LHC, but may be accessible at 14 TeV, especially if the NLSP is the lightest stau.

4.1 Introduction

The discovery of a Higgs boson near 126 GeV [1, 2] has profound implications for supersymmetry as a solution to the electroweak hierarchy problem. This is especially the case

in minimal supersymmetry, where the stops must either be unnaturally heavy ($\gtrsim 10$ TeV) or have a large trilinear coupling to the Higgs [26–29, 16, 30–33]. The former possibility leaves little hope for preserving naturalness or observational signals at the LHC, so we will focus on the latter scenario. This requires a plausible mechanism for generating such large A-terms without introducing large flavor violation or other unwanted effects.

The lack of decisive deviations in searches for flavor and CP violation has long favored low-scale gauge mediation by virtue of its flavor universality. However, in its minimal form, gauge mediation is challenged by the Higgs sector, since it generates neither the μ and B_μ parameters necessary for electroweak symmetry breaking (EWSB), nor the A-terms suggested by the Higgs mass measurement. These terms may be generated in a flavor universal manner by adding interactions between the Higgs sector and the messenger sector,

$$W \supset \lambda_u O_u H_u + \lambda_d O_d H_d \tag{4.1}$$

where $O_{u,d}$ are messenger-sector operators. Although the μ and A-terms are obtained trivially in such a setup, viable solutions must confront two thorny problems: the "μ/B_μ problem" [22] and the "A/m_H^2 problem" [77]. Both problems arise because adding Higgs-messenger interactions that generate a μ (A) term also tend to produce a B_μ (m_H^2) term that is too large for viable electroweak symmetry breaking.

The most stringent form of the A/m_H^2 problem may be resolved if the sole source of messenger mass is a single SUSY-breaking spurion [47, 77], as in minimal gauge mediation (MGM) [42–44]. But even in this case the μ/B_μ problem remains unaddressed, and requires a further extension of the model. Moreover, there is a residual "little A/m_H^2 problem", as any weakly-coupled model that generates large A-terms through Higgs-messenger interactions also generates contributions to the Higgs soft masses proportional to A^2 [77]. Even if these contributions do not prevent electroweak symmetry breaking, they significantly increase the fine-tuning associated with the weak scale.

In this paper, we present an alternative framework which uses strong dynamics in the hidden sector to economically solve both the μ/B_μ and A/m_H^2 problems. Two ingredients are required for this: that there exists a hierarchy between the messenger scale M and the SUSY-breaking scale $\sqrt{F}$; and that the anomalous dimensions of the operators responsible

for SUSY-breaking are large and positive. The former property is a generic prediction of dynamical supersymmetry breaking [85], while the latter property is constrained, but still allowed by the conformal bootstrap [81]. If both these conditions are met, strong renormalization effects in the hidden sector can suppress the soft masses of the scalars (including B_μ [69, 71, 70] and m_H^2 [49]), an idea more generally known as "conformal sequestering" or "scalar sequestering" [86–88]. We will demonstrate that with such a strongly coupled hidden sector, even the very simplest example for the messenger sector yields a large viable parameter space. The simplicity of our model contrasts sharply with most fully weakly-coupled solutions, which address the μ/B_μ problem by elaborately extending either the Higgs sector or the messenger sector (or both).

In recent years, there has been tremendous progress in our understanding of 4D conformal field theory, starting with the work of [89]. This revival of the conformal bootstrap program has led to strong bounds on the dimensions of operators appearing in the OPE. Applying these bounds to the operators responsible for SUSY-breaking has in turn strongly limited the efficacy of the conformal sequestering scenario [81]. In particular, it is now very difficult to achieve full suppression of B_μ and $m_{H_u}^2$,

$$B_\mu \ll |\mu|^2 \quad \text{and} \quad m_{H_u}^2 + |\mu|^2 \ll |A_u|^2. \tag{4.2}$$

On the other hand, a *partial* suppression of the dangerous contributions such that

$$B_\mu \lesssim |\mu|^2 \quad \text{and} \quad m_{H_u}^2 + |\mu|^2 \lesssim |A_u|^2. \tag{4.3}$$

is still possible and may be sufficient to facilitate electroweak symmetry breaking. In this case the details of the hidden sector dynamics do not fully decouple from the low energy observables, and testing for viable electroweak symmetry breaking requires a robust framework to explicitly compute the MSSM soft parameters in terms of the hidden sector data (such as the spectrum of operators, their scaling dimensions, and their OPE coefficients).

General Messenger Higgs Mediation (GMHM), developed recently in [49], provides precisely such a framework. Following [78], the idea of GMHM is to go beyond the single-sector frameworks of [56, 57, 23] and explicitly separate the messenger sector and SUSY-breaking sector, so that it becomes possible to take $\sqrt{F} \ll M$. Specifically, we parametrize the coupling between the messenger sector and the SUSY-breaking hidden sector via a perturbative

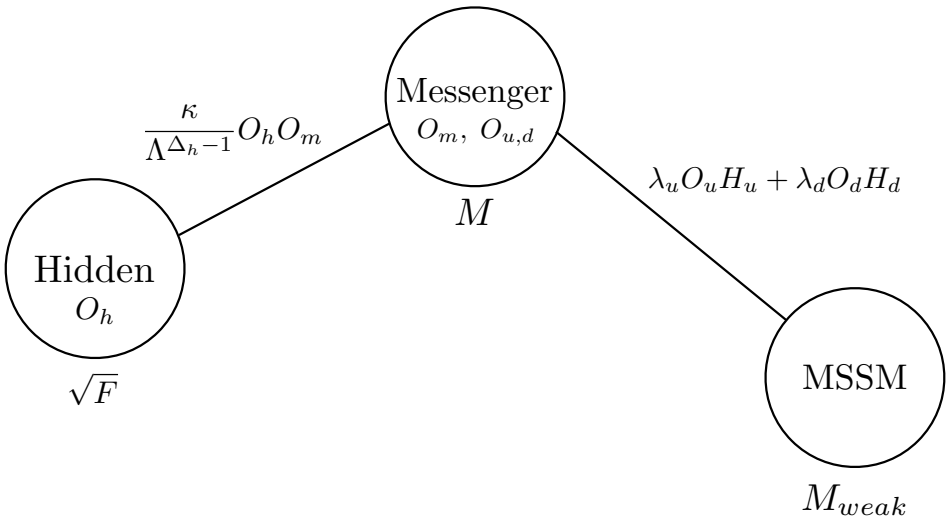

Figure 4.1: Schematic representation of the various sectors and couplings. This paper we take the messenger sector to be weakly coupled but allow for strong dynamics in the hidden sector.

superpotential interaction as in [78]:

$$W \supset \frac{\kappa}{\Lambda^{\Delta_h-1}} O_h O_m \tag{4.4}$$

where O_h is an operator in the SUSY-breaking sector with dimension Δ_h, O_m is an operator in the messenger sector, and Λ is the cut-off scale associated with the irrelevant operator in (4.4). The complete setup of GMHM is shown in figure 4.1. By expanding in the portal couplings κ, $\lambda_{u,d}$ of (4.1) and (4.4), we can express the soft parameters in terms of products of separate correlation functions over the messenger sector and the hidden sector. Under the assumption that the hidden sector is near a conformal fixed point between the scales M and $\sqrt{F}$, the correlators simplify dramatically. The GMHM formalism then allows, for the first time, for a full calculation of soft masses directly in terms of hidden sector scaling dimensions, OPE coefficients, and expectation values.

Although GMHM applies to any hidden sector and messenger sector coupled through the portals (4.1), (4.4), in this paper we will focus on weakly-coupled messenger sectors in order to preserve calculability and predictivity.[1] We will explore the phenomenology of this entire class of models, as well as present a very simple explicit example. Concretely, the

[1]For this reason we will assume for simplicity that $\Delta_m = \Delta_u = \Delta_d = 2$ (while allowing for arbitrary Δ_h), which is well motivated for a weakly coupled messenger sector. This explains the powers of Λ or lack thereof implicitly taken in (4.1) and (4.4).

model for the messenger sector that we consider is given by

$$W = \left(\frac{\kappa}{\Lambda^{\Delta_h - 1}} O_h + M\right)\left(\tilde{\phi}_D \phi_D + \tilde{\phi}_S \phi_S\right) + \lambda_u \tilde{\phi}_D \phi_S H_u + \lambda_d \phi_D \tilde{\phi}_S H_d. \tag{4.5}$$

where ϕ_D, $\tilde{\phi}_D$ and ϕ_S, $\tilde{\phi}_S$ are $SU(2)$ doublets and gauge singlets respectively. Although this model is the prime example of a model that does *not* solve the μ/B_μ problem when the hidden sector is trivial [22], with partial hidden-sector sequestering it becomes an elegant solution to both the μ/B_μ and A/m_H^2 problems. We find that electroweak symmetry breaking and $m_h = 126$ GeV are easy to achieve in this model, and instead the most interesting constraints on the parameter space originate from stau tachyons. Nevertheless there is a large viable parameter space, which can accommodate $\mathcal{O}(1)$ OPE coefficients and roughly 10% suppression from conformal sequestering. The collider phenomenology is similar to that of standard gaugino mediation [90, 91], with all the colored states above 1 TeV. The NLSP is always long-lived, which leads to spectacular collider signatures if the NLSP is a stau.

The paper is organized as follows. Section 2 is a brief review of the mechanism of conformal sequestering as well as the most important features of the GMHM formalism. In section 3 we discuss the model-independent constraints on the parameter space from weak scale requirements such as EWSB and the Higgs mass, prior to presenting a full analysis of our explicit example in section 4. Section 5 is a short discussion of the collider phenomenology of this class of models. Section 6 contains our conclusions, and we reserve various technical details for the appendices.

4.2 Review of GMHM and Conformal Sequestering

4.2.1 The GMHM formalism

In this subsection, we review the calculation of the Higgs soft parameters μ, B_μ, $A_{u,d}$ and $m^2_{H_{u,d}}$ through the GMHM formalism. For the derivation of the various results we refer to [49]. At the scale $\sqrt{F}$, conformal symmetry and supersymmetry are broken by an F-term expectation value for the hidden sector operator O_h with dimension Δ_h:

$$\langle Q^2 O_h \rangle_h \equiv \sqrt{F}^{\Delta_h + 1}, \tag{4.6}$$

To leading order, the dimension-one soft parameters (gaugino masses, μ, and $A_{u,d}$) are only sensitive to this vacuum expectation value.

Meanwhile, the dimension-two soft parameters (sfermion mass-squareds, B_μ, and $m^2_{H_{u,d}}$) are sensitive to the dynamics of the hidden sector. The leading contribution of such dynamics is packaged in the hidden-sector two-point function

$$\langle Q^4[O_h^\dagger(x)O_h(x')]\rangle_h, \tag{4.7}$$

In the spurion limit, this correlation function simply factorizes into $|\langle Q^2 O_h\rangle_h|^2$, but in a non-trivial hidden sector this is not necessarily a good approximation. For calculable models of the supersymmetry breaking sector one could address this issue by explicitly evaluating (4.7) and then studying its effects on the low energy physics. In this paper we will take a different approach: we will remain agnostic about the precise mechanism of supersymmetry breaking, but instead assume that the hidden sector is approximately conformal before it breaks SUSY. In the GMHM framework, the hidden sector correlator in (4.7) is always convolved with a short-distance messenger correlator, which then enforces $|x-x'| \sim \frac{1}{M} \ll \frac{1}{\sqrt{F}}$. It is therefore justified to simplify (4.7) by making use of the operator product expansion:

$$O_h(x)O_h^\dagger(x') \sim |x-x'|^{-2\Delta_h}\mathbf{1} + C|x-x'|^{\Delta-2\Delta_h}O_\Delta(x) + \dots \tag{4.8}$$

where the ellipses denote terms with higher dimension and/or spin. The supercharges annihilate the unit operator such that the correlation function is reduced to

$$\langle Q^4[O_h(x)O_h^\dagger(x')]\rangle_h \approx C|x-x'|^{\Delta-2\Delta_h}\langle Q^4 O_\Delta\rangle_h \tag{4.9}$$

where we only keep the leading non-vanishing term in the OPE. Dimensional analysis then demands that the D-term expectation value of O_Δ takes the form $\langle Q^4 O_\Delta\rangle \equiv \xi_\Delta F^{(\Delta+2)/2}$, where Δ is the scaling dimension of O_Δ and ξ_Δ is a dimensionless number. The parameters ξ_Δ and C are degenerate at the level of our analysis, and to facilitate the notation we thus introduce an 'effective OPE coefficient' :

$$\hat{C} \equiv C\xi_\Delta. \tag{4.10}$$

Note that ξ_Δ (and therefore $\hat{C}$) is a real number, but can have either sign.

To leading order in $\lambda_{u,d}$, the μ term and the A-terms are given by

$$\mu = -\lambda_u \lambda_d \kappa \frac{\sqrt{F}^{\Delta_h+1}}{\Lambda^{\Delta_h-1}} \int d^4y\, d^4x \langle O_m^\dagger(y) Q^\alpha O_u(x) Q_\alpha O_d(0)\rangle_m \tag{4.11}$$

$$A_{u,d} = |\lambda_{u,d}|^2 \kappa \frac{\sqrt{F}^{\Delta_h+1}}{\Lambda^{\Delta_h-1}} \int d^4y d^4x \langle O_m^\dagger(y) \bar{Q}^2 \big[O_{u,d}^\dagger(x) O_{u,d}(0)\big]\rangle_m \tag{4.12}$$

The Higgs sector soft masses are specified by the correlators

$$B_\mu = -\lambda_u \lambda_d \kappa^2 \hat{C} \frac{\sqrt{F}^{\Delta+2}}{\Lambda^{2\Delta_h-2}} \int d^4y\, d^4y'\, d^4x\, |y-y'|^\gamma \Big\langle O_m(y) O_m^\dagger(y') Q^2 O_u(x) Q^2 O_d(0)\Big\rangle_m \tag{4.13}$$

$$\hat{m}^2_{H_{u,d}} = -|\lambda_{u,d}|^2 \kappa^2 \hat{C} \frac{\sqrt{F}^{\Delta+2}}{\Lambda^{2\Delta_h-2}} \int d^4y\, d^4y'\, d^4x\, |y-y'|^\gamma \Big\langle O_m(y) O_m^\dagger(y') Q^2 O_{u,d}(x) \bar{Q}^2 O_{u,d}^\dagger(0)\Big]\Big\rangle_m \tag{4.14}$$

with $\gamma \equiv \Delta - 2\Delta_h$. Here we have introduced the following notational convenience:

$$\hat{m}^2_{H_{u,d}} \equiv m^2_{H_{u,d}} + |\mu|^2 \tag{4.15}$$

where the $m^2_{H_{u,d}}$ are the usual soft masses for the Higgs fields.

Although the Higgs sector parameters are generated by the portal (4.1), for the rest of the MSSM soft parameters we need a different source. In this paper, we assume that these arise through standard gauge mediation, i.e. the messenger sector in figure 4.1 also couples to the MSSM through gauge interactions. For completeness, let us exhibit the usual gauge-mediated contributions to the soft masses. These can be assembled from the GGM correlators [56, 57]:

$$\begin{aligned} M_i &= g_i^2 B_i \\ m^2_{\tilde{f}} &= \sum_{i=1}^{3} g_i^4 c_2(f,i) A_i \end{aligned} \tag{4.16}$$

where f labels the matter representations of the MSSM, and $c_2(f,i)$ is the quadratic Casimir of f with respect to the gauge group i. In the GMGM formalism the B_i and A_i correlators can be written as a convolution of a messenger sector correlator with a hidden sector correlator [78]. Crucially, the hidden sector correlator appearing in the expression for the A_i

is precisely (4.7). Using the OPE, the expressions for B_i and A_i then reduce to

$$B_i = \frac{\kappa}{4}\frac{\sqrt{F}^{\Delta_h+1}}{\Lambda^{\Delta_h-1}}\int d^4y\, d^4x \langle Q^2 O_m^\dagger(y) J_i(x) J_i(0)\rangle_m \tag{4.17}$$

$$A_i = -\frac{\kappa^2}{128\pi^2}\hat{C}\frac{\sqrt{F}^{\Delta+2}}{\Lambda^{2\Delta_h-2}}\int d^4y\, d^4y'\, d^4x\, |y-y'|^\gamma \Big\langle Q^4\big[O_m(y)O_m^\dagger(y')\big] J_i(x) J_i(0)\Big\rangle_m \log[M^2x^2] \tag{4.18}$$

The $J_i(x)$ are the bottom components of the current superfields through which the messengers couple to gauge group i. In contrast with (4.13) and (4.14), the expression for sfermion mass-squareds in (4.18) is suppressed by an extra loop factor, in addition to any loop factors that may be generated by the messenger correlator itself.

4.2.2 Conformal sequestering

For a generic weakly-coupled messenger sector, all the messenger correlators in equations (4.11)-(4.14) are non-zero at one loop, which implies that B_μ and $\hat{m}^2_{H_{u,d}}$ are too large to facilitate viable electroweak symmetry breaking. However just by applying naive dimensional analysis on the correlators in the previous section, we can already identify several possible avenues to address the problem:

$$\begin{aligned}\frac{B_\mu}{\mu^2} &\sim \frac{16\pi^2}{\lambda_u\lambda_d}\frac{\hat{C}}{N}\left(\frac{\sqrt{F}}{M}\right)^\gamma \\ \frac{\hat{m}^2_{H_{u,d}}}{|A_{u,d}|^2} &\sim \frac{16\pi^2}{|\lambda_{u,d}|^2}\frac{\hat{C}}{N}\left(\frac{\sqrt{F}}{M}\right)^\gamma\end{aligned} \tag{4.19}$$

A well known method to mitigate the infamous loop factor is to increase the messenger number, which we denote by N. However, this is limited by Landau poles in the gauge couplings and cannot be responsible for completely suppressing the loop factor. Secondly, if $\gamma > 0$ and $\sqrt{F} \ll M$, the last factor on each line of (4.19) can in principle suppress the loop factor. This is the conformal sequestering mechanism. Finally, one could consider an SCFT with $\hat{C} \ll 1$, such that the effective OPE coefficient provides the desired suppression factor, possibly in combination with some suppression from sequestering.

Meanwhile, from equations (4.16)-(4.18) we see that since the gaugino and sfermion masses are generated through gauge mediation, they satisfy:

$$\frac{m^2_{\tilde{f}}}{M_i^2} \sim \frac{\hat{C}}{N}\left(\frac{\sqrt{F}}{M}\right)^\gamma \tag{4.20}$$

In particular, the sfermion masses come with an extra loop factor with respect to B_μ and $\hat{m}^2_{H_{u,d}}$, but are subject to the same suppression from the hidden sector. This implies that the sfermion masses are always suppressed with respect to the gaugino masses if the μ/B_μ and A/m_H^2 problems are solved. The phenomenology will therefore be similar to that of gaugino mediation [90, 91].

The idealized cases where $\gamma \gg 1$ or $\hat{C} \to 0$ lead to the extremely simple boundary conditions at the scale $\sqrt{F}$:

$$B_\mu \approx \hat{m}^2_{H_{u,d}} \approx m^2_{\tilde{f}} \approx 0 \tag{4.21}$$

Interestingly, this part of the UV boundary conditions becomes completely model-independent. The sensitivity of these parameters to the details of the hidden sector and messenger sector has been completely erased.

Unfortunately this scenario is severely challenged in several ways. First, it has been known for some time that achieving suitable EWSB is nontrivial for these boundary conditions [79, 80]. Second, even if one succeeds in breaking electroweak symmetry, the amount of sequestering through the factor $\left(\frac{\sqrt{F}}{M}\right)^\gamma$ is now severely limited by powerful upper bounds on γ from the internal consistency of the hidden sector SCFT [81].

To see this, consider some reference values in table 4.1, taken from figure 7 of [81]. The bounds are clearly very strong for low values of Δ_h, but could going to larger Δ_h allow for enough sequestering? (This is indeed suggested by figure 9 of [81].) In fact, increasing Δ_h runs into a competing constraint. Because the messenger sector portal (4.4) becomes a higher-dimension operator, it becomes increasingly challenging to achieve realistic gaugino masses.[2] These are given by (4.16) and (4.17):

$$M_i = \frac{g_i^2}{16\pi^2} N \frac{\sqrt{F}^{\Delta_h+1}}{M\Lambda^{\Delta_h-1}}. \tag{4.22}$$

Requiring TeV-scale gaugino masses leads to the following rough limit on the suppression that can be achieved from conformal sequestering:

$$\left(\frac{\sqrt{F}}{M}\right)^\gamma \gtrsim \left(\frac{100 \text{ TeV}}{N\epsilon^{\Delta_h-1}\sqrt{F}}\right)^{\frac{\gamma}{\Delta_h}} \tag{4.23}$$

[2] An identical argument applies to μ and $A_{u,d}$, which implies that this constraint cannot be be simply circumvented by arranging the gaugino masses to arise from a separate source of supersymmetry breaking.

Δ_h	$(\gamma)_{max}$
1.20	0.1
1.45	0.4
2.00	0.7

Table 4.1: Maximum allowed value of γ for selected values of Δ_h, as extracted from figure 7 of [81].

where we made the rough order of magnitude estimate $\frac{16\pi^2}{g_i^2} M_i \sim 100$ TeV and defined $\epsilon \equiv \frac{M}{\Lambda} < 1$. Figure 4.2 shows this as a function of $\sqrt{F}$ and Δ_h (with γ saturating the bootstrap bound), for two choices of ϵ. For larger Δ_h, the hierarchy between the messenger and hidden sector scales is greatly reduced in comparison to the hierarchy that one would obtain in the spurion limit. In combination with the upper bound on γ from [81], this severely limits the amount of sequestering that can be achieved. Some more comments on this result:

- Equation (4.23) and the requirement that $M > \sqrt{F}$ also provide a rough lower bound on $\sqrt{F} \gtrsim \frac{100 \text{ TeV}}{N \epsilon^{\Delta_h - 1}}$. This is the same type of lower bound as found for any model with weakly coupled messengers, except that in the case at hand the bound is further strengthened for smaller values of ϵ and larger values of Δ_h.

- For $\Delta_h \gtrsim 1.7$, increasing Δ_h barely improves the sequestering, because of the competing effects described above.

- The estimate in (4.23) also shows that the achievable sequestering somewhat improves for higher N, however the gain is limited due to the $\sqrt{F}$-dependent upper bound on N from Landau poles in the gauge couplings.

By comparing figure 4.2 with figure 9 of [81], we see that the bound on the sequestering has been strengthened considerably by accounting for TeV scale gaugino masses and by factoring in the UV scale Λ, here parametrized by the variable ϵ. In particular, a full loop factor suppression is only feasible for $\sqrt{F} \gtrsim 10^{11}$ GeV. In this case the separation with the weak scale may be sufficiently high such that MSSM RG-running could suffice to generate a large A-term, without the need for Higgs mediation [16]. Moreover, such a high scale of supersymmetry breaking introduces various subtleties in the model: firstly, the gravitino is no longer the LSP. While this is interesting if the new LSP is a neutralino [70, 92, 93], it is a

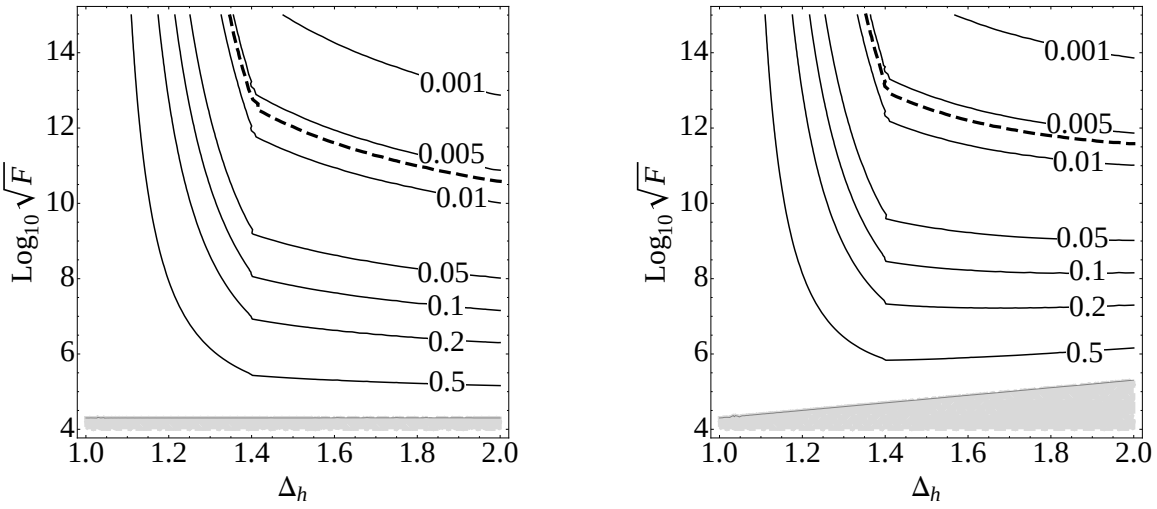

(a) $\epsilon = 1$ (b) $\epsilon = 0.1$

Figure 4.2: Contours of the maximal suppression factor that can be achieved from conformal sequestering as a function of Δ_h and $\sqrt{F}$ for various values of ϵ with $N = 5$. The dashed contour indicates the suppression needed to precisely overcome the factor $16\pi^2$ that constitutes the μ/B_μ and A/m_H^2 problems. The gray region corresponds to the unphysical case $\sqrt{F} > M$. The contours should be taken as a rough estimate using (4.23). The precise value of the sequestering is model-dependent.

disaster if the new LSP is a stau. Secondly, for $\sqrt{F} \gtrsim 10^{11}$ GeV, contributions from anomaly and/or gravity mediation may not be negligible. Especially the latter could be problematic, as they generically induce large flavor violation in the A-terms and the sfermion masses. (On the other hand, it is possible that the very same mechanism of conformal sequestering may help to suppress dangerous flavor violation [86–88].) While these are certainly interesting issues, we do not wish to confront them in this paper. For simplicity we therefore restrict our discussion to $\sqrt{F} < 10^{10}$ GeV, to ensure that the gravitino is always the NLSP and that gravity-induced flavor violation is always automatically small.

From figure 4.2 we then conclude that for $\sqrt{F} < 10^{10}$ GeV conformal sequestering is not sufficiently powerful to achieve the fully suppressed boundary conditions in (4.21). The best we can hope for is to achieve a partial suppression from sequestering given by

$$\left(\frac{\sqrt{F}}{M}\right)^{\gamma} \sim 0.01 - 0.1. \tag{4.24}$$

This may be sufficient – especially in combination with some additional suppression from $\hat{C} < 1$ and/or $N > 1$ – to achieve viable EWSB, provided that the boundary conditions at

the scale $\sqrt{F}$ still satisfy

$$B_\mu \lesssim |\mu|^2 \quad \text{and} \quad \hat{m}^2_{H_u} \lesssim |A_u|^2, \tag{4.25}$$

rather than the overly stringent requirement in (4.21). Such partially suppressed boundary conditions imply that the details of the dynamics in the hidden and messenger sectors are not erased at the scale $\sqrt{F}$. Instead, both sectors should leave an observable imprint on the low energy spectrum. Using the GMHM formalism developed in [49], we are able for the first time to explicitly evaluate this imprint for a weakly messenger sector of our choice. We will present an explicit example in section 4.4, but before doing so, it is useful to study the available parameter space in a (semi) model-independent way. This will be the subject of the next section.

4.3 Exploring the Parameter Space

The correlator formalism described in the previous section a priori involves a very large parameter space; in the most general case the boundary conditions are described by no less than 10 free parameters:

$$M_1,\ M_2,\ M_3,\ A_u,\ A_d,\ \mu,\ B_\mu,\ \hat{m}^2_{H_u},\ \hat{m}^2_{H_d},\ \sqrt{F}. \tag{4.26}$$

with $m^2_{\tilde{f}} \approx 0$. (Recall from the discussion around equation (4.20) that the sfermion masses are suppressed at the scale $\sqrt{F}$.) Here and onwards, the parameters in (4.26) are always to be thought of as evaluated at the scale $\sqrt{F}$, unless indicated otherwise. Following the discussion of the previous section, to maximize the impact of the conformal sequestering we choose $\sqrt{F} = 10^9$ GeV. At the end of section 4.4 we briefly comment on lower values for $\sqrt{F}$.

Before even writing down a specific UV model, we can restrict this parameter space through phenomenological considerations in the IR such as EWSB and the Higgs mass. This approach has a double advantage: it serves as a valuable intermediate step in the full analysis and provides some model independent information about the UV soft parameters. Despite the restrictions from the IR boundary conditions, the remaining parameter space in (4.26) is still rather daunting to analyze in full generality. In this paper, we instead

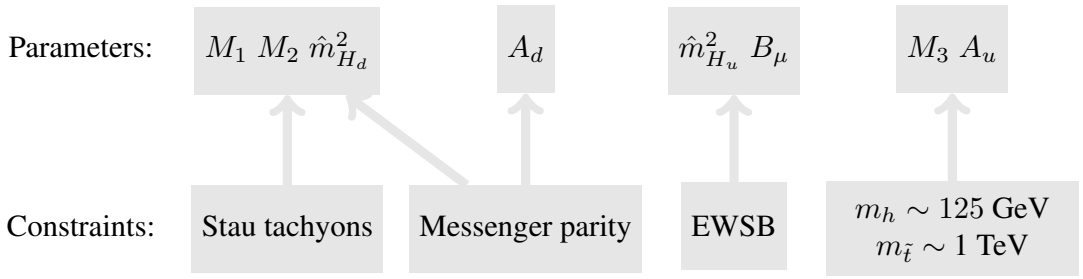

Figure 4.3: Schematic representation of the various constraints and how they impact the parameter space. We use the electroweak symmetry breaking conditions to eliminate B_μ in favor of $\tan\beta$. Our assumption regarding the action of the messenger parity on the operators O_u and O_d allows us to eliminate A_d as an independent variable and to constrain $\hat{m}_{H_d}$ to be positive.

choose to impose one more condition on the UV soft parameters purely for simplicity. This condition – an extension of messenger parity to the Higgs-messenger portal – renders the parameter space in (4.26) manageable. Moreover it is a property of a broad class of models, and it is motivated in particular by the model we will study in section 4.4. The impact of each of the constraints on the soft parameters is summarized in figure 4.3, and in this section we will describe each one in turn.

4.3.1 Simplifying assumptions for the UV soft parameters

In GGM, a standard ingredient is that the hidden sector possesses a "messenger parity" symmetry that forbids dangerous hypercharge tadpoles [94, 56]. To reduce the size of the parameter space here, we choose to extend this symmetry to the Higgs-messenger interactions. Specifically, we assume that messenger parity exchanges O_u and O_d. This greatly simplifies our analysis, since it implies that the correlators for A_u and A_d in (4.12) must be identical. The same is true for the correlators for $\hat{m}^2_{H_u}$ and $\hat{m}^2_{H_d}$ in (4.14). The soft parameters must therefore obey the following relation at the scale $\sqrt{F}$:

$$\frac{A_d}{A_u} = \frac{\hat{m}^2_{H_d}}{\hat{m}^2_{H_u}} = \frac{|\lambda_d|^2}{|\lambda_u|^2} > 0. \tag{4.27}$$

We can conveniently use this constraint to eliminate A_d as a free parameter, and thus reduce size of the parameter space. In addition, (4.27) determines the relative sign of A_u and A_d, as well as the relative sign of $\hat{m}^2_{H_u}$ and $\hat{m}^2_{H_d}$. We emphasize that this extension of messenger

parity to O_u and O_d is motivated purely on the grounds of convenience; although messenger parity is usually included in the definition of gauge mediation, in general it does not need to act on O_u and O_d in this specific way.

For any concrete model, the UV soft parameters must be realized in terms of the underlying parameters of the model, which generally leads to additional restrictions on top of (4.27). For example, a minimal messenger sector with only messengers in a $\mathbf{5}$-$\bar{\mathbf{5}}$ representation of an SU(5) GUT yields the following relation between the gaugino masses:

$$M_1 = \frac{3}{5}\frac{g_1^2}{g_2^2}M_2 + \frac{2}{5}\frac{g_1^2}{g_3^2}M_3. \tag{4.28}$$

In this section we discuss this special case as well as the more general case where all three gaugino masses are independent. Any further restrictions on the UV boundary conditions are typically highly model-dependent, and we deal with them only when we commit to a specific example in section 4.4.

4.3.2 IR boundary conditions

The restrictions on the IR soft masses are purely given by phenomenological considerations, and as such they are independent of the precise composition of the messenger sector. In particular, we demand that a realistic spectrum at the weak scale satisfies the following requirements:

1. Viable electroweak symmetry breaking.
2. $m_h \approx 126$ GeV and TeV-scale stops.
3. Charge, color and CP must be unbroken in the vacuum on cosmological time scales.

In what follows, we will go step by step through the IR constraints mentioned above, and use them to reduce the size of the parameter space until it becomes tractable. More details on our numerical procedure are given in appendix 4.B.

Constraints from EWSB

As usual, the tadpole equations in the Higgs sector allow us to eliminate $\hat{m}_{H_u}^2$ and B_μ at the weak scale in favor of m_Z and $\tan\beta$. In order not to exacerbate the fine-tuning, we

only consider $|\mu| \leq 500$ GeV, but this is by no means essential. This assumption has the additional benefit that the parameter μ now has little impact on the IR spectrum, with the exception of course of the mass of the Higgsino, which may be the NLSP. A small number of discrete choices therefore suffices to obtain a good qualitative picture of the parameter space. In addition, we fix $\tan\beta = 10$.

Constraints from the Higgs mass

The parameters A_u and M_3 are the most important parameters as far as the mass of the lightest CP even Higgs is concerned, as they set the stop A-term as well as the stop masses. To appreciate the latter, consider the system of RG equations

$$\begin{aligned} 16\pi^2 \frac{d}{dt} m_{Q_3}^2 &= 2y_t^2(\hat{m}_{H_u}^2 + m_{Q_3}^2 + m_{u_3}^2 + |A_u|^2) - \frac{32}{3} g_3^2 |M_3|^2 - 6g_2^2 |M_2|^2 \\ 16\pi^2 \frac{d}{dt} m_{u_3}^2 &= 4y_t^2(\hat{m}_{H_u}^2 + m_{Q_3}^2 + m_{u_3}^2 + |A_u|^2) - \frac{32}{3} g_3^2 |M_3|^2 \\ 16\pi^2 \frac{d}{dt} \hat{m}_{H_u}^2 &= 6y_t^2(\hat{m}_{H_u}^2 + m_{Q_3}^2 + m_{u_3}^2 + |A_u|^2) - 6g_2^2 |M_2|^2 \end{aligned} \tag{4.29}$$

where we neglected contributions proportional to y_b and g_1. We also dropped the dependence on the μ parameter, since we assumed it to be smaller than the other soft masses. The key fact is that the stop masses and $\hat{m}_{H_u}^2$ are essentially zero at the scale $\sqrt{F}$ (due to sequestering) and at the weak scale (due to EWSB), respectively. Therefore, the running of the stops and $\hat{m}_{H_u}^2$ must be determined primarily by the sources M_3, M_2 and A_u. Of these parameters, the effect of M_2 is typically subleading compared to the other two. It is therefore justified to fix the parameters A_u and M_3 by insisting on $m_h \approx 126$ GeV with TeV-scale stop masses.[3] This is illustrated in figure 4.4 for some representative values of M_2. Given both the theory and the experimental errors on the Higgs mass, this is necessarily a somewhat loose constraint, and for the purpose of our analysis, we simply choose a representative point in the allowed region, indicated with a star in figure 4.4. Other choices are certainly possible, but the qualitative features of what will follow are preserved.

[3] A priori, a large A_u may cause our vacuum to decay to a lower, color-breaking vacuum on a time scale shorter than the age of the universe. The recently improved empirical constraint on this process [95] does not impact the parameter space plotted in figure 4.4. (See also [96] for a similar recent result.)

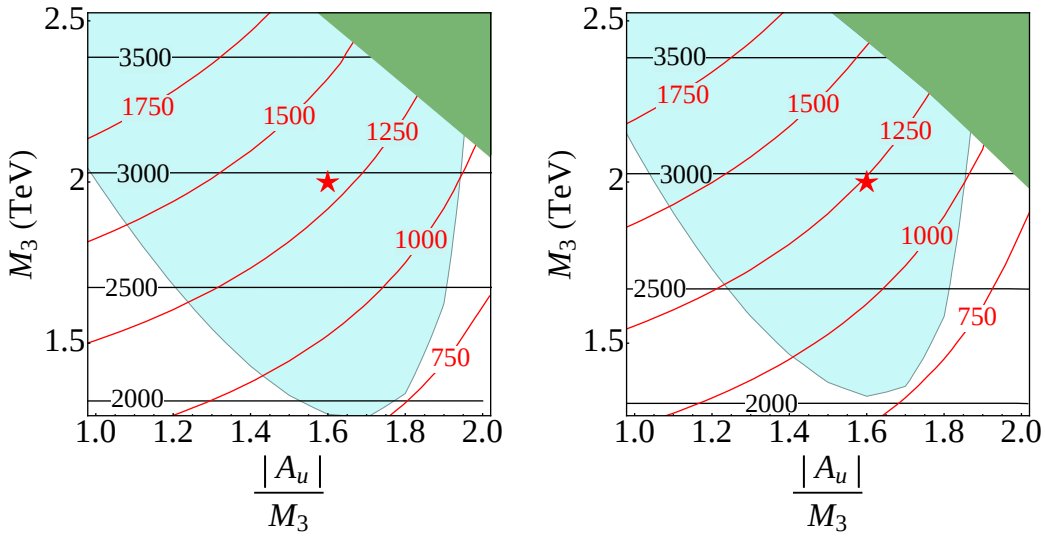

(a) $M_2 = 0.5$ TeV

(b) $M_2 = 2$ TeV

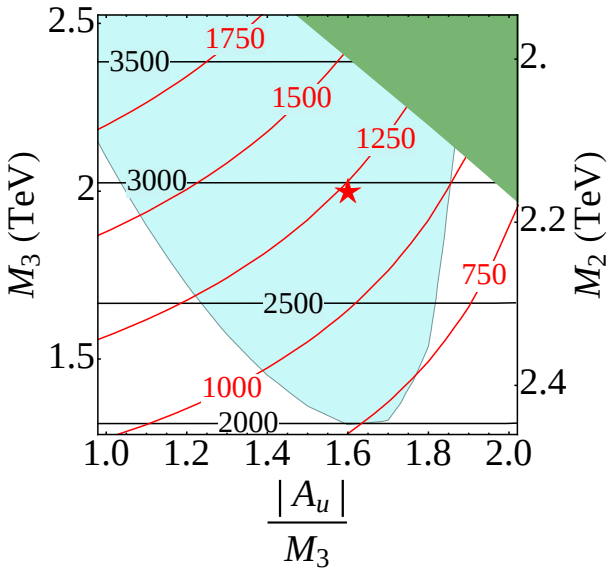

(c) **5-$\bar{\mathbf{5}}$** messengers

Figure 4.4: Contours of the pole masses (in GeV) of the lightest stop (red) and the gluino (black), as a function of M_3 and $|A_u|/M_3$, for different choices of M_2. The other parameters are fixed to $\tan\beta = 10$, $\mu = 200$ GeV, $\sqrt{F} = 10^9$ GeV, $M_1 = 1.2$ TeV and $m_{A^0} = 1.5$ TeV. The pseudoscalar pole mass m_{A^0} was used instead of $\hat{m}^2_{H_d}$ for purely technical reasons; all other parameters are defined at the scale $\sqrt{F}$. The blue region represents 123 GeV $< m_h <$ 129 GeV; the green region is ruled out by stau tachyons. The star indicates the benchmark point plotted in figure 4.5.

Constraints from tachyons and (meta)stability

Having fixed A_u and M_3 from requiring TeV-scale stops and $m_h \approx 126$ GeV, we are left with just the independent parameters M_1, M_2 and $\hat{m}^2_{H_d}$ (see figure 4.3). All of these will be constrained by requiring the absence of slepton tachyons. Since the Yukawa interaction pushes the sleptons down in the RG running, the third generation is always the most constraining. The relevant RG equations are[4]

$$16\pi^2 \frac{d}{dt} m^2_{L_3} = 2y^2_\tau |A_d|^2 - 6g^2_2 |M_2|^2 - \frac{6}{5} g^2_1 |M_1|^2 - \frac{3}{5} g^2_1 S \tag{4.30}$$

$$16\pi^2 \frac{d}{dt} m^2_{e_3} = 4y^2_\tau |A_d|^2 - \frac{24}{5} g^2_1 |M_1|^2 + \frac{6}{5} g^2_1 S \tag{4.31}$$

with

$$S = \mathrm{Tr}[Y_i m^2_{\phi_i}]. \tag{4.32}$$

At the scale $\sqrt{F}$, $S \approx \hat{m}^2_{H_u} - \hat{m}^2_{H_d}$, since all sfermion masses are small. Given that $y^2_\tau \ll g^2_1$, we neglect all the terms proportional to y^2_τ, except for $|A_d|^2$, which may be very large. The right-handed stau is the more fragile of the two staus, since its mass is not sensitive to the upwards pull of M_2. Moreover recall that $\hat{m}^2_{H_u}$ and A_d have already been fixed by EWSB plus the Higgs mass constraint and the extension of messenger parity, respectively. The most interesting slicing of the parameter space is therefore in terms of M_1 and $\hat{m}^2_{H_d}$. This is shown in the plots in figure 4.5, and we now proceed to discuss these plots in more detail.[5]

Let us first consider the case where M_2 is held fixed, as shown in figure 4.5(a) and figure 4.5(b) for two representative values of M_2.

- Since $\hat{m}^2_{H_d}$ pushes down $m^2_{L_3}$ in the RGE, as $\hat{m}^2_{H_d}$ is increased, it eventually results in a snutau tachyon. This is indicated by the red shaded region in figure 4.5(a). This is less of an issue for larger M_2, which is why there is no analogous constraint from snutau tachyons in figure 4.5(b).

[4]Keep in mind that $\hat{m}^2_{H_d}$ does not exhibit strong RG running and can usually be approximated fairly well by its UV value. The story is very different for the stau masses: although in absolute terms their RG running is small as well, their UV threshold value is highly suppressed and the running therefore provides the dominant contribution to the IR stau masses.

[5]Note that in these plots we have considered only positive $\hat{m}^2_{H_d}$. This is because $\hat{m}^2_{H_u}$ (at the scale $\sqrt{F}$) is positive for our choices of M_3, M_2 and A_u, and our simplifying assumption about messenger parity relates the sign of $\hat{m}^2_{H_d}$ to that of $\hat{m}^2_{H_u}$ through equation (4.27).

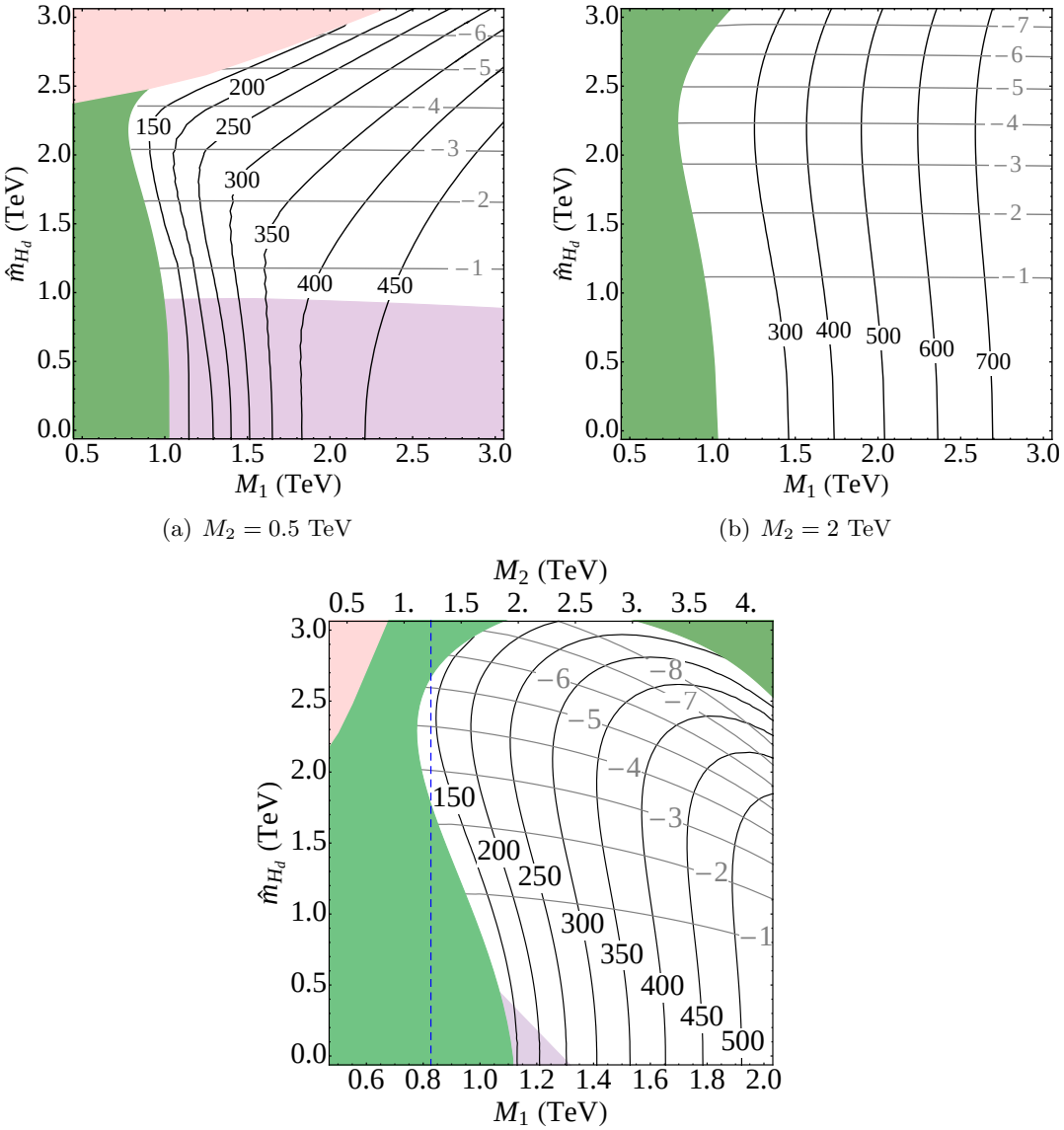

(a) $M_2 = 0.5$ TeV

(b) $M_2 = 2$ TeV

(c) **5-$\bar{\mathbf{5}}$** messengers

Figure 4.5: The pole mass of the lightest stau in GeV (black) and A_d in TeV (gray) as a function of M_1 and $\hat{m}_{H_d}$. $M_3 = 2.0$ TeV and $A_u = -3.2$ TeV and were chosen such that a $m_h \approx 126$ GeV is achieved with TeV-scale stop masses (see the red star on figure 4.4). The other parameters were fixed to $|\mu| = 400$ GeV, $\sqrt{F} = 10^9$ GeV and $\tan\beta = 10$. All soft parameters are defined at the scale $\sqrt{F}$. The green (red) shaded region indicates a stau (snutau) tachyon. If the $\mu < 0$, the purple region is ruled out by an A^0 tachyon. The blue dashed line in 4.5(c) indicates the slice of parameter space where the gaugino masses unify at the GUT scale.

- For smaller M_1, either the S-term or the $|A_d|^2$ term drives the right-handed stau tachyonic. This is indicated by the green shaded regions in figure 4.5.

- Another interesting feature in figure 4.5(a) and figure 4.5(b) is that A_d is fairly independent of M_1 and monotonically increases as a function of $\hat{m}^2_{H_d}$. This is a direct consequence of (4.27) and the fact that (as we just discussed) $\hat{m}^2_{H_u}$ is basically constant in these plots.

- A final noteworthy special case occurs if $M_2 \ll M_1$, as the lightest stau mass eigenstate may be predominantly composed out of the left-handed stau, due to the smaller coefficient for the $|M_1|$ term in (4.30) compared to its analogue in (4.31).

In models with only $\mathbf{5}$-$\bar{\mathbf{5}}$ messengers, M_2 is a function of M_1 and M_3 rather than an independent variable. The constraints on this case are shown in figure 4.5(c).

- We see from figure 4.5(c) that M_2 is always larger than M_1, so snutau tachyons no longer constrain the parameter space, as a stau tachyon is always generated first.

- The relation between the gaugino masses has some interesting implications on A_d and the lightest stau as shown in figure 4.5(c). In particular, the A_d contours bend downwards for large values of M_2. This is again easily understood from (4.27) and (4.29): for large values of M_2, $\hat{m}_{H_u}$ is smaller at the scale $\sqrt{F}$, which in turn leads to a large and negative A_d. Since A_d pulls the staus down, the stau contours eventually start tracking the A_d contours for sufficiently large A_d, and ultimately a stau tachyon is induced. Interestingly, this leads to an *upper* bound on M_1 from stau tachyons, a priori a somewhat counterintuitive notion.

- Also note that the special scenario where all the gaugino masses unify at the GUT scale (dashed blue line in figure 4.5(c)) is only viable in a small sliver of the parameter space for $\hat{m}_{H_d} \sim 2$ TeV.

Finally, we verified using `Vevacious-1.0.11` [97] that there are no further significant constraints from metastable vacuum decay to a charge breaking minimum (even with such

large A_d). However, the parameter space is constrained by demanding the absence of CP-breaking vacua. If $\mu < 0$ and $|A_u| \gg M_2$, the pseudoscalar may end up tachyonic by virtue of a large radiative correction. This constraint is indicated by the purple region in figure 4.5.

4.3.3 Summary of the constraints

This concludes the discussion of the (semi) model-independent constraints on the parameter space. Since the discussion was rather lengthy and involved, a brief summary is appropriate:

- Our assumptions on the extension of messenger parity let us eliminate A_d as a free parameter through (4.27) and restrict $\hat{m}^2_{H_d}$ to be positive at the scale $\sqrt{F}$.
- Through the EWSB conditions we eliminate $\hat{m}^2_{H_u}$ and trade B_μ for $\tan\beta$. Except for the Higgsino mass, the IR physics has little sensitivity to the μ parameter.
- Requiring $m_h \approx 126$ GeV for a minimal SUSY scale roughly fixes M_3 and A_u. As an extra consequence, this requirement also more or less determines $\hat{m}^2_{H_u}$ at the scale $\sqrt{F}$.
- The absence of a charge and CP breaking vacuum imposes restrictions on the parameters M_1, M_2 and $\hat{m}^2_{H_d}$. Roughly speaking, this leads to a lower bound on M_1 and an upper bound on $\hat{m}^2_{H_d}$.

Now that we have exhausted all (semi) model-independent constraints, we will write down an explicit example and compute the associated UV boundary conditions using GMHM. These boundary conditions then yield a prediction for the conformal sequestering and the effective OPE coefficient $\hat{C}$.

4.4 A Minimal Example

Perhaps the simplest example of a messenger sector which generates both μ and A_u at one loop is

$$W = \left(\frac{\kappa}{\Lambda^{\Delta_h - 1}} O_h + M\right)\left(\tilde{\phi}_D \phi_D + \tilde{\phi}_S \phi_S\right) + \lambda_u \tilde{\phi}_D \phi_S H_u + \lambda_d \phi_D \tilde{\phi}_S H_d. \tag{4.33}$$

where the ϕ_D and ϕ_S are a $SU(2)$ doublet and a gauge singlet respectively. In the spurion limit this model notoriously yields the disastrous relation $B_\mu \sim 16\pi^2\mu^2$ [22]. However, as we will show, when hidden sector effects are accounted for this is not necessarily the case.

To obtain a complete model we embed the doublet messengers in **5**-$\bar{\mathbf{5}}$ representations of $SU(5)$ and exploit the full parametric freedom of the model. The full superpotential is then

$$\begin{aligned} W =& \frac{O_h}{\Lambda^{\Delta_h-1}}\left(\kappa_T\tilde{\phi}_T\phi_T + \kappa_D\tilde{\phi}_D\phi_D + \kappa_S\tilde{\phi}_S\phi_S\right) + M_T\tilde{\phi}_T\phi_T + M_D\tilde{\phi}_D\phi_D + M_S\tilde{\phi}_S\phi_S \\ &+ \lambda_u\tilde{\phi}_D\phi_S H_u + \lambda_d\phi_D\tilde{\phi}_S H_d \end{aligned} \tag{4.34}$$

where the ϕ_T, $\tilde{\phi}_T$ are $SU(3)$ triplets. Note that they do not participate in the Higgs mediation; their sole purpose is to complete the $SU(5)$ multiplet and to give a mass to the gluino through standard gauge mediation. M_T, M_D and M_S can all be chosen positive without loss of generality. As is conventional, we allow for N identical copies of these messengers, as long as no Landau poles are introduced below the GUT scale.

4.4.1 UV boundary conditions

The threshold contributions to the gaugino masses are the usual ones in gauge mediation, and may be obtained from (4.16) and (4.17):

$$\begin{aligned} M_3 &= \frac{g_3^2}{16\pi^2}\Lambda_T \\ M_2 &= \frac{g_2^2}{16\pi^2}\Lambda_D \\ M_1 &= \frac{3}{5}\frac{g_1^2}{16\pi^2}\Lambda_D + \frac{2}{5}\frac{g_1^2}{16\pi^2}\Lambda_T \end{aligned} \tag{4.35}$$

with

$$\Lambda_{D,T} = N\kappa_{D,T}\frac{\sqrt{F}^{\Delta_h+1}}{M_{D,T}\Lambda^{\Delta_h-1}}. \tag{4.36}$$

Since the messenger sector consists out of **5**-$\bar{\mathbf{5}}$ messengers, the only two out of the three gaugino masses are independent and the relation in (4.28) is satisfied.

At one loop, the threshold corrections to the Higgs sector obtained from integrating out (4.34) are symmetric under interchange of (κ_S, M_S) $\leftrightarrow$ (κ_D, M_D). This symmetry is made

manifest if we introduce the notation:

$$\kappa = \sqrt{\kappa_D \kappa_S}, \quad M = \sqrt{M_D M_S}, \quad a = \sqrt{\frac{M_D}{M_S}}, \quad b = \sqrt{\frac{\kappa_D}{\kappa_S}} \tag{4.37}$$

and

$$\Lambda_H \equiv N\kappa \frac{\sqrt{F}^{\Delta_h+1}}{M\Lambda^{\Delta_h-1}} \tag{4.38}$$

Then the symmetry becomes $a \to 1/a$, $b \to 1/b$ with κ, M and Λ_H unchanged. The soft parameters can be written as:

$$\mu = \frac{\lambda_u \lambda_d}{16\pi^2} f_\mu(a,b)\Lambda_H \tag{4.39}$$

$$A_{u,d} = \frac{|\lambda_{u,d}|^2}{16\pi^2} f_A(a,b)\Lambda_H \tag{4.40}$$

The dimensionless functions f_μ and f_A can be obtained from explicit computation of the appropriate correlation functions in section 4.2:

$$f_\mu(a,b) = \frac{ab}{(a^4-1)^2}\left(1 - a^4 + 4\log a\right) + (a \leftrightarrow \frac{1}{a}, b \leftrightarrow \frac{1}{b}) \tag{4.41}$$

$$f_A(a,b) = \frac{a^3 b}{(a^4-1)^2}\left(1 - a^4 + 4\log a\right) + (a \leftrightarrow \frac{1}{a}, b \leftrightarrow \frac{1}{b}) \tag{4.42}$$

Similarly, the dimension two soft parameters are given by

$$B_\mu = \frac{\lambda_u \lambda_d}{16\pi^2} f_B(a,b,\gamma)\, \frac{\hat{C}}{N} \left(\frac{\sqrt{F}}{M}\right)^\gamma \Lambda_H^2 \tag{4.43}$$

$$\hat{m}^2_{H_{u,d}} = \frac{|\lambda_{u,d}|^2}{16\pi^2} f_{m_H}(a,b,\gamma)\, \frac{\hat{C}}{N} \left(\frac{\sqrt{F}}{M}\right)^\gamma \Lambda_H^2 \tag{4.44}$$

where $\hat{C}$ is the effective OPE coefficient as defined in section 4.2, the suppression factor

$\left(\frac{\sqrt{F}}{M}\right)^{\gamma}$ is the result of the conformal sequestering, and

$$f_B(a,b,\gamma) = \frac{\pi^{3/2}\csc\left(\frac{\pi\gamma}{2}\right)\Gamma\left(\frac{\gamma}{2}+2\right)\Gamma\left(\frac{\gamma}{2}\right)}{4\left(a^4-1\right)^2\Gamma\left(-\frac{\gamma}{2}\right)\Gamma\left(\frac{\gamma+3}{2}\right)}\left(b^2a^{-\gamma}\left(\gamma-a^4(\gamma+4)\right)+2\left(a^4+1\right)a^{\gamma+2}\right.$$
$$\left.-2\left(a^4-2a^2b^2+1\right)a^{\gamma+2}\,{}_2F_1\left(\frac{\gamma}{2},\frac{\gamma+2}{2};\gamma+2;1-a^4\right)\right)+\left(a\leftrightarrow\frac{1}{a},b\leftrightarrow\frac{1}{b}\right) \tag{4.45}$$

$$f_{m_H}(a,b,\gamma) = \frac{\pi^{3/2}\csc\left(\frac{\pi\gamma}{2}\right)\Gamma\left(\frac{\gamma}{2}+1\right)\Gamma\left(\frac{\gamma}{2}+2\right)}{2\left(a^4-1\right)^2\gamma\Gamma\left(-\frac{\gamma}{2}\right)\Gamma\left(\frac{\gamma+3}{2}\right)}\left(4a^{\gamma+4}-a^{6-\gamma}b^2(\gamma+2)+a^{2-\gamma}b^2(\gamma-2)\right.$$
$$\left.+2\left(a^4b^2-2a^2+b^2\right)a^{\gamma+2}\,{}_2F_1\left(\frac{\gamma}{2},\frac{\gamma+2}{2};\gamma+2;1-a^4\right)\right)+\left(a\leftrightarrow\frac{1}{a},b\leftrightarrow\frac{1}{b}\right) \tag{4.46}$$

In the limit $\gamma \to 0$ the hidden sector reduces to the spurion limit and the formulas simplify drastically. In this limit the model was first discussed in [22], and was later leveraged as a weakly coupled solution to the A/m_H^2 problem in the special case where $a = b = 1$ [48, 77]. Another interesting special case occurs if $a = 1$ and $b = i$ (corresponding to $M_D = M_S$ and $\kappa_D = -\kappa_S$), in which case a symmetry argument forbids both $A_{u,d}$ and μ at one loop. Both of these special limits serve as important consistency checks of our formulas. We elaborate on them further in Appendix 4.A.

4.4.2 Solutions to the UV boundary conditions

As is usual in models with factorizable messenger and hidden sectors, there are some degeneracies in the parametrization of the soft masses in terms of the fundamental parameters of the model. Concretely, all soft masses are left invariant by three different reparametrizations of the fundamental parameters

$$\begin{aligned}
&\kappa_T \to x\kappa_T, \quad M_T \to xM_T \\
&\kappa_D \to y\kappa_D, \quad M_D \to yM_D, \quad \kappa_S \to y\kappa_S, \quad M_S \to yM_S, \quad \hat{C} \to y^{\gamma}\hat{C} \\
&M_{D,T} \to zM_{D,T}, \quad \Lambda \to z^{\frac{1}{1-\Delta_h}}\Lambda
\end{aligned} \tag{4.47}$$

where the x, y and z are arbitrary real constants. As we will see in a moment, these degeneracies are relevant when we attempt to map soft parameters onto the various model-specific couplings and mass scales.

One important subtlety is that the conformal sequestering and the effective OPE coefficient would seem to be degenerate, as can be seen from (4.43), (4.44), and the second line of (4.47). It would seem to imply that a small effective OPE coefficient with little or no sequestering can be traded for a larger OPE coefficient with more sequestering and vice versa, without affecting the soft parameters. However in practice, the effect of this rescaling is limited by the requirement that the $\kappa_{D,S}$ are perturbative and that $\sqrt{F} < \text{Min}[M_T, M_D, M_S]$. The two other degeneracies in (4.47) are restricted by similar consistency conditions.

In general, the model-independent restrictions discussed in section 4.3 are supplemented by the additional requirement that the soft parameters can all be realized in terms of the fundamental parameters of the model. In other words, one must establish that there exists a solution to the set of 10 boundary conditions for the soft parameters

$$M_1, M_2, M_3, A_u, A_d, \mu, B_\mu, \hat{m}^2_{H_u}, \hat{m}^2_{H_d} \text{ and } \sqrt{F} \tag{4.48}$$

in terms of a realistic choice for the 13 continuous 'fundamental' parameters

$$\lambda_u, \lambda_d, \kappa_T, \kappa_D, \kappa_S, M_T, M_D, M_S, \hat{C}, \Delta_h, \gamma, \sqrt{F} \text{ and } \Lambda \tag{4.49}$$

plus the discrete messenger number N. Of the 10 soft parameters, only 9 are really independent since we imposed a messenger parity that related A_d to A_u, $\hat{m}_{H_u}$ and $\hat{m}_{H_d}$. Naively this system of equations appears to be underconstrained, and one would expect that generically a solution should exist. However the situation is bit more subtle.

First, we have used the results of the conformal bootstrap program (summarized in table 4.1) to choose the maximum γ allowed for a given Δ_h, so they are no longer independent. Secondly, 3 out of the 12 remaining continuous fundamental parameters are degenerate as in (4.47). For definiteness, we break the degeneracies[6] in (4.47) by fixing $\kappa_T = \kappa_D = 2$ and $\Lambda = 2 \max[M_T, M_D, M_S]$. This choice attempts to maximize the impact of the conformal sequestering, while preserving perturbativity in $\kappa_{D,T}$. (Even more sequestering, and thus larger $\hat{C}$, can be obtained from (4.47) if one is willing to tolerate a larger value for κ_D.)

After fixing the degeneracies, we are left with only with 9 independent fundamental parameters to determine 9 independent soft parameters. Since the boundary conditions are

[6]Our choice for Λ corresponds to the most optimistic case as far as the impact of the sequestering is concerned. For a different choice of Λ the messenger scale and the sequestering can be obtained by the rescaling in (4.47).

soft parameters		fundamental parameters			
$\sqrt{F}$	10^9 GeV	γ	0.1	0.4	0.7
M_1	1.75 TeV	Δ_h	1.20	1.45	2.00
M_2	3.53 TeV	N	6	6	6
M_3	2.0 TeV	λ_u	0.66	0.68	0.70
A_u	-3.2 TeV	λ_d	0.60	0.62	0.63
A_d	-2.6 TeV	κ_S	-0.19	-0.25	-0.30
μ	400 GeV	M_T	4.3×10^{12} GeV	9.0×10^{11} GeV	1.6×10^{11} GeV
$\hat{m}_{H_u}$	1.66 TeV	M_D	1.5×10^{12} GeV	3.2×10^{11} GeV	4.0×10^{10} GeV
$\hat{m}_{H_d}$	1.50 TeV	M_S	2.4×10^{11} GeV	6.4×10^{10} GeV	9.7×10^{9} GeV
B_μ	0.35 TeV^2	$\left(\frac{\sqrt{F}}{M}\right)^\gamma$	0.53	0.14	0.12
		$\hat{C}$	0.071	0.30	0.30

Table 4.2: An example of a point with its interpretation in terms of the fundamental parameters, for various values of γ. For this point $\tan\beta = 10$.

highly non-linear in some of the fundamental parameters, a solution is not guaranteed, and requiring its existence can further constrain the acceptable range of the soft parameters in (4.48). Such solutions must be obtained numerically; details on our algorithm are provided in appendix 4.B. We do not attempt to find all possible solutions for a given set of soft parameters, but are content with a single viable solution per set of soft parameters. A 'viable' solution in this context means that all masses, couplings and the effective OPE coefficient are real, that the couplings λ_u, λ_d and κ_S are perturbative and that $\sqrt{F} < \text{Min}[M_T, M_D, M_S]$. The latter will turn out to be a stringent condition if $\sqrt{F} \leq 10^7$ GeV.

Table 4.2 contains an example of a point and its solution in terms of the fundamental parameters for various choices of γ. Unsurprisingly, conformal sequestering is not efficient for $\gamma = 0.1$ and the effective OPE coefficient must be very small to accommodate a solution. For $\gamma = 0.4$ and $\gamma = 0.7$ on the other hand, conformal sequestering provides roughly an order of magnitude suppression for the one-loop contributions to B_μ and $\hat{m}^2_{H_{u,d}}$.[7] Moreover, if we choose $N = 6$ the $\frac{1}{N}$ factor in (4.43) and (4.44) in combination with conformal sequestering provides a sufficient amount of suppression to facilitate an $\mathcal{O}(1)$ effective OPE coefficient.

More generally, the solutions for the effective OPE coefficient as a function of M_1 and $\hat{m}_{H_d}$ are shown in figure 4.6 for various values of γ. Almost all of the viable parameter space

[7]Notice that the sequestering for $\gamma = 0.7$ is essentially the same as the sequestering for $\gamma = 0.4$, despite the higher anomalous dimension of the former. We have encountered this already in figure 4.2. It is due to the competing effects of increased sequestering from larger γ, but decreased sequestering from larger Δ_h.

in figure 4.5(c) of the previous section can be covered by our example, except for a small region for low $\hat{m}^2_{H_d}$ where our numerical method fails to converge on a suitable solution. It is conceivable that these points may be recovered with a more sophisticated numerical procedure. This result suggests that it should be possible to cover the full parameter space with weakly coupled models for the messenger sector; however this is beyond the scope of this work.

It is interesting to compare the precise effectiveness of the conformal sequestering in our model as a function of $\sqrt{F}$ with our rough estimates in figure 4.2. The sequestering as computed in our example is shown in figure 4.7, as well as the effective OPE coefficient needed to obtain viable EWSB. In fairly good agreement with our rough estimate in figure 4.2, conformal sequestering becomes less efficient for lower $\sqrt{F}$, and its effect completely disappears for $\sqrt{F} \sim 10^6$ GeV. As we have seen, the reason is that for a fixed gaugino mass and lower $\sqrt{F}$, the separation between M and $\sqrt{F}$ must decrease, limiting the capabilities of the sequestering.

From the left-hand panel of figure 4.7 one also learns that increasing the messenger number has a double advantage: on the one hand it provides an extra $\frac{1}{N}$ suppression in (4.43) and (4.44). In addition, a larger N in (4.35) allows for a slightly larger splitting between M_D and $\sqrt{F}$ and thus slightly more efficient suppression from conformal sequestering. For low N and low $\sqrt{F}$, a smaller $\hat{C}$ is needed to compensate for the loss in sequestering and messenger number suppression. This is illustrated in the right-hand panel figure 4.7, where for completeness we added the extreme limit of $\gamma = 0$, which corresponds to no contribution from sequestering.

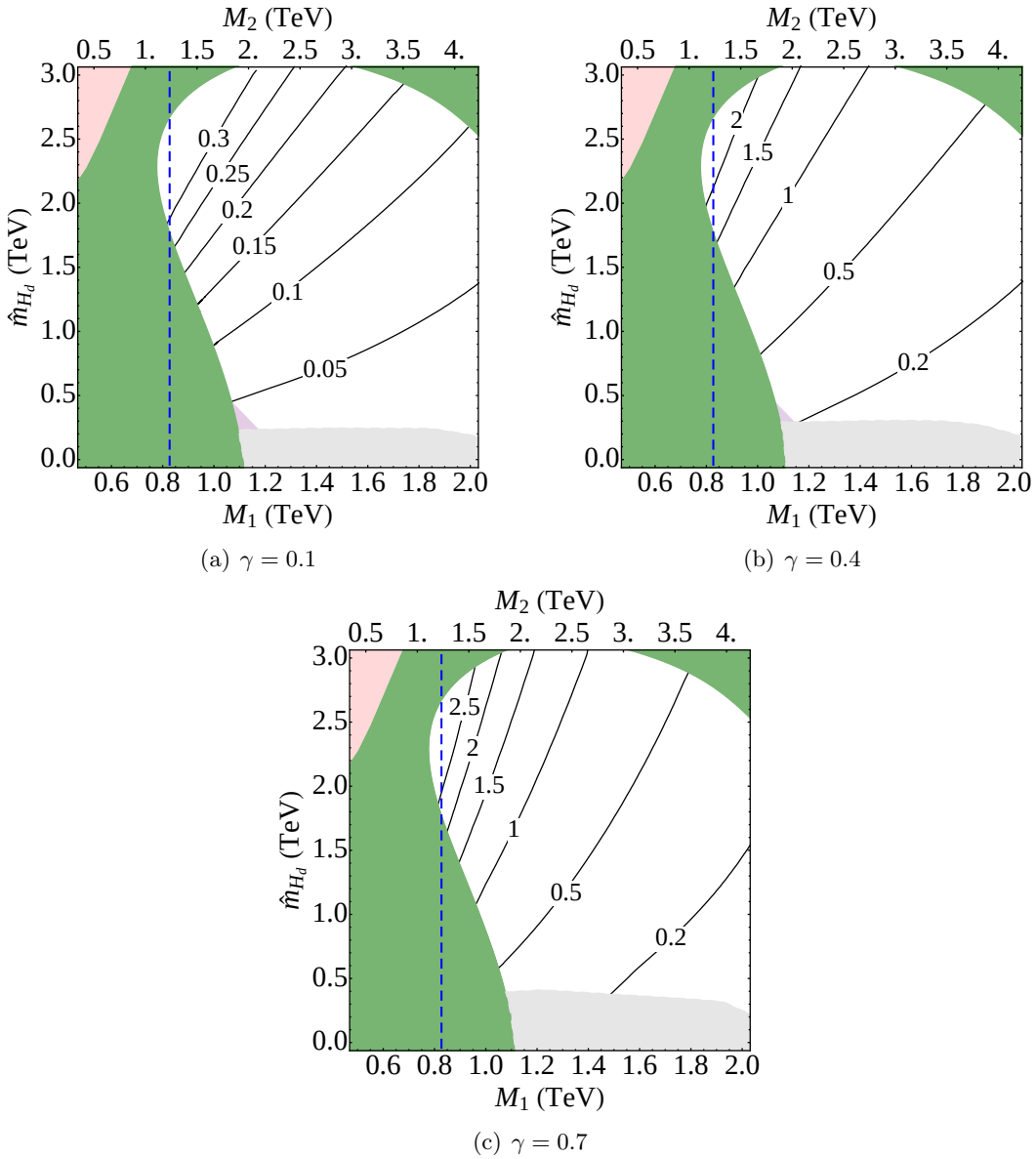

(a) $\gamma = 0.1$

(b) $\gamma = 0.4$

(c) $\gamma = 0.7$

Figure 4.6: $\hat{C}$ as a function of M_1 and $\hat{m}_{H_d}$ for $N = 6$. The light gray area indicates the region where our algorithm does not converge on a suitable solution for the UV boundary conditions. All other parameters and colors are as in figure 4.5(c).

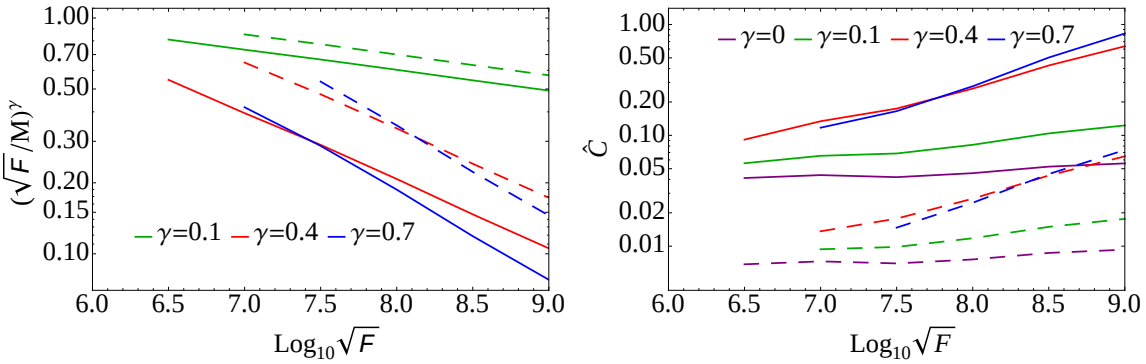

Figure 4.7: Plots of $\left(\frac{\sqrt{F}}{M}\right)^{\gamma}$ and $\hat{C}$ as a function of $\log_{10}\sqrt{F}$ for $m_{A^0} = 1.5$ TeV, $M_1 = 1.2$ TeV, $\mu = 400$ GeV and $\tan\beta = 10$. For each value of $\sqrt{F}$, M_3 and A_u are fixed such that $\sqrt{m_{\tilde{t}_1} m_{\tilde{t}_2}}$ is minimized under the constraint $m_h > 125$ GeV. Dashed lines represent $N = 1$, full lines represent $N = 6$. The various curves are cut off at the point where the consistency condition $\sqrt{F} < \mathrm{Min}[M_T, M_D, M_S]$ is no longer satisfied.

4.5 Collider Phenomenology

In this section we briefly discuss the collider phenomenology and the current constraints on the model. Since all the sfermion masses are suppressed at the scale $\sqrt{F}$, their IR values are primarily set through gaugino mediation. We emphasize once more that this is a general property of models that attempt to address the μ/B_μ and the A/m_H^2 problems with strong hidden sector dynamics. This implies a number of generic features of the low energy spectrum which are independent of the precise content of the hidden and messenger sectors:

- The gluino tends to be heavier than the squarks, the wino tends to be heavier than the left-handed sleptons, and the bino tends to be heavier than the right-handed sleptons.
- The colored sfermions are typically heavier than the electroweak sfermions, because only the former are pulled up by M_3. One exception is the lightest stop, which may be pushed down due to mixing effects.
- The NLSP is a stau or a Higgsino and is sufficiently long-lived[8] to escape the detector, except if $\sqrt{F} \sim 10^6$ GeV, in which case it decays through a displaced vertex.

[8]This is assuming R-parity conservation. If R-parity is violated, the NLSP could still decay promptly despite a high supersymmetry breaking scale.

- The LSP is the gravitino if $\sqrt{F} \lesssim 10^{10}$ GeV as we have assumed in this paper. (If $\sqrt{F} > 10^{10}$ GeV, the gravitino mass may be lifted to the extent that it is no longer the LSP [70, 92, 93].)

Unsurprisingly, this class of models is subject to a variety of collider constraints. Conceptually, it is important to distinguish constraints on the colored part of the spectrum from constraints on the electroweak part. Regarding the former, the masses of the colored sparticles are almost exclusively controlled by M_3 and A_u. As we saw in section 4.3.2, these two parameters are determined by the requirement of a 126 GeV Higgs with TeV-scale stops. Therefore, we expect robust predictions on the typical masses of the colored sparticles. As shown in figure 4.4, the lightest stop is always the lightest colored state and must be heavier than 750 GeV, while the minimum gluino mass is roughly 2 TeV. The masses of the electroweak states on the other hand are controlled by the bino and wino masses, and may be as light as several hundreds of GeV. The phenomenology of these electroweak states is very rich and radically different depending on the nature of the NLSP. In what follows we discuss stau and Higgsino NLSP separately.[9] A typical spectrum is shown in figure 4.8.

Since the NLSP is nearly always detector-stable in these models, there are already very powerful collider constraints if the stau is the NLSP. In particular, CMS has excluded such long-lived staus with a cross section above 0.3 fb [99]. (A slightly weaker limit from ATLAS is also available [100].) This translates to a lower limit on the mass of 339 GeV. As can be seen from figure 4.5, this constraint implies that the stau NLSP scenario is now experimentally disfavored.

Since these searches are inclusive, they are also likely to be sensitive to the production of the entire superpartner spectrum, and not just to the staus themselves (see e.g. the discussion in [101, 102]). By comparing their production cross sections [103] with the CMS limit, one can estimate the bounds on the masses of other sparticles. For instance, we find that the gluino and the stops should be heavier than ~ 1400 GeV and ~ 1000 GeV respectively. According to the preceding discussion of the colored spectrum (see again figure 4.4), this is not a very stringent constraint on these models, where the gluinos and stops

[9] In a narrow corner of the parameter space the sneutrino can be the NLSP. For a discussion on the phenomenology of this scenario we refer to [98].

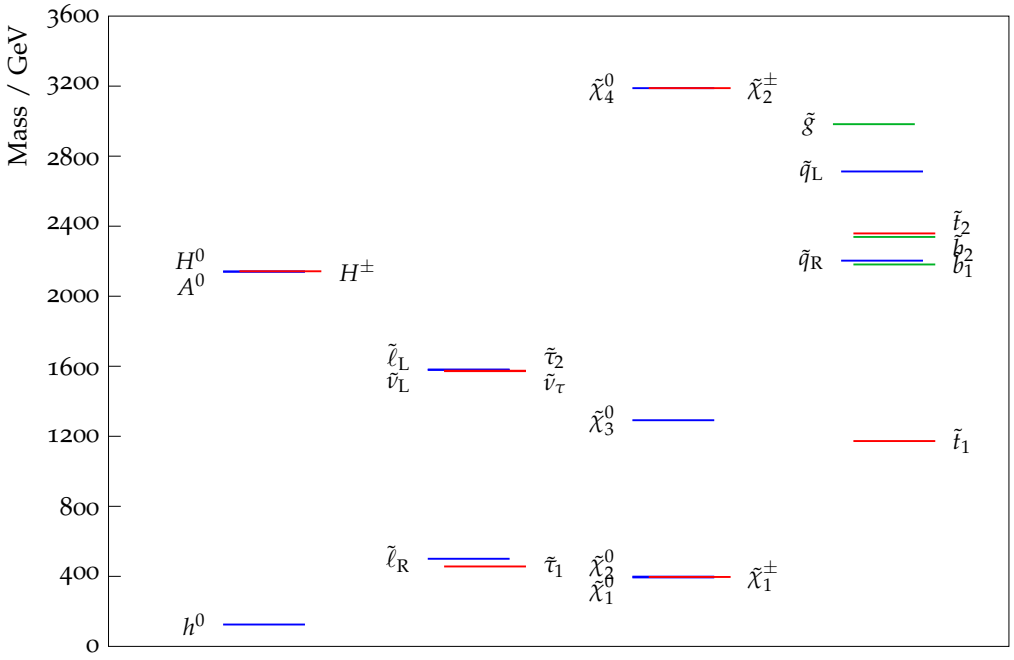

Figure 4.8: The spectrum for the point in table 4.2, with Higgsino NLSP. The spectrum with stau NLSP is nearly identical, since the μ parameter has only a small effect on the other masses.

are already heavy to begin with. Meanwhile, the Higgsino is excluded below ~ 600 GeV, where we estimated the production cross section with Prospino 2.1 [104]. In the discussion in section 4.3 we restricted ourselves to $|\mu| < 500$ GeV for simplicity, however we verified that Higgsino masses which evade the constraint can easily be obtained.

The collider phenomenology of a detector stable Higgsino NLSP is essentially identical to that of a Higgsino LSP in gravity mediation models. Unsurprisingly, from an experimental point of view a long-lived Higgsino NLSP is much more challenging than a long-lived stau NLSP. If the other states decouple, the only robust bound comes from LEP, and requires the charged Higgsino component to be heavier than 92.4 GeV [105]. Since the sfermion masses are generated through gaugino mediation, the next state in the spectrum is typically the lightest stau mass eigenstate, possibly degenerate with the right-handed light flavor sleptons. With a Higgsino heavier than the LEP bound, there is currently no bound on these right-handed sleptons if they are Drell-Yan produced [106, 107]. The left-handed sleptons on the other hand have a higher production cross section and are constrained to be heavier than 300 GeV if the Higgsino is lighter than 160 GeV [106, 107], however this bound does not yet

significantly constrain our minimal model with **5**-$\bar{\mathbf{5}}$ messengers. The lightest colored state is always the lightest stop and is always outside the reach of the 8 TeV LHC, but its direct production could be a promising channel at the 14 TeV run. Although the spectrum is not natural in the strict sense, this signature is covered by existing "Natural SUSY" search strategies.

4.6 Discussion and Outlook

Strong hidden sector dynamics may provide an elegant framework in which both the μ/B_μ and the A/m_H^2 problems can be addressed through a single mechanism. Rather than relying on a cleverly designed messenger sector, this class of models counters the disastrous $16\pi^2$ enhancement of B_μ and m_H^2 by a suppression from strong dynamics in the hidden sector. This suppression can arise from conformal sequestering, a small effective OPE coefficient, large messenger number, or a combination of all three. We provide a simple example of a complete model, as well as the first explicit calculation of the low energy observables in terms of scaling dimensions, vacuum expectation values and OPE coefficients of the leading operators in the hidden sector. The essential tool enabling this calculation is the GMHM framework [49].

Accounting for the bounds on the anomalous dimension from the conformal bootstrap program [81], we make a general estimate of the impact of conformal sequestering for this class of models and validate our estimate in an explicit example. In either case, conformal sequestering is insufficient to produce a full loop factor suppression, but a suppression of roughly one order of magnitude is possible if $\sqrt{F} \sim 10^9$ GeV. In this case viable electroweak symmetry breaking can be achieved for effective OPE coefficients roughly between 1 and 0.1, depending on the details of the messenger sector. It is still an open question whether the upper bound on γ from the bootstrap program can be saturated, as currently no examples are known. Such an example would necessarily need to be strongly coupled, as weakly coupled SCFT's were shown not to produce the required inequalities for the scaling dimensions of the operators [83].

An important and generic feature of this class of models is that the suppression from conformal sequestering is only appreciable for $\sqrt{F}$ as high as roughly 10^9 GeV. From this

fairly high scale of supersymmetry breaking one would expect a degree of fine-tuning of roughly 1 in 10^3 at best, and a priori the tuning may be aggravated by large cancellations in the UV boundary conditions, as is the case in Higgs mediation models without appreciable hidden sector dynamics. In most of the parameter space of our example such large cancellations do not occur, indicating that the tuning estimates from the high scale RG running are a fair estimate of the total tuning of the model. The model therefore constitutes a solution to the "little A/m_H^2 problem" as presented in [77], although a moderate price in tuning had to be paid from the higher supersymmetry breaking scale.

This problem would be alleviated to some degree by considering lower values $\sqrt{F}$, where the suppression of the loop factor must be obtained from the smallness of the effective OPE coefficient rather than from the conformal sequestering.[10] At this point it is not clear whether such small OPE coefficients can be achieved in a realistic model. The conformal bootstrap program has resulted in interesting lower bounds on OPE coefficients, provided that there is a gap in the spectrum of operators [81]. Implicitly, we assumed the existence of such a gap by truncating the OPE after the leading term, and it seems plausible that our scenario may be constrained from this end as well.[11] A detailed quantitative analysis of this type of constraint is beyond the scope of this paper, but is certainly worth exploring.

Even if very small OPE coefficients could be made compatible with the bootstrap constraints, within our simple example, we found it very challenging to find viable solutions with $\sqrt{F} \sim 10^6$ GeV. But we strongly suspect that even extending the model slightly would allow for many more solutions with low $\sqrt{F}$. A broader question which is also interesting is whether it is possible to completely cover the rest of the parameter space in (4.26). It is encouraging that even with our simple example we were able to sample a large part of it. We therefore suspect that it should be possible to cover the full parameter with a set of perturbative messenger models. Here are some promising ideas in this direction. First we could relax our assumption on the action of the messenger parity on O_u and O_d. For instance, one could consider multiple portals between the messenger sector and the MSSM

[10] Alternatively, we could conceivably avoid the loop factors altogether with a strongly-coupled messenger sector. Although such a setup may greatly alleviate the fine-tuning by allowing for lower $\sqrt{F}$, it may also lose much of its predictivity and calculability.

[11] We thank David Simmons-Duffin for bringing this to our attention.

Higgs sector, of the form:

$$W \supset \sum_i \lambda_u^{(i)} O_u^{(i)} H_u + \sum_i \lambda_d^{(i)} O_d^{(i)} H_d \tag{4.50}$$

Another idea would be to allow for portals of the form

$$W \supset \lambda S H_u H_d \tag{4.51}$$

where S is a gauge singlet. This is interesting since the singlet portal does not generate $A_{u,d}$ and $\hat{m}^2_{H_{u,d}}$ at the same loop order as μ and B_μ [23] and therefore provides a clean way to untangle these two soft parameters from the others. Finally, in our simple model we assumed **5**-$\bar{\mathbf{5}}$ messengers. A model including **10**-$\overline{\mathbf{10}}$ messengers (as in [80]) would offer more parametric freedom.

In our analysis we restricted ourselves to $\sqrt{F} < 10^{10}$ GeV in order to avoid problems with charged LSPs and to automatically eliminate Planck-induced flavor violation. However it is conceivable that with enough assumptions about the hidden sector, conformal sequestering could also suppress dangerous Planck-induced operators [86–88]. If this is true, then our model could be extended beyond $\sqrt{F} \sim 10^{10}$ GeV (at least with the Higgsino being the LSP). Such a scenario deserves further study, especially since with larger $\sqrt{F}$, the impact of the conformal sequestering can be further enhanced beyond what we have found in this paper.

The collider phenomenology in this class of models is generically similar to the phenomenology of gaugino mediation with large A-terms and depends strongly on the nature of the NLSP. If the NLSP is the Higgsino, the phenomenology is similar to that of a neutralino LSP. The constraints on this scenario are currently rather weak and prospects for the 14 TeV run depend heavily on the spectrum of the colored states. On the other hand, if the NLSP is a stau, our model is already strongly constrained by current searches. Moreover, in this case direct stop production would be a spectacular channel at the 14 TeV run of the LHC, which should allow us to definitively test this scenario.

Appendices

4.A Simplifying Limits

The boundary conditions for B_μ and $\hat{m}_{H_{u,d}}$ for our example in section 4.4 simplify dramatically in the spurion limit ($\gamma \to 0$ and $\hat{C} \to 1$). Specifically, the dimensionless functions reduce to:

$$\begin{aligned} f_B(a,b,0) =& \frac{1}{(a^4-1)^3}\Big[b^2\left(-a^8+8a^4\log a+1\right) \\ & -a^2\left(a^4+1\right)\left(1-a^4+2\left(a^4+1\right)\log a\right)\Big] + (a \leftrightarrow 1/a, b \leftrightarrow 1/b) \end{aligned} \tag{4.52}$$

$$f_{m_H}(a,b,0) = -\frac{2a^2(a^2-b^2)}{(a^4-1)^3}\left(1-a^4+2\left(a^4+1\right)\log a\right) + (a \leftrightarrow 1/a, b \leftrightarrow 1/b) \tag{4.53}$$

If in addition we take $a = b$, the model reduces to the model first presented by Dvali, Giudice and Pomarol [22] and we can verify that in this limit our results agree with theirs. Concretely, the dimensionless functions further reduce to

$$\begin{aligned} f_\mu(a,a) &= \frac{a^2\log a^4}{1-a^4} \\ f_A(a,a) &= -1 \\ f_B(a,a,0) &= \frac{a^2\log a^4}{1-a^4} \\ f_{m_H}(a,a,0) &= 0 \end{aligned} \tag{4.54}$$

Observe that $\hat{m}_{H_u}$ and $\hat{m}_{H_d}$ vanish at one loop; this was the basis of the weakly coupled solution to the A/m_H^2 problem presented in [77]. In that paper we considered the special limit $\lambda_d = 0$ which ensures that μ, B_μ, A_d and $\hat{m}_{H_d}$ vanish. In such a setup, the μ/B_μ problem is postponed and must dealt with separately, for instance by extending the MSSM with an extra singlet.

For the case $a \neq b$, DGP also provide an expression for $\hat{m}^2_{H_{u,d}}$.[12] Their notation is somewhat different from ours, and the Λ_1 and Λ_2 in equation (22) of [22] correspond to

$$\Lambda_1 = \frac{a}{b}\Lambda_H \quad \text{and} \quad \Lambda_2 = \frac{b}{a}\Lambda_H \tag{4.55}$$

With this change of notation in (4.53), our expression for $\hat{m}^2_{H_{u,d}}$ becomes

$$\hat{m}^2_{H_{u,d}} = \frac{|\lambda_{u,d}|^2}{16\pi^2}(\Lambda_1-\Lambda_2)^2 g(a) \tag{4.56}$$

[12] To 1 loop order, the distinction between $\hat{m}^2_{H_{u,d}} \equiv m^2_{H_{u,d}} + |\mu|^2$ and $m^2_{H_{u,d}}$ is moot.

with

$$g(a) = -a^4 \frac{1 - a^4 + (1 + a^4)\log(a^4)}{(1 - a^4)^3} \tag{4.57}$$

The magnitude of our expression agrees with equation (22) in [22], however we disagree on the sign. We find $\hat{m}^2_{H_{u,d}} > 0$ and since the Higgs fields can be considered as pseudomoduli in a model with only fields of R-charge 0 and 2, we have confidence in our result [108, 109].

The second interesting special limit is when $a = 1$ and $b = i$, as in this case μ and $A_{u,d}$ vanish at one loop. The superpotential reduces now to

$$W = \kappa \frac{O_h}{\Lambda^{\Delta_h - 1}} \left(\tilde{\phi}_D \phi_D - \tilde{\phi}_S \phi_S \right) + M \left(\tilde{\phi}_D \phi_D + \tilde{\phi}_S \phi_S \right) + \lambda_u \tilde{\phi}_D \phi_S H_u + \lambda_d \phi_D \tilde{\phi}_S H_d. \tag{4.58}$$

with $\kappa \equiv \kappa_D = -\kappa_S$ and $M \equiv M_D = M_S$. The model now has an enhanced discrete symmetry:

$$\phi_D \leftrightarrow \tilde{\phi}_S \quad \tilde{\phi}_D \leftrightarrow \phi_S \quad O_h \rightarrow -O_h \tag{4.59}$$

which forbids the correlators (4.11) and (4.12) at the one loop level[13] since the operator O_m is odd under (4.59). This feature may be useful when attempting to cover the full GMHM parameter space with weakly coupled models for the messenger sector.

4.B Numerical Procedure

Our general philosophy is to front-load the part of the calculation that involves integrating the RGE's, and delay the implementation of the model-specific boundary conditions as long as possible. This allows us to study various tachyons and EWSB requirements in terms of the familiar soft parameters, rather than the somewhat unintuitive parameters $\lambda_{u,d}$, $\hat{C}$ etc. This approach also should allow for a more straightforward generalization to other models, since the model-independent, more time consuming steps are performed first. Concretely, we parametrize our scan in terms of the independent variables

$$M_{1,2,3}, A_u, A_d, \tan\beta, \mu, m_A(\text{pole}) \text{ and } \sqrt{F} \tag{4.60}$$

[13] Of course the discrete symmetry does not commute with the gauge symmetry, and is therefore not a symmetry of the full theory. However for the 1 loop Higgs mediated contributions the gauge charge of ϕ_D is irrelevant.

where all parameters are specified at the scale $\sqrt{F}$, except the pole mass of the pseudoscalar m_A. We choose the latter rather than $\hat{m}_{H_d}$ such that our scan is maximally compatible with the inputs that must be provided to `SOFTSUSY-3.3.9` [67]. For the case where the messengers fit into **5-$\bar{\mathbf{5}}$** representations, we solve for M_2 from the outset by using (4.28). Our method can be further broken down in the following steps:

1. For a given choice of (4.60), `SOFTSUSY-3.3.9` computes the RG-running and imposes the EWSB conditions, a procedure which results in a value for $\hat{m}^2_{H_u}$ and $\hat{m}^2_{H_d}$ at the scale $\sqrt{F}$. Furthermore we determine A_d as a function of the other soft parameters by imposing (4.27). Since (4.27) involves $\hat{m}^2_{H_u}$ and $\hat{m}^2_{H_d}$, this must be done through an iterative procedure, which we repeat until convergence is achieved. At this point we are done with integrating the RGE's, and there is no more need to run `SOFTSUSY-3.3.9` in the remainder of the calculation.

2. At this stage we can express Λ_H as a function of M_2, a and b. At the level of finding a solution for the boundary conditions, the variables $\hat{C}$, N and $\left(\frac{\sqrt{F}}{M}\right)^\gamma$ are degenerate. We therefore define an auxiliary variable

$$\tilde{C} \equiv \frac{\hat{C}}{N}\left(\frac{\sqrt{F}}{M}\right)^\gamma \tag{4.61}$$

to simplify the solution finding procedure. Solving the UV boundary conditions specified in (4.39), (4.40), (4.43) and (4.44) thus corresponds to solving 6 algebraic equations in terms of the 5 variables $\lambda_{u,d}$, a, b and $\tilde{C}$. In the previous step we already eliminated A_d by solving (4.27) through the iterative procedure. This leaves us with 5 equations with 5 unknowns, and a much better chance of obtaining a viable solution than if we would have attacked all 6 equations at once. This translates into a much improved computation time per point than if we would have performed a brute force scan over $\lambda_{u,d}$, a, b and $\tilde{C}$. Next we can isolate a simple set of two equations by taking a clever combination of the boundary conditions:

$$\begin{aligned}\frac{\mu^2}{A_u A_d} &= \left(\frac{f_\mu(a,b)}{f_A(a,b)}\right)^2 \\ \frac{B_\mu^2}{(\mu^2+m^2_{H_u})(\mu^2+m^2_{H_d})} &= \left(\frac{f_B(a,b,\gamma)}{f_{m_H}(a,b,\gamma)}\right)^2\end{aligned} \tag{4.62}$$

This system of equations is independent of $\lambda_{u,d}$ and $\tilde{C}$ and can be solved analytically for b. At this point we have to commit to a concrete choice of γ, after which we can solve the remaining equation for a numerically.

3. Now that we have solved for a and b for a given choice of γ, it is trivial to solve the remaining boundary conditions for $\lambda_{u,d}$ and $\tilde{C}$. At this point we discard the solution if any of these parameters does not have a real solution, if $|\lambda_u| > 3$, if $|\lambda_d| > 3$ or if $\tilde{C} > 100$. These cuts are chosen arbitrarily to ensure no non-physical solutions where kept. We verified that the results are not sensitive to the precise value of these cuts.

4. In the final step we recover M_D from (4.35) and table 4.1, and use this to unpack $\tilde{C}$ in terms of the suppression factor from conformal sequestering and the effective OPE coefficient $\hat{C}$. At this step we also must commit to a choice of messenger number N.

By delaying an explicit choice for γ and N as long as possible we gained in both flexibility and computation speed.

Chapter 5

Conclusion and outlook

In the context of supersymmetry, the observation of a SM-like Higgs boson with a mass near 126 GeV either requires a non-trivial extension of the MSSM or stops heavier than roughly 1 TeV. Furthermore the lower bound on the stops in the latter case can only be saturated if the stops are equipped with a large trilinear coupling with the H_u Higgs field, which results in a large positive threshold contribution to the mass of the lightest CP-even Higgs. In this work, we have attempted to systematically study the implications of requiring such a large A-term on possible UV completions of the MSSM, without sacrificing the MFV ansatz. Since it is very challenging to obtain sizable A-terms from mere RG running without jeopardizing electroweak symmetry breaking [17], one must allow for direct interactions between the MSSM matter fields and the messenger fields. If such extra interactions are restricted to the MSSM Higgs sector, the MFV ansatz is trivially preserved. Moreover such Higgs-messenger couplings are well motivated as a solution to the μ/B_μ problem.

In chapter 2 we showed that Higgs mediation suffers from an A/m_H problem, just as it suffers from the more well known μ/B_μ problem. Concretely this means that in a generic model, the soft supersymmetry breaking terms in the Higgs sector satisfy

$$B_\mu \sim 16\pi^2|\mu|^2 \tag{5.1}$$

$$m_{H_u}^2 \sim 16\pi^2|A_t|^2. \tag{5.2}$$

Both relations have a detrimental effect on the Higgs potential and prevent electroweak symmetry from being broken spontaneously. In a fully weakly coupled context, there exists a simple solution to the A/m_H problem, which also appears to be unique. Concretely, we consider a simple model of the form

$$W = X\left(\tilde{\phi}_1\phi_1 + \tilde{\phi}_2\phi_2\right) + \phi_1\tilde{\phi}_2 H_u. \tag{5.3}$$

where X is responsible for spontaneous supersymmetry breaking. Upon integrating out the ϕ, $\tilde{\phi}$ fields, the 1-loop field strength renormalization factor for H_u is

$$Z_{H_u}(X, X^\dagger) \sim \frac{1}{16\pi^2} \log\left(\frac{XX^\dagger}{\Lambda^2}\right) \tag{5.4}$$

At one loop, $m^2_{H_u}$ is computed by differentiating $Z_{H_u}(X, X^\dagger)$ with respect to X and $X^\dagger$. For the case at hand, $Z_{H_u}(X, X^\dagger)$ is the sum of a holomorphic and an anti-holomorphic piece, and therefore vanishes under differentiation with respect to both X and $X^\dagger$. This implies that $m^2_{H_u}$ must vanish at one loop and we are therefore able circumvent the dangerous relation in (5.2). This behavior is however spoiled if extra mass scales are introduced in the model defined by (5.3).

We further constructed an explicit example which incorporates this solution, in addition to a solution to the μ/B_μ problem by means of an extra singlet as in the NMSSM. Although this solution allows for low messenger scales, it is nevertheless significantly fine tuned. The reason is a large, positive two loop contribution to $m^2_{H_u}$ which must be cancelled off partially to facilitate electroweak symmetry breaking. These contributions arise from integrating out the auxiliary component of the Higgs field:

$$A_u F_{H_u} H_u^\dagger \to |A_u|^2 H_u H_u^\dagger \tag{5.5}$$

where A_u is of course large by construction, to facilitate a physical Higgs mass near 126 GeV. We find that this 'little A/m_H problem' is present in all weakly coupled Higgs mediation models that strive towards large A-terms.

Since fully weakly coupled models are always plagued by this little A/m_H problem, partially strongly coupled solutions are of special interest. Strongly coupled messenger sectors may be viable but lose most, if not all of their predictivity. On the other hand, models where only the hidden sector is strongly coupled can be made calculable to a very high degree. We lay the theoretical groundwork for this in chapter 3 and provide and explicit, fully worked out example in chapter 4. As it turns out both the μ/B_μ and A/m_H problems may be resolved by a single, simple mechanism, provided that certain anomalous dimensions and OPE coefficients in the hidden sector satisfy certain inequalities. Concretely, in a strong hidden sector the operators O_h and O_Δ, responsible for respectively the A-term

and for $m^2_{H_u}$, do not need to be related in an obvious way. In this case $m^2_{H_u}$ will be proportional to the ratio of the susy breaking scale $\sqrt{F}$ and messenger scale M, such that

$$m^2_{H_u} \sim 16\pi^2 C_\Delta \left(\frac{\sqrt{F}}{M}\right)^{\Delta-2\Delta_h} |A_u|^2 \tag{5.6}$$

where C_Δ is an OPE coefficient in the hidden sector and Δ and Δ_h the scaling dimensions of O_Δ and O_h respectively. If $\Delta > 2\Delta_h$ and $M \gg \sqrt{F}$, this results in the desired suppression of $m^2_{H_u}$. In chapter 4 we clarified the theoretical foundations of this scenario in terms of a correlator formalism. This allows us to clear up some disagreements that have persisted in the literature, as well as to extend the calculability of this class of models. In chapter 5 we show that recent constraints from the conformal boothstrap program [81] rule out the scenario where the power suppression is sufficiently strong to fully counter the $16\pi^2$ enhancement in (5.6). Nevertheless a successful solution is still possible if the OPE coefficient C_Δ is smaller than one. We provide an explicit example of model and show that this type of solutions are characterized by fairly high supersymmetry breaking scales, which once again increases the fine tuning of the model. On the other hand, such high supersymmetry breaking scales may lead to very interesting collider signatures in the form of a long lived stau NLSP.

On general grounds, one may claim that if the MSSM or a close variant is indeed realized in nature, it is not surprising that none of the superpartners have been discovered at the 8 TeV LHC. If the A-terms are small, the stop are bound to be out of the reach of the 14 TeV as well, and a much more powerful experiment would be needed. On the other hand, if the A-terms are sizable, the stops may be accessible, depending on the rest of the spectrum, in particular the properties of the LSP. In this sense we enjoy the exciting prospect that much of the work in this thesis will be experimentally tested in the early phase of the 14 TeV run.

On the model building side there are two main avenues to build further on this work. In chapter 4 we studied the full parameter space of general Higgs mediation by means of correlation functions, as was done for gauge mediation in [56, 57, 78]. For gauge mediation it was shown that the full parameter space could be spanned with explicit models [57, 84]. At this time, no such proof exists for Higgs mediation, but the example provided in chapter 4 may be a fruitful starting point to pursue this goal.

The second major question that currently remains unanswered is whether the two solutions to the A/m_H problem in Higgs mediation presented in this thesis are unique or whether other solutions exists. This is especially important since both the weak and strongly coupled solutions appear fairly fine-tuned, although for different reasons. An especially promising direction is to obtain the A-term through an effective superpotential operator of the form

$$W_{eff} = y_{ij}\frac{X}{M}HQ_iU_j. \tag{5.7}$$

This type of operator may be obtained by integrating out fields at tree-level, and is therefore not subject to the detrimental relation in (5.2). A priori one may think that such a model does not need to generate any soft mass at all, however we find that in a generic model contributions of the form

$$m^2_{soft} \sim \frac{1}{\kappa^2}|A_u|^2 \tag{5.8}$$

cannot be avoided [110]. The soft mass in question may be $m^2_{H_u}$ or a squark soft mass, where the former is MFV and the latter is not. κ is a particular coupling constant in the model under consideration. Although its precise meaning is model dependent, we find that all models of this type contain a coupling constant which can be identified with κ such that (5.8) holds. Although the dreaded soft masses cannot be avoided entirely, this scenario may nevertheless constitute an improvement over the other models presented in this thesis because of the presence of the coupling constant κ in (5.8). In particular it is notable that the little A/m_H problem from (5.5) is reduced in (5.8) is κ is allowed to be large. This in turn leads to better fine tuning properties of the model. In [110] we show that a realistic UV completion of this idea can be constructed if either the Higgs or the squarks are (partial) composites of a new strongly coupled sector.

Finally, although Higgs mediation is the perhaps the most straightforward method to obtain manifestly MFV A-terms, it is likely not to be the only possibility. In particular, one may allow for squark-messenger couplings, which may not suffer from the same problems which Higgs-messenger couplings are prone to. In this sense this type of models is expected to be less fine tuned, and perhaps a minimally tuned model can be constructed. On the other hand, in such a scenario MFV is no longer manifest and a full or partial flavor model is needed to generate properly aligned A-terms, which introduces another set of challenges

for the model builder [19–21].

Bibliography

[1] **ATLAS Collaboration** , G. Aad *et al.*, *Observation of a new particle in the search for the Standard Model Higgs boson with the ATLAS detector at the LHC*, *Phys.Lett.* **B716** (2012) 1–29, [arXiv:1207.7214].

[2] **CMS Collaboration** , S. Chatrchyan *et al.*, *Observation of a new boson at a mass of 125 GeV with the CMS experiment at the LHC*, *Phys.Lett.* **B716** (2012) 30–61, [arXiv:1207.7235].

[3] **CMS Collaboration** , S. Chatrchyan *et al.*, *Measurement of the properties of a Higgs boson in the four-lepton final state*, arXiv:1312.5353.

[4] **ATLAS Collaboration** , G. Aad *et al.*, *Measurements of Higgs boson production and couplings in diboson final states with the ATLAS detector at the LHC*, *Phys.Lett.* **B726** (2013) 88–119, [arXiv:1307.1427].

[5] *https://twiki.cern.ch/twiki/bin/view/cmspublic/physicsresultshig*, tech. rep., CMS, Geneva, 2014.

[6] L. D. Landau, *On the angular momentum of a two-photon system", journal =*, .

[7] C.-N. Yang, *Selection Rules for the Dematerialization of a Particle Into Two Photons", journal =*, .

[8] **ATLAS Collaboration** , *Study of the spin of the new boson with up to 25 fb^{-1} of ATLAS data*, Tech. Rep. ATLAS-CONF-2013-040, CERN, Geneva, Apr, 2013.

[9] G. Marques Tavares, M. Schmaltz, and W. Skiba, *Higgs mass naturalness and scale invariance in the UV*, *Phys.Rev.* **D89** (2014) 015009, [arXiv:1308.0025].

[10] S. P. Martin, *A Supersymmetry primer*, hep-ph/9709356.

[11] N. Craig, *The State of Supersymmetry after Run I of the LHC*, arXiv:1309.0528.

[12] **LUX Collaboration** , D. Akerib *et al.*, *First results from the LUX dark matter experiment at the Sanford Underground Research Facility*, arXiv:1310.8214.

[13] **CMS Collaboration** , *Search for supersymmetry using razor variables in events with b-jets in pp collisions at 8 TeV*, Tech. Rep. CMS-PAS-SUS-13-004, CERN, Geneva, 2013.

[14] **CMS Collaboration** , S. Chatrchyan *et al.*, *Search for top-squark pair production in the single-lepton final state in pp collisions at $\sqrt{s}$ = 8 TeV*, *Eur.Phys.J.* **C73** (2013) 2677, [arXiv:1308.1586].

[15] **CMS Collaboration** , S. Chatrchyan *et al.*, *Search for supersymmetry in pp collisions at $\sqrt{s}$ = 8 TeV in events with a single lepton, large jet multiplicity, and multiple b jets*, arXiv:1311.4937.

[16] P. Draper, P. Meade, M. Reece, and D. Shih, *Implications of a 125 GeV Higgs for the MSSM and Low-Scale SUSY Breaking*, arXiv:1112.3068.

[17] D. Redigolo, S. Knapen, and D. Shih, *In progress*, .

[18] J. Wess and J. Bagger, *Supersymmetry and supergravity", journal =*, .

[19] J. A. Evans and D. Shih, *Surveying Extended GMSB Models with m_h=125 GeV*, *JHEP* **1308** (2013) 093, [arXiv:1303.0228].

[20] Y. Shadmi and P. Z. Szabo, *Flavored Gauge-Mediation*, *JHEP* **1206** (2012) 124, [arXiv:1103.0292].

[21] M. Abdullah, I. Galon, Y. Shadmi, and Y. Shirman, *Flavored Gauge Mediation, A Heavy Higgs, and Supersymmetric Alignment*, *JHEP* **1306** (2013) 057, [arXiv:1209.4904].

[22] G. Dvali, G. Giudice, and A. Pomarol, *The Mu problem in theories with gauge mediated supersymmetry breaking*, *Nucl.Phys.* **B478** (1996) 31–45, [hep-ph/9603238].

[23] Z. Komargodski and N. Seiberg, *mu and General Gauge Mediation*, *JHEP* **0903** (2009) 072, [arXiv:0812.3900].

[24] **ATLAS** , G. Aad *et al.*, *Combined search for the Standard Model Higgs boson using up to 4.9 fb-1 of pp collision data at sqrt(s) = 7 TeV with the ATLAS detector at the LHC*, *Phys.Lett.* **B710** (2012) 49–66, [arXiv:1202.1408].

[25] **CMS** , S. Chatrchyan *et al.*, *Combined results of searches for the standard model Higgs boson in pp collisions at sqrt(s) = 7 TeV*, *Phys.Lett.* **B710** (2012) 26–48, [arXiv:1202.1488].

[26] L. J. Hall, D. Pinner, and J. T. Ruderman, *A Natural SUSY Higgs Near 126 GeV*, *JHEP* **1204** (2012) 131, [arXiv:1112.2703].

[27] S. Heinemeyer, O. Stal, and G. Weiglein, *Interpreting the LHC Higgs Search Results in the MSSM*, *Phys.Lett.* **B710** (2012) 201–206, [arXiv:1112.3026].

[28] A. Arbey, M. Battaglia, A. Djouadi, F. Mahmoudi, and J. Quevillon, *Implications of a 125 GeV Higgs for supersymmetric models*, *Phys.Lett.* **B708** (2012) 162–169, [arXiv:1112.3028].

[29] A. Arbey, M. Battaglia, and F. Mahmoudi, *Constraints on the MSSM from the Higgs Sector*, *Eur.Phys.J.* **C72** (2012) 1906, [arXiv:1112.3032].

[30] M. Carena, S. Gori, N. R. Shah, and C. E. Wagner, *A 125 GeV SM-like Higgs in the MSSM and the $\gamma\gamma$ rate*, *JHEP* **1203** (2012) 014, [arXiv:1112.3336].

[31] J. Cao, Z. Heng, J. M. Yang, Y. Zhang, and J. Zhu, *A SM-like Higgs near 125 GeV in low energy SUSY: a comparative study for MSSM and NMSSM*, *JHEP* **1203** (2012) 086, [arXiv:1202.5821].

[32] N. D. Christensen, T. Han, and S. Su, *MSSM Higgs Bosons at The LHC*, arXiv:1203.3207.

[33] F. Brummer, S. Kraml, and S. Kulkarni, *Anatomy of maximal stop mixing in the MSSM*, arXiv:1204.5977.

[34] G. Giudice and R. Rattazzi, *Theories with gauge mediated supersymmetry breaking*, *Phys.Rept.* **322** (1999) 419–499, [hep-ph/9801271].

[35] Z. Chacko and E. Ponton, *Yukawa deflected gauge mediation*, *Phys.Rev.* **D66** (2002) 095004, [hep-ph/0112190].

[36] Z. Chacko, E. Katz, and E. Perazzi, *Yukawa deflected gauge mediation in four dimensions*, *Phys.Rev.* **D66** (2002) 095012, [hep-ph/0203080].

[37] J. L. Evans, M. Ibe, and T. T. Yanagida, *Relatively Heavy Higgs Boson in More Generic Gauge Mediation*, *Phys.Lett.* **B705** (2011) 342–348, [arXiv:1107.3006].

[38] J. L. Evans, M. Ibe, S. Shirai, and T. T. Yanagida, *A 125GeV Higgs Boson and Muon g-2 in More Generic Gauge Mediation*, *Phys.Rev.* **D85** (2012) 095004, [arXiv:1201.2611].

[39] T. Jelinski, J. Pawelczyk, and K. Turzynski, *On Low-Energy Predictions of Unification Models Inspired by F-theory*, *Phys.Lett.* **B711** (2012) 307–312, [arXiv:1111.6492].

[40] M. Dine, Y. Nir, and Y. Shirman, *Variations on minimal gauge mediated supersymmetry breaking*, *Phys.Rev.* **D55** (1997) 1501–1508, [hep-ph/9607397].

[41] G. Giudice and R. Rattazzi, *Extracting supersymmetry breaking effects from wave function renormalization*, *Nucl.Phys.* **B511** (1998) 25–44, [hep-ph/9706540].

[42] M. Dine and A. E. Nelson, *Dynamical supersymmetry breaking at low-energies*, *Phys.Rev.* **D48** (1993) 1277–1287, [hep-ph/9303230].

[43] M. Dine, A. E. Nelson, and Y. Shirman, *Low-energy dynamical supersymmetry breaking simplified*, *Phys.Rev.* **D51** (1995) 1362–1370, [hep-ph/9408384].

[44] M. Dine, A. E. Nelson, Y. Nir, and Y. Shirman, *New tools for low-energy dynamical supersymmetry breaking*, *Phys.Rev.* **D53** (1996) 2658–2669, [hep-ph/9507378].

[45] S. Dimopoulos, G. Dvali, R. Rattazzi, and G. Giudice, *Dynamical soft terms with unbroken supersymmetry*, *Nucl.Phys.* **B510** (1998) 12–38, [hep-ph/9705307].

[46] A. Delgado, G. Giudice, and P. Slavich, *Dynamical mu term in gauge mediation*, *Phys.Lett.* **B653** (2007) 424–433, [arXiv:0706.3873].

[47] G. F. Giudice, H. D. Kim, and R. Rattazzi, *Natural mu and B mu in gauge mediation*, *Phys.Lett.* **B660** (2008) 545–549, [arXiv:0711.4448].

[48] Z. Kang, T. Li, T. Liu, C. Tong, and J. M. Yang, *A Heavy SM-like Higgs and a Light Stop from Yukawa-Deflected Gauge Mediation*, arXiv:1203.2336.

[49] N. Craig, S. Knapen, and D. Shih, *General Messenger Higgs Mediation*, *JHEP* **1308** (2013) 118, [arXiv:1302.2642].

[50] A. de Gouvea, A. Friedland, and H. Murayama, *Next-to-minimal supersymmetric standard model with the gauge mediation of supersymmetry breaking*, *Phys.Rev.* **D57** (1998) 5676–5696, [hep-ph/9711264].

[51] T. Han, D. Marfatia, and R.-J. Zhang, *A Gauge mediated supersymmetry breaking model with an extra singlet Higgs field*, *Phys.Rev.* **D61** (2000) 013007, [hep-ph/9906508].

[52] U. Ellwanger, C.-C. Jean-Louis, and A. Teixeira, *Phenomenology of the General NMSSM with Gauge Mediated Supersymmetry Breaking*, *JHEP* **0805** (2008) 044, [arXiv:0803.2962].

[53] D. E. Morrissey and A. Pierce, *Modified Higgs Boson Phenomenology from Gauge or Gaugino Mediation in the NMSSM*, *Phys.Rev.* **D78** (2008) 075029, [arXiv:0807.2259].

[54] U. Ellwanger, C. Hugonie, and A. M. Teixeira, *The Next-to-Minimal Supersymmetric Standard Model*, *Phys.Rept.* **496** (2010) 1–77, [arXiv:0910.1785].

[55] **CMS** , S. Chatrchyan *et al.*, *Search for anomalous production of multilepton events in pp collisions at sqrt(s)=7 TeV*, arXiv:1204.5341.

[56] P. Meade, N. Seiberg, and D. Shih, *General Gauge Mediation*, *Prog.Theor.Phys.Suppl.* **177** (2009) 143–158, [arXiv:0801.3278].

[57] M. Buican, P. Meade, N. Seiberg, and D. Shih, *Exploring General Gauge Mediation*, *JHEP* **0903** (2009) 016, [arXiv:0812.3668].

[58] M. Dine, *Some issues in gauge mediation*, *Nucl.Phys.Proc.Suppl.* **62** (1998) 276–280, [hep-ph/9707413].

[59] C. Csaki, A. Falkowski, Y. Nomura, and T. Volansky, *New Approach to the mu-Bmu Problem of Gauge-Mediated Supersymmetry Breaking*, *Phys.Rev.Lett.* **102** (2009) 111801, [arXiv:0809.4492].

[60] A. De Simone, R. Franceschini, G. F. Giudice, D. Pappadopulo, and R. Rattazzi, *Lopsided Gauge Mediation*, *JHEP* **1105** (2011) 112, [arXiv:1103.6033].

[61] C. Cheung, A. L. Fitzpatrick, and D. Shih, *(Extra)ordinary gauge mediation*, *JHEP* **0807** (2008) 054, [arXiv:0710.3585].

[62] S. Dimopoulos, G. Giudice, and A. Pomarol, *Dark matter in theories of gauge mediated supersymmetry breaking*, *Phys.Lett.* **B389** (1996) 37–42, [hep-ph/9607225].

[63] S. P. Martin, *Generalized messengers of supersymmetry breaking and the sparticle mass spectrum*, *Phys.Rev.* **D55** (1997) 3177–3187, [hep-ph/9608224].

[64] I. Donkin and A. K. Knochel, *NMSSM with Lopsided Gauge Mediation*, arXiv:1205.5515.

[65] U. Ellwanger, J. F. Gunion, and C. Hugonie, *NMHDECAY: A Fortran code for the Higgs masses, couplings and decay widths in the NMSSM*, *JHEP* **0502** (2005) 066, [hep-ph/0406215].

[66] U. Ellwanger and C. Hugonie, *NMHDECAY 2.0: An Updated program for sparticle masses, Higgs masses, couplings and decay widths in the NMSSM*, *Comput.Phys.Commun.* **175** (2006) 290–303, [hep-ph/0508022].

[67] B. Allanach, *SOFTSUSY: a program for calculating supersymmetric spectra*, *Comput.Phys.Commun.* **143** (2002) 305–331, [hep-ph/0104145].

[68] R. Barbieri and G. Giudice, *Upper Bounds on Supersymmetric Particle Masses*, *Nucl.Phys.* **B306** (1988) 63.

[69] M. Dine, P. Fox, E. Gorbatov, Y. Shadmi, Y. Shirman, *et al.*, *Visible effects of the hidden sector*, *Phys.Rev.* **D70** (2004) 045023, [hep-ph/0405159].

[70] H. Murayama, Y. Nomura, and D. Poland, *More visible effects of the hidden sector*, *Phys.Rev.* **D77** (2008) 015005, [arXiv:0709.0775].

[71] T. S. Roy and M. Schmaltz, *Hidden solution to the mu/Bmu problem in gauge mediation*, *Phys.Rev.* **D77** (2008) 095008, [arXiv:0708.3593].

[72] N. J. Craig and D. Green, *On the Phenomenology of Strongly Coupled Hidden Sectors*, *JHEP* **0909** (2009) 113, [arXiv:0905.4088].

[73] S. P. Martin, *A Supersymmetry primer*, hep-ph/9709356.

[74] J. Casas, J. Espinosa, M. Quiros, and A. Riotto, *The Lightest Higgs boson mass in the minimal supersymmetric standard model*, *Nucl.Phys.* **B436** (1995) 3–29, [hep-ph/9407389].

[75] M. S. Carena, J. Espinosa, M. Quiros, and C. Wagner, *Analytical expressions for radiatively corrected Higgs masses and couplings in the MSSM*, *Phys.Lett.* **B355** (1995) 209–221, [hep-ph/9504316].

[76] H. E. Haber, R. Hempfling, and A. H. Hoang, *Approximating the radiatively corrected Higgs mass in the minimal supersymmetric model*, *Z.Phys.* **C75** (1997) 539–554, [hep-ph/9609331].

[77] N. Craig, S. Knapen, D. Shih, and Y. Zhao, *A Complete Model of Low-Scale Gauge Mediation*, *JHEP* **1303** (2013) 154, [arXiv:1206.4086].

[78] T. T. Dumitrescu, Z. Komargodski, N. Seiberg, and D. Shih, *General Messenger Gauge Mediation*, *JHEP* **1005** (2010) 096, [arXiv:1003.2661].

[79] G. Perez, T. S. Roy, and M. Schmaltz, *Phenomenology of SUSY with scalar sequestering*, *Phys.Rev.* **D79** (2009) 095016, [arXiv:0811.3206].

[80] M. Asano, J. Hisano, T. Okada, and S. Sugiyama, *A Realistic Extension of Gauge-Mediated SUSY-Breaking Model with Superconformal Hidden Sector*, *Phys.Lett.* **B673** (2009) 146–151, [arXiv:0810.4606].

[81] D. Poland, D. Simmons-Duffin, and A. Vichi, *Carving Out the Space of 4D CFTs*, *JHEP* **1205** (2012) 110, [arXiv:1109.5176].

[82] S. Knapen and D. Shih, *Higgs Mediation with Strong Hidden Sector Dynamics*, arXiv:1311.7107.

[83] D. Green and D. Shih, *Bounds on SCFTs from Conformal Perturbation Theory*, *JHEP* **1209** (2012) 026, [arXiv:1203.5129].

[84] L. M. Carpenter, M. Dine, G. Festuccia, and J. D. Mason, *Implementing General Gauge Mediation*, *Phys.Rev.* **D79** (2009) 035002, [arXiv:0805.2944].

[85] E. Witten, *Dynamical Breaking of Supersymmetry*, *Nucl.Phys.* **B188** (1981) 513.

[86] L. Randall and R. Sundrum, *Out of this world supersymmetry breaking*, *Nucl.Phys.* **B557** (1999) 79–118, [hep-th/9810155].

[87] M. A. Luty and R. Sundrum, *Supersymmetry breaking and composite extra dimensions*, *Phys.Rev.* **D65** (2002) 066004, [hep-th/0105137].

[88] M. Luty and R. Sundrum, *Anomaly mediated supersymmetry breaking in four-dimensions, naturally*, *Phys.Rev.* **D67** (2003) 045007, [hep-th/0111231].

[89] R. Rattazzi, V. S. Rychkov, E. Tonni, and A. Vichi, *Bounding scalar operator dimensions in 4D CFT*, *JHEP* **0812** (2008) 031, [arXiv:0807.0004].

[90] Z. Chacko, M. A. Luty, A. E. Nelson, and E. Ponton, *Gaugino mediated supersymmetry breaking*, *JHEP* **0001** (2000) 003, [hep-ph/9911323].

[91] D. E. Kaplan, G. D. Kribs, and M. Schmaltz, *Supersymmetry breaking through transparent extra dimensions*, *Phys.Rev.* **D62** (2000) 035010, [hep-ph/9911293].

[92] N. J. Craig and D. R. Green, *Sequestering the Gravitino: Neutralino Dark Matter in Gauge Mediation*, *Phys.Rev.* **D79** (2009) 065030, [arXiv:0808.1097].

[93] N. J. Craig and D. Green, *Building a Better mSUGRA: WIMP Dark Matter Without Flavor Violation*, *Phys.Rev.* **D80** (2009) 085012, [arXiv:0906.2022].

[94] S. Dimopoulos and G. Giudice, *Multimessenger theories of gauge mediated supersymmetry breaking*, *Phys.Lett.* **B393** (1997) 72–78, [hep-ph/9609344].

[95] N. Blinov and D. E. Morrissey, *Vacuum Stability and the MSSM Higgs Mass*, arXiv:1310.4174.

[96] J. E. Camargo-Molina, B. O'Leary, W. Porod, and F. Staub, *On the vacuum stability of SUSY models*, arXiv:1310.1260.

[97] J. Camargo-Molina, B. O'Leary, W. Porod, and F. Staub, *Vevacious: A Tool For Finding The Global Minima Of One-Loop Effective Potentials With Many Scalars*, arXiv:1307.1477.

[98] A. Katz and B. Tweedie, *Signals of a Sneutrino (N)LSP at the LHC*, *Phys.Rev.* **D81** (2010) 035012, [arXiv:0911.4132].

[99] **CMS Collaboration** , S. Chatrchyan *et al.*, *Searches for long-lived charged particles in pp collisions at $\sqrt{s}$=7 and 8 TeV*, arXiv:1305.0491.

[100] *A search for heavy long-lived sleptons using 16 fb^{-1} of pp collisions at $\sqrt{s} = 8$ tev with the ATLAS detector*, Tech. Rep. ATLAS-CONF-2013-058, CERN, Geneva, Jun, 2013.

[101] J. Heisig and J. Kersten, *Long-lived staus from strong production in a simplified model approach*, *Phys.Rev.* **D86** (2012) 055020, [arXiv:1203.1581].

[102] J. Heisig, J. Kersten, B. Panes, and T. Robens, *A survey for low stau yields in the MSSM*, arXiv:1310.2825.

[103] *https://twiki.cern.ch/twiki/bin/view/lhcphysics/susycrosssections*, tech. rep., LHC SUSY Cross Section Working Group, 2014.

[104] W. Beenakker, M. Klasen, M. Kramer, T. Plehn, M. Spira, *et al.*, *The Production of charginos / neutralinos and sleptons at hadron colliders*, *Phys.Rev.Lett.* **83** (1999) 3780–3783, [hep-ph/9906298].

[105] *Combined LEP chargino results, up to 208 gev for low δm*, Tech. Rep. LEPSUSYWG/02-04.1, LEP susy working group, Geneva, 2002.

[106] *Search for direct-slepton and direct-chargino production in final states with two opposite-sign leptons, missing transverse momentum and no jets in 20/fb of pp collisions at sqrt(s) = 8 tev with the atlas detector*, Tech. Rep. ATLAS-CONF-2013-049, CERN, Geneva, May, 2013.

[107] *Search for electroweak production of charginos, neutralinos, and sleptons using leptonic final states in pp collisions at 8 tev*, Tech. Rep. CMS-PAS-SUS-13-006, CERN, Geneva, 2013.

[108] D. Shih, *Spontaneous R-symmetry breaking in O'Raifeartaigh models*, *JHEP* **0802** (2008) 091, [hep-th/0703196].

[109] D. Curtin, Z. Komargodski, D. Shih, and Y. Tsai, *Spontaneous R-symmetry Breaking with Multiple Pseudomoduli*, *Phys.Rev.* **D85** (2012) 125031, [arXiv:1202.5331].

[110] A. Basirnia, D. Egana, S. Knapen, and D. Shih, *In progress*, .